

RESISTIVITY AND SEISMIC REFRACTION SURVEYS OVER
PLEISTOCENE DEPOSITS IN SOUTHERN MANITOBA

A Thesis

Submitted to

The Faculty of Graduate Studies and Research

The University of Manitoba

In Partial Fulfillment

of the Requirements for the Degree of

Master of Science

by

Pakiraiah Chagarlamudi

April, 1971

© Pakiraiah Chagarlamudi 1972



TABLE OF CONTENTS

	Page
List of Tables	v
List of Figures	vii
Abstract	x
Acknowledgements	xi
CHAPTER I - INTRODUCTION	1
CHAPTER II - FIELD PROCEDURES AND INTERPRETATIONS	3
Resistivity Surveys	3
Resistivity Interpretation Techniques	5
Seismic Surveys	9
Seismic Refraction Interpretation	10
CHAPTER III - FIELD RESULTS	18
Broomhill Experimental Aquifer, Melita.	18
Geology of the Area	18
Resistivity Results	20
Seismic Results	36
Conclusions	44
Whiteshell Nuclear Research Establishment Plant Site, Pinawa	48
Geology of the Area	48
Resistivity Results	48
Seismic Results	57
Conclusions	65

	Page
Metro Winnipeg Area	67
Geology of the Area	67
Resistivity Results	68
Seismic Results	85
Conclusions	90
Wilson Creek Experimental Watershed, McCreary	92
Geology of the Area	92
Resistivity Results	93
Seismic Results	98
Conclusions	106
CHAPTER IV - GENERAL CONCLUSIONS	110
References	114

LIST OF TABLES

	Page
<u>Broomhill Experimental Aquifer</u>	
1. Resistivity and depth values from curve matching method.	25
2. Resistivity and depth values from inverse slope method.	29
3. Depth values from cumulative method.	37
4. Resistivity and depth values from Tagg's method.	39
5. Velocity and depth values from seismic profiles.	42
<u>Whiteshell Nuclear Research Establishment Plant Site</u>	
6. Resistivity and depth values from curve matching method.	54
7. Resistivity and depth values from inverse slope method.	55
8. Depth values from cumulative method.	59
9. Velocity and depth values from seismic profiles.	61
<u>Metro Winnipeg Area</u>	
10. Resistivity and depth values from curve matching method.	74
11. Resistivity and depth values from inverse slope method.	79
12. Depth values from cumulative method.	81
13. Velocity and depth values from seismic profiles.	86

	Page
<u>Wilson Creek Experimental Watershed</u>	
14. Resistivity and depth values from curve matching method.	96
15. Resistivity and depth values from inverse slope method.	100
16. Depth values from cumulative method.	102
17. Velocity and depth values from seismic profiles.	104

LIST OF FIGURES

Figure	Page
1. Index map showing study area locations.	2
2. Wenner electrode configuration.	4
3. Diagram showing inverse slope method interpretation.	4
4. Time-distance plot and refraction path for a single horizontal discontinuity.	11
5. Time-distance plot and refraction paths for two horizontal discontinuities.	12
6. Refraction paths and time-distance plots for up dip and down dip profiles.	14
7. Elevation correction.	16
8. Test well and drill hole location map - Broomhill Experimental Aquifer, Melita.	19
9. Resistivity sounding - seismic profile location map - Broomhill Experimental Aquifer, Melita.	21
10. Sounding #65 typical resistivity sounding of the area - Broomhill Experimental Aquifer, Melita.	22
11. Sounding #79 typical resistivity sounding of the area - Broomhill Experimental Aquifer, Melita.	23
12. Depth to till layer shown - Broomhill Experimental Aquifer, Melita.	24
13. Normalized histogram of resistivities - Broomhill Experimental Aquifer, Melita.	28
14. Resistivity sounding #79 inverse slope method interpretation - Broomhill Experimental Aquifer, Melita.	31

	Page
15. Cross section AA'.	33
16. Cross section BB'.	34
17. Resistivity sounding #79 cumulative method - Broomhill Experimental Aquifer, Melita.	35
18. Normalized histogram of velocities - Melita.	41
19. Seismic profile 239-240 near well 46 - Broomhill Experimental Aquifer, Melita.	45
20. Seismic profile 226-227 near well 24 - Broomhill Experimental Aquifer, Melita.	46
21. Resistivity sounding and seismic profile locations Whiteshell Nuclear Research Establishment Plant Site, Pinawa.	49
22. Map showing depth to bedrock -Pinawa.	51
23. Sounding #18, curve matching method -Pinawa.	52
24. Normalized histogram of resistivities -Pinawa.	53
25. Sounding #18 (a) cumulative (b) inverse slope.	56
26. Sounding #20 (a) cumulative (b) inverse slope.	58
27. Normalized histogram of velocities - Pinawa.	63
28. Seismic profile 179-180 (at sounding #18) - Pinawa.	64
29. Map showing well locations - Metro Winnipeg.	69
30. Map showing resistivity sounding and seismic profile locations - Metro Winnipeg.	70
31. Resistivity sounding #112 - curve matching method.	71
32. Resistivity sounding #120 - curve matching method.	72
33. Normalized histogram of resistivities - Metro Winnipeg.	76
34. Resistivity sounding #109 - curve matching method.	77
35. Resistivity sounding #112 (a) cumulative (b) inverse slope method.	83

	Page
36. Resistivity sounding #120 (a) cumulative (b) inverse slope method.	84
37. Normalized histogram of seismic velocities - Metro Winnipeg.	87
38. Seismic profile 414-415 - Metro Winnipeg.	89
39. Location map - Wilson Creek Experimental Watershed.	94
40. Resistivity sounding and Seismic profile locations - Wilson Creek Experimental Watershed.	95
41. Normalized histogram of resistivities - Wilson Creek Experimental Watershed.	97
42. Resistivity sounding #7 curve matching method.	99
43. Resistivity sounding #7 inverse slope method.	101
44. Resistivity sounding #7 cumulative method.	103
45. Normalized histogram of velocities, Wilson Creek Experimental Watershed.	107
46. Seismic profile 24-23 - Wilson Creek Experimental	108

ABSTRACT

Electrical resistivity and seismic refraction surveys were conducted at four different areas in southern Manitoba having widely varying geologic settings. This study was undertaken to determine the advantages and usefulness of these methods in evaluation of Pleistocene deposits.

This study indicates that resistivity and seismic refraction methods can be successfully used in the evaluation of Pleistocene deposits in Manitoba. The resistivity method is effective both in evaluating the individual superficial deposits and in mapping the overburden-bedrock interface. The seismic refraction method is less sensitive to the character of the individual superficial deposits. The best use for the seismic refraction method is in mapping the overburden-bedrock interface.

The results of this work indicate that a combination of geophysical methods with selected drilling is the best approach to studying Pleistocene deposits. The individual methods to be applied and the spacing to be used depends on the specific problem under consideration and the features of the deposits to be studied.

ACKNOWLEDGEMENTS

The writer wishes to express his sincere thanks to Drs. C. D. Anderson, D. H. Hall, and R. Newbury for their direction and supervision during his M.Sc. studies, and thesis work. Thanks are also due to Dr. J. A. Cherry for his help in the initial planning of this study. It is also a pleasure to acknowledge the help from Dr. Z. Hajnal during the field work.

The writer wishes to acknowledge the contributions from Messrs. M. Chekryn, T. Duffy, R. Altonen, H. Bhaktiari, F. Render and J. Thomlinson in the field studies.

This work was supported by grants from the National Research Council of Canada and the Agassiz Center for Water Studies, University of Manitoba.

CHAPTER I

INTRODUCTION

The main purpose of this study was to check the advantages and usefulness of the application of electrical resistivity and seismic refraction techniques to ground water problems in selected areas of southern Manitoba. The field data were collected with a view to study the sensitivity of these two methods to the character of the Pleistocene deposits. Whenever possible, the data were collected where drill hole information is available.

The particular areas chosen for this study were:

- (a) Broomhill Experimental Aquifer, Melita
- (b) Whiteshell Nuclear Research Establishment
Plant Site, Pinawa
- (c) Metropolitan Winnipeg area
- (d) Wilson Creek Experimental Aquifer, McCreary

Figure 1 is an index map showing the location of these areas.

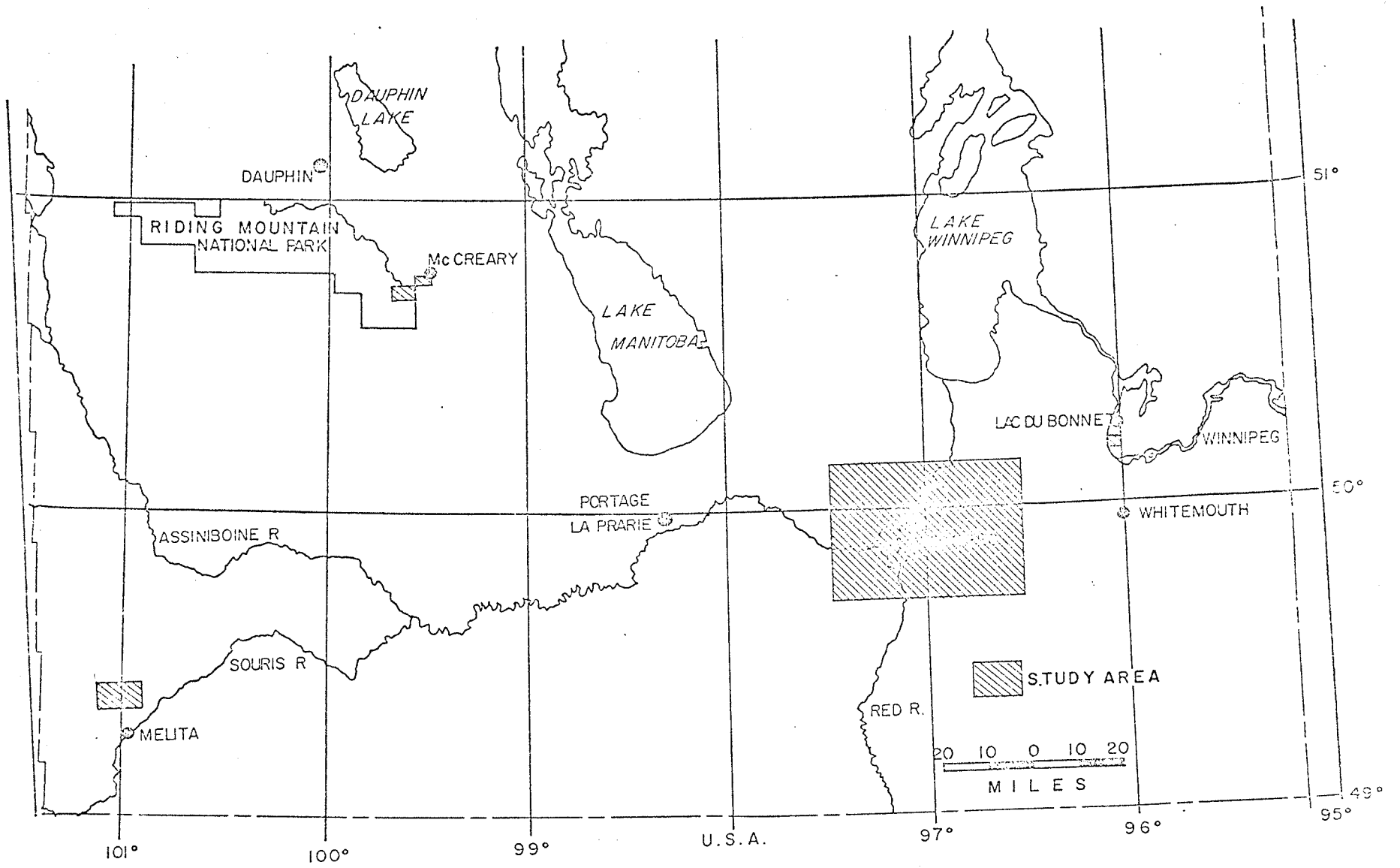


Fig. 1. Map showing study area locations.

CHAPTER II

FIELD PROCEDURES AND INTERPRETATIONS

Resistivity Surveys

All resistivity soundings were done using a Wenner electrode configuration. The major advantages of this configuration over other standard configurations are that it minimizes the effects of local surface inhomogeneities and there are a greater number of interpretation techniques available.

In the Wenner electrode configuration the four electrodes are spaced along a line at equal inter-electrode distances (Wenner, 1915). The current is passed through two outer electrodes, designated C_1 and C_2 and the potential difference is measured between two inner electrodes, designated P_1 and P_2 (Figure 2).

The apparent resistivity (ρ_a) for the Wenner configuration is given by

$$\rho_a = 2\pi a \frac{V}{I}$$

where 'V' is the potential difference (in volts) between P_1 and P_2 when current 'I' (in amperes) flows between current electrodes C_1 and C_2 . The electrode separation

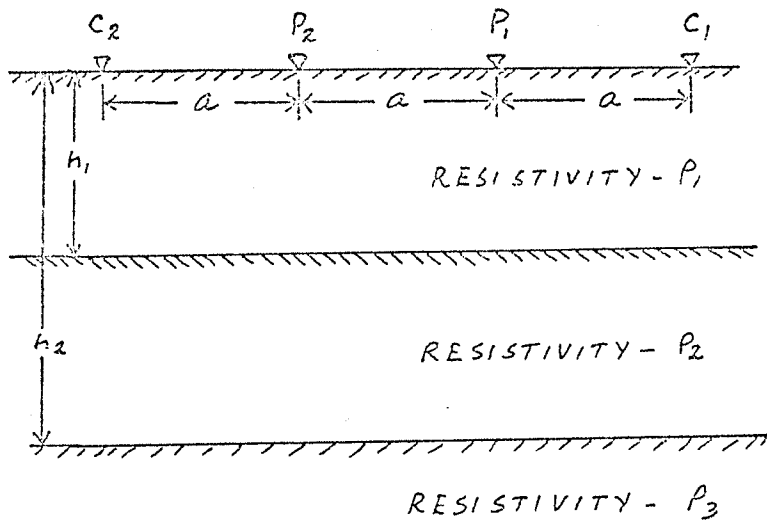


Fig. 2. Wenner electrode configuration

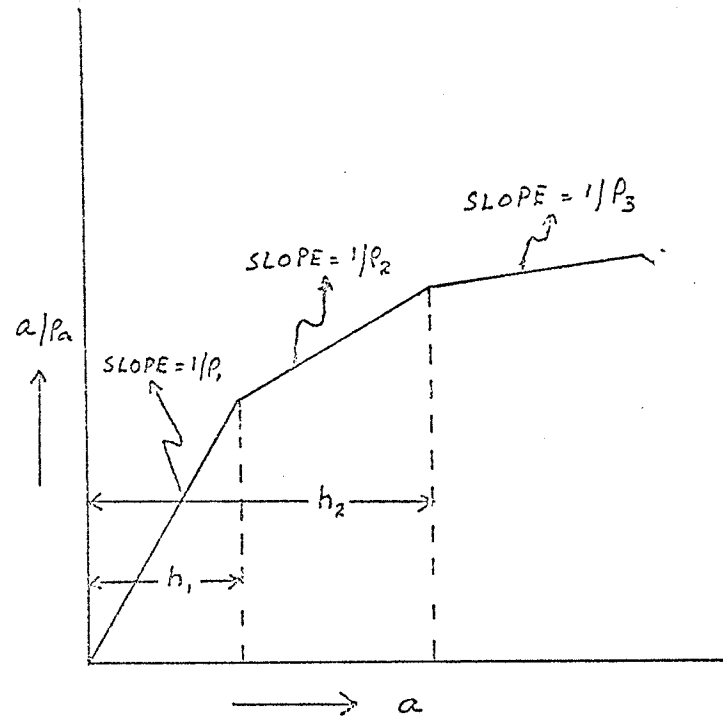


Fig. 3. Diagram showing inverse slope method interpretation

is 'a' (in meters) and the apparent resistivity is ρ_a (in ohmmeters).

Equipment Set Up

Power is supplied by a bank of ten 45 volt batteries connected in a series-parallel combination to provide a maximum of 225 volts D.C. at the current terminals. One ampere of current was used whenever possible. Potential differences are measured with a Hewlett-Packard Model 419-A D.C. null voltmeter. Current is measured on a d'arsonval type ammeter. Round steel stakes (24 in. x 0.75 in.) were used as current electrodes. Porous pots, 2 in. in diameter and 4 in. deep with 0.75 in. diameter copper coated electrodes in a copper sulphate solution were used as potential electrodes. Self potential is nullified using an adjustable voltage source in the potential circuit. The potential measurements were taken at electrode separations 5, 10, 25, 50, 100, 150, 200, 300, 400 and 500 feet.

Resistivity Interpretation Techniques

Depth determinations were done using the curve matching method (Mooney and Wetzel, 1956), the inverse slope method (Sankernarain and Ramanujachary, 1967), and Tagg's method (Tagg, 1934) with extention to three layer cases by successive approximation (Pirson, 1934).

Curve Matching Method

Mooney and Wetzel theoretical curves were used to interpret the field results. For comparison the field data is plotted on double logarithmic paper with the electrode separation along the horizontal axis and the observed resistivity along the vertical axis. The resistivity ρ_1 of the first layer is the observed resistivity value on the field curve which overlies apparent resistivity = 1.0 on the theoretical curve. The depth to the lowermost interface is the electrode separation (a) on the field curve which overlies depth index = 6.0 on the theoretical curve. The unknown resistivities and depths can be calculated from the resistivity and depth ratios which identify the theoretical curve.

Inverse Slope Method

Sankernarain and Ramanujachary (1967) described the method as follows:

For the Wenner configuration (Fig. 2)

$$\rho_a = 2\pi a \frac{V}{I}$$

for small values of a, $\rho_a = \rho_1$, and

$$\frac{a}{\rho_a} = \frac{a}{\rho_1} = [2\pi \frac{V}{I}]^{-1}$$

A plot of $\frac{a}{\rho_a}$ versus 'a' will give a straight line passing through the origin. The slope of the line equals $\frac{1}{\rho_1}$. For a horizontal layer (using Hummel's principle) they arrive at the equation

$$\frac{h_1(\rho_2 - \rho_1)}{\rho_1\rho_2} + \frac{a}{\rho_2} \approx \frac{a}{\rho_a}$$

The first term of the equation is a constant. The graph of $\frac{a}{\rho_a}$ versus 'a' is a straight line with slope $\frac{1}{\rho_2}$ and it intersects the segment of slope $\frac{1}{\rho_1}$ at a point whose abscissa gives the thickness h_1 of the first layer. With another layer the above equation takes the form

$$\frac{(h_1 + h_2)(\rho_3 - \rho_{ave})}{\rho_{ave}\rho_3} + \frac{a}{\rho_3} \approx \frac{a}{\rho_a}$$

where ρ_{ave} is the average resistivity of layers 1 and 2. On the graph in Fig. 3 this equation represents the segment of slope $\frac{1}{\rho_3}$. The intersection of this segment with the previous one projected down to the 'a' axis gives the quantity h_2 . In the same manner this approach can be extended for additional layers.

Cumulative Method

In this method the cumulative values of apparent resistivity are plotted against the electrode separation

on a linear scale. The point of intersection of tangents (straight lines) drawn to intersect at zones of maximum curvature in the cumulative curve indicates the depth to the underlying layer. The greatly reduced scale required for plotting the cumulative values of resistivity together with the effect of summation of the individual values serves to minimize the effect of purely local surface anomalies and inadvertent errors of measurement.

Successive Approximation Method

An average value of the resistivity of the top layer (ρ_1) is estimated from the curve obtained by plotting ' ρ_a ' versus 'a' on a linear scale and a graphic approximation curve is drawn from ρ_1 meeting the first part of the curve tangentially. Tagg's method is then applied to the first part of the curve, which yields the resistivity of the second layer (ρ_2), the thickness of the first layer (h_1) and the resistivity factor K_1 . The depth to the third layer is estimated by the method of Lancaster Jones (1930). Thus $h_1 + h_2 = \frac{2}{3}d$, where 'd' is the spacing at which occurs the inflection point comprised between the two lower maximum curvature points, and ' h_2 ' is the thickness of the second layer. The equivalent resistivity ' ρ'_1 ' of the two layers in parallel is calculated by Kirchhoff's law and Tagg's method is then applied to the lower part of the curve. From the curves of the depth resistivity

factor the depth $h_1 + h_2'$ and the resistivity factor

$K_2 = \frac{\rho_3 - \rho_2}{\rho_3 + \rho_2}$ are known and the third layer resistivity

can be calculated. The process may be repeated using

$h_1 + h_2'$ instead of $\frac{2}{3}d$ for a successive approximation.

Seismic Surveys

The basic seismic theory is discussed adequately by such authorities as Heiland (1963), Dobrin (1960) and Nettleton (1940). The basic formulae set out by them uses velocities of the layers involved and either the interception times or the critical distances.

In this study profile shooting was done. All the profiles are reversed and dip determinations are made whenever necessary. The depth determinations are carried out using the time-distance plots.

Equipment Set-Up

The refraction surveys were conducted using Geospace Model GT-2 portable refraction equipment. This equipment has 12 channels and a polaroid film read-out device. The travel time accuracy is ± 0.5 m. sec. With normal cable spread the distance between successive geophones is 110 ft. The energy source used in this work was a small explosion caused by a 75% forcite stick, which weighs about two-fifths of a pound. The shot holes were two feet deep on the average.

Seismic Refraction Interpretation

Single Horizontal Layer

The time-distance plot for the case of two media with respective speeds V_1 and V_2 separated by a horizontal discontinuity at depth z is shown in Fig. 4.

The depth z to the interface can be calculated from the intercept time using the equation

$$z = \frac{T_i}{2} \cdot \frac{V_2 V_1}{\sqrt{V_2^2 - V_1^2}}$$

The depth can be solved for in terms of critical distance, x_c , using the equation

$$z = \frac{x_c}{2} \cdot \sqrt{\frac{V_2 - V_1}{V_2 + V_1}}$$

Two Horizontal Layers

The time-distance plot for the case of three media with respective speeds V_1 , V_2 , and V_3 with discontinuities at depths z_1 and $z_1 + z_2$ is shown in Fig. 5. The depth z_1 can be calculated as shown for single horizontal discontinuity.

The depth z_2 can be calculated from time intercept using the formula

$$z = \frac{1}{2} (T_{i_2} - 2z_1 \sqrt{\frac{V_3^2 - V_1^2}{V_3 V_1}}) \cdot \frac{V_3 V_2}{\sqrt{V_3^2 - V_2^2}}$$

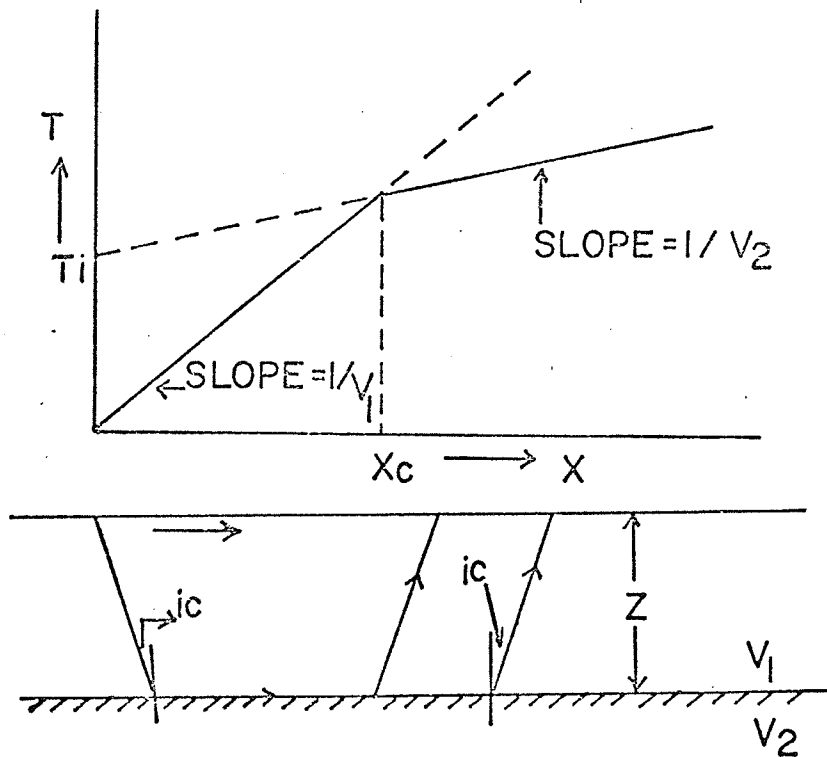


Fig. 4. Time-distance plot and refraction path for a single horizontal discontinuity.

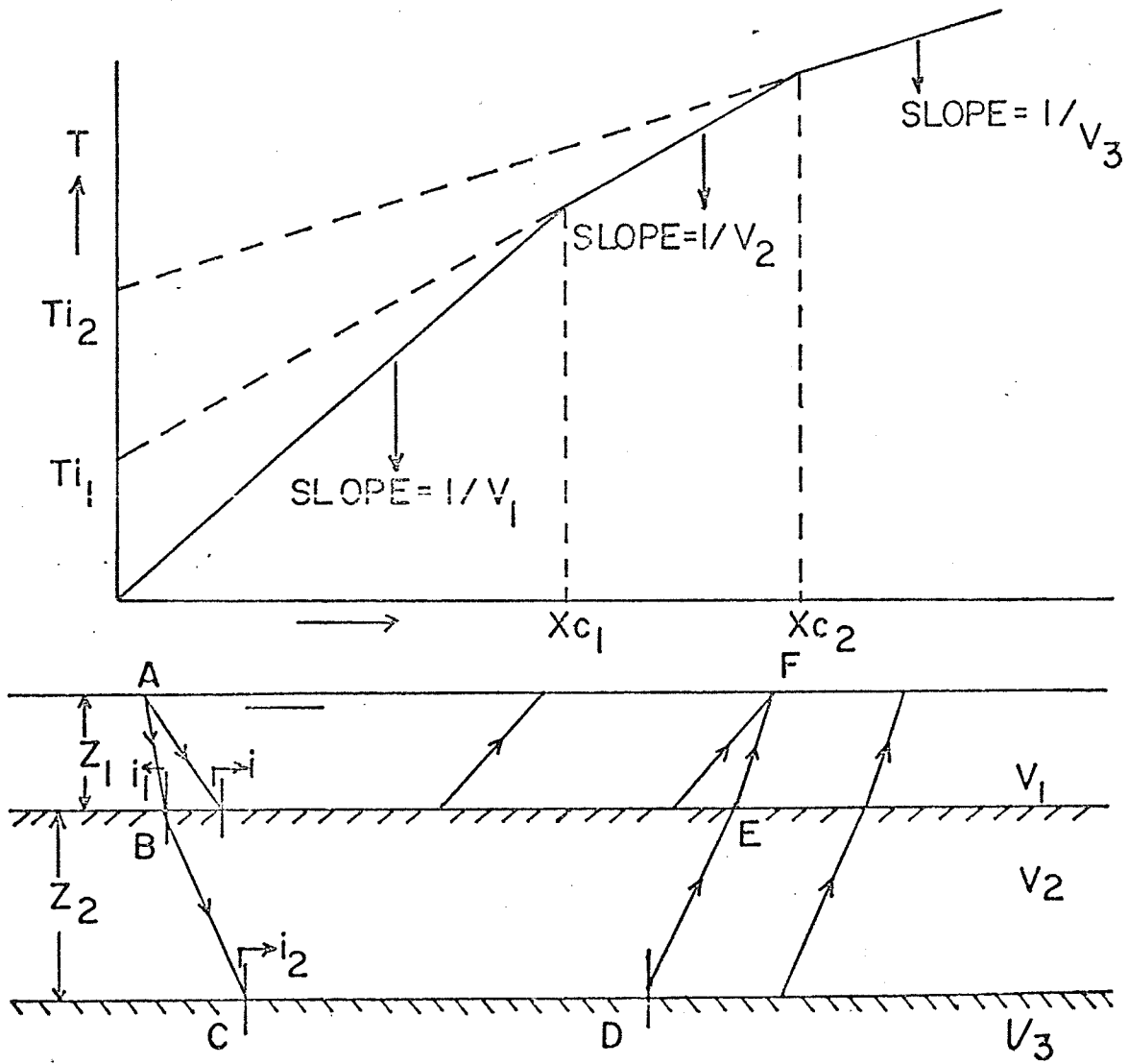


Fig. 5. Time-distance plot and refraction paths for two horizontal discontinuities.

Using critical distances the depth to the bottom of the second layer can be calculated from the equation

$$z_1 + z_2 = \frac{x_{c2}}{2} \sqrt{\frac{V_3 - V_2}{V_3 + V_2}} + z_1 \left[1 + \frac{1}{\sin i \cos i_2} (\cos i - \cos i_1) \right]$$

The value of z_1 can be obtained from the critical distance formula given for a single horizontal discontinuity.

Single Dipping Layer

The time-distance plot for a sloping interface is shown in Fig. 6. Using the slopes of the up-dip and down-dip segments (m_u and m_d); and

$$i_c = \frac{1}{2} (\sin^{-1} V_1 \cdot m_d + \sin^{-1} V_1 \cdot m_u)$$

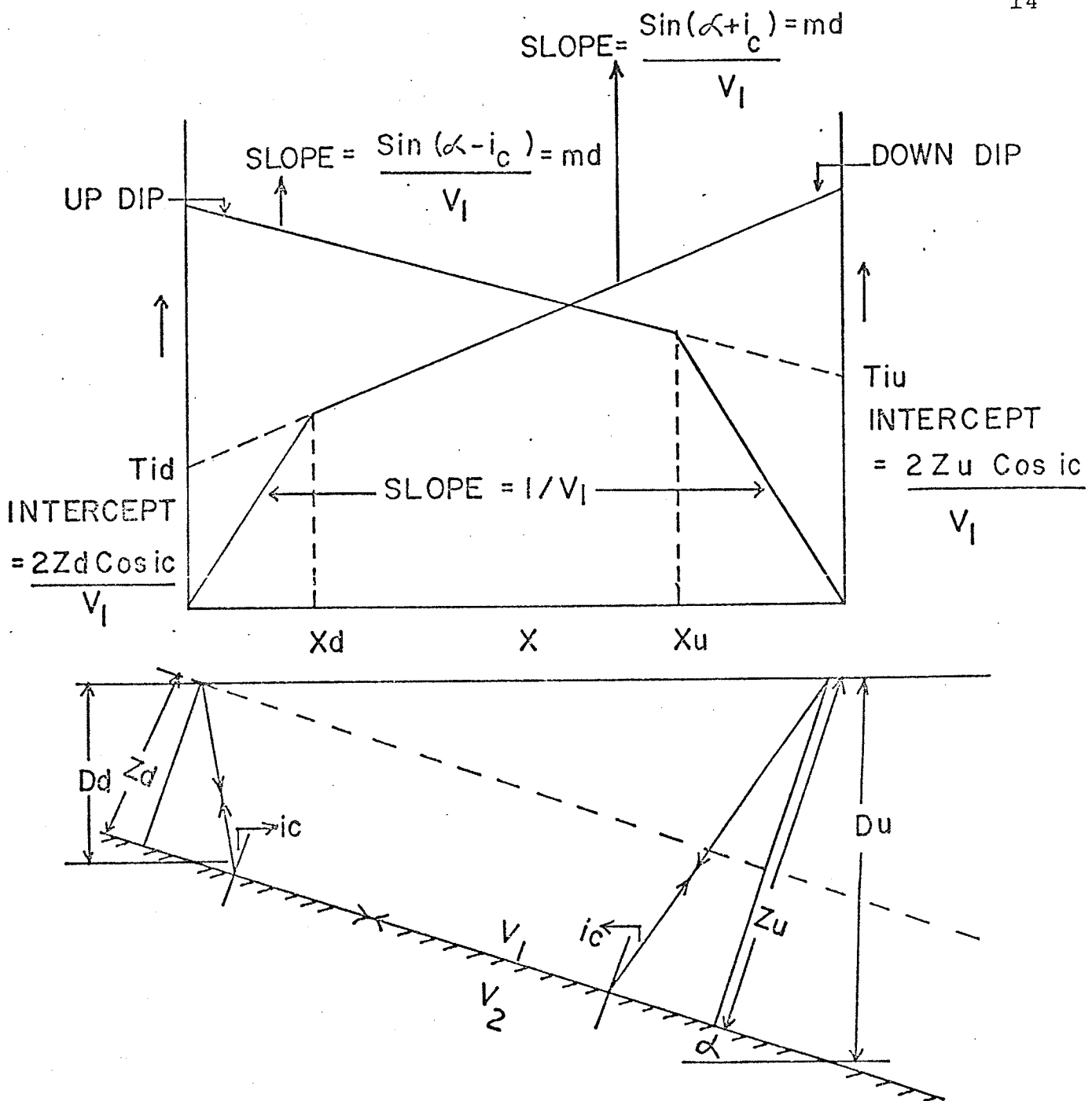
$$\alpha = \frac{1}{2} (\sin^{-1} V_1 \cdot m_d - \sin^{-1} V_1 \cdot m_u)$$

With i_c determined, V_2 is obtained from the relation

$$V_2 = \frac{V_1}{\sin i_c}$$

The perpendicular distance z_u can be calculated from the relation

$$z_u = \frac{V_1 \cdot T_{i_u}}{2 \cos i_c}$$



α = dip

z_d = perpendicular distance from the shot to the interface at the up-dip end of the line.

z_u = perpendicular distance from the shot to the interface at the down-dip end of the line.

d_d and d_u = the depths at the up-dip end and down-dip end respectively.

Fig. 6. Refraction paths and time distance plots for up-dip and down-dip profiles.

and z_d can be calculated from the relation

$$z_d = \frac{V_1 \cdot T_{i_d}}{2 \cos i_c}$$

The depths D_u and D_d can be calculated using the equations

$$D_u = \frac{z_u}{\cos \alpha} \quad \text{and} \quad D_d = \frac{z_d}{\cos \alpha}$$

Once the dip (α) is determined, the depths can be calculated using the critical distance formulae

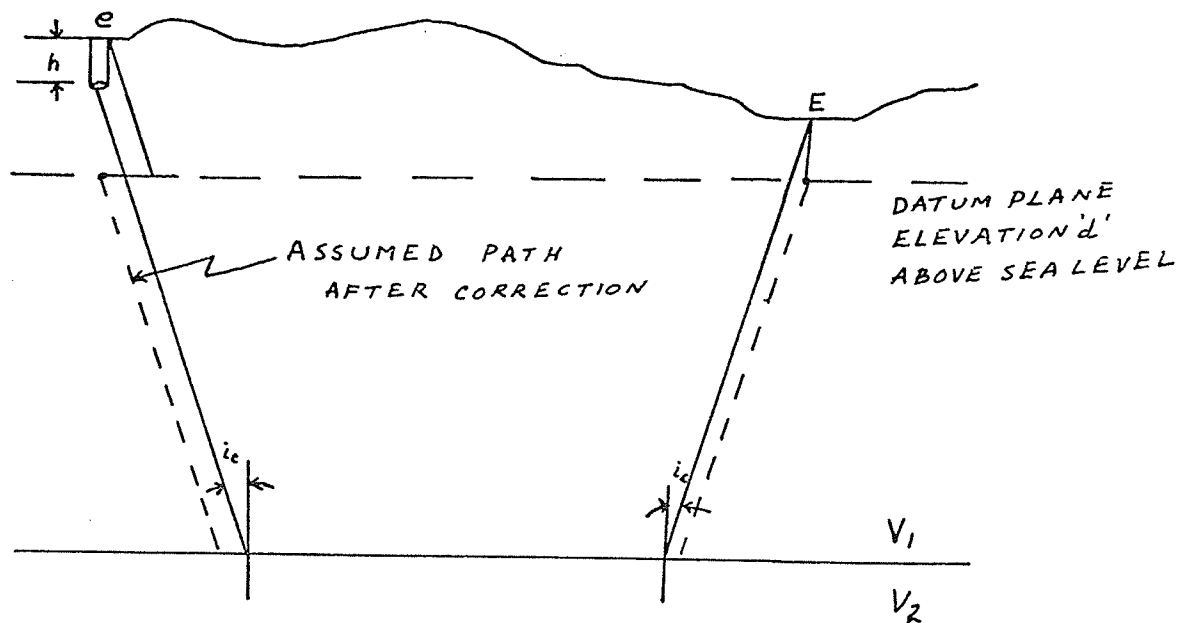
$$D_u = x_u \cdot \frac{1 - \sin(i_c - \alpha)}{2 \cos \alpha \cos i_c}$$

and

$$D_d = x_d \cdot \frac{1 - \sin(i_c + \alpha)}{2 \cos \alpha \cos i_c}$$

Elevation Corrections

A common procedure is to put both the shot and the detector on the same imaginary datum plane by subtracting the times that would be required for the wave to travel from the datum to the actual shot or detector locations if the latter are higher than the datum, or by adding the times that would be required if they are lower. Figure 7 demonstrates how this is done. At the shot end the delay time associated with the layer between the bottom of the



'e' is shot elevation

'E' is detector elevation above sea level.

Fig. 7. Elevation correction

shot at elevation $(e - h)$ and the datum plane at elevation 'd' is

$$D_s = \frac{(e - h - d) \cos i_c}{V_1} = \frac{(e - h - d) \sqrt{V_2^2 - V_1^2}}{V_1 V_2}$$

At the detector end, where the elevation is E , the delay time associated with the path from the surface to the datum is

$$D_d = \frac{(E - d) \sqrt{V_2^2 - V_1^2}}{V_1 V_2}$$

The sum of these corrections in delay time should be subtracted from the observed intercept time in order to place both the shot and detector effectively on the datum plane. Thus, the final elevation correction to be applied to the intercept time is

$$\frac{(e - h + E - 2d) \sqrt{V_2^2 - V_1^2}}{V_1 V_2}$$

CHAPTER III

FIELD RESULTS

Broomhill Experimental Aquifer, Melita

Geology of the Area

The experimental aquifer is located between Bede and Broomhill, approximately seven miles north of Melita in southwestern Manitoba (Fig. 8). The hydrogeology of the aquifer is studied by Bhaktiari (1971) and the geology of the area is described in Groundwater Availability Studies Report No. 1 (1968).

The area investigated is underlain by shale of the Riding Mountain formation. The thickness of the Riding Mountain formation in southwestern Manitoba is about 1,100 ft. The thickness of the superficial deposit (mainly till) varies from 200-300 ft. Thin beds of sand and gravel are interbedded in the till at various depths but appear to be more common in a zone approximately 70 to 100 ft. below ground level. Overlying the till is an outwash delta deposit which mainly consists of gravel and coarse sand. The outwash deposit is somewhat stratified and varies in thickness from 5 to 50 feet in the study area.

For hydrogeological purposes the geological contact

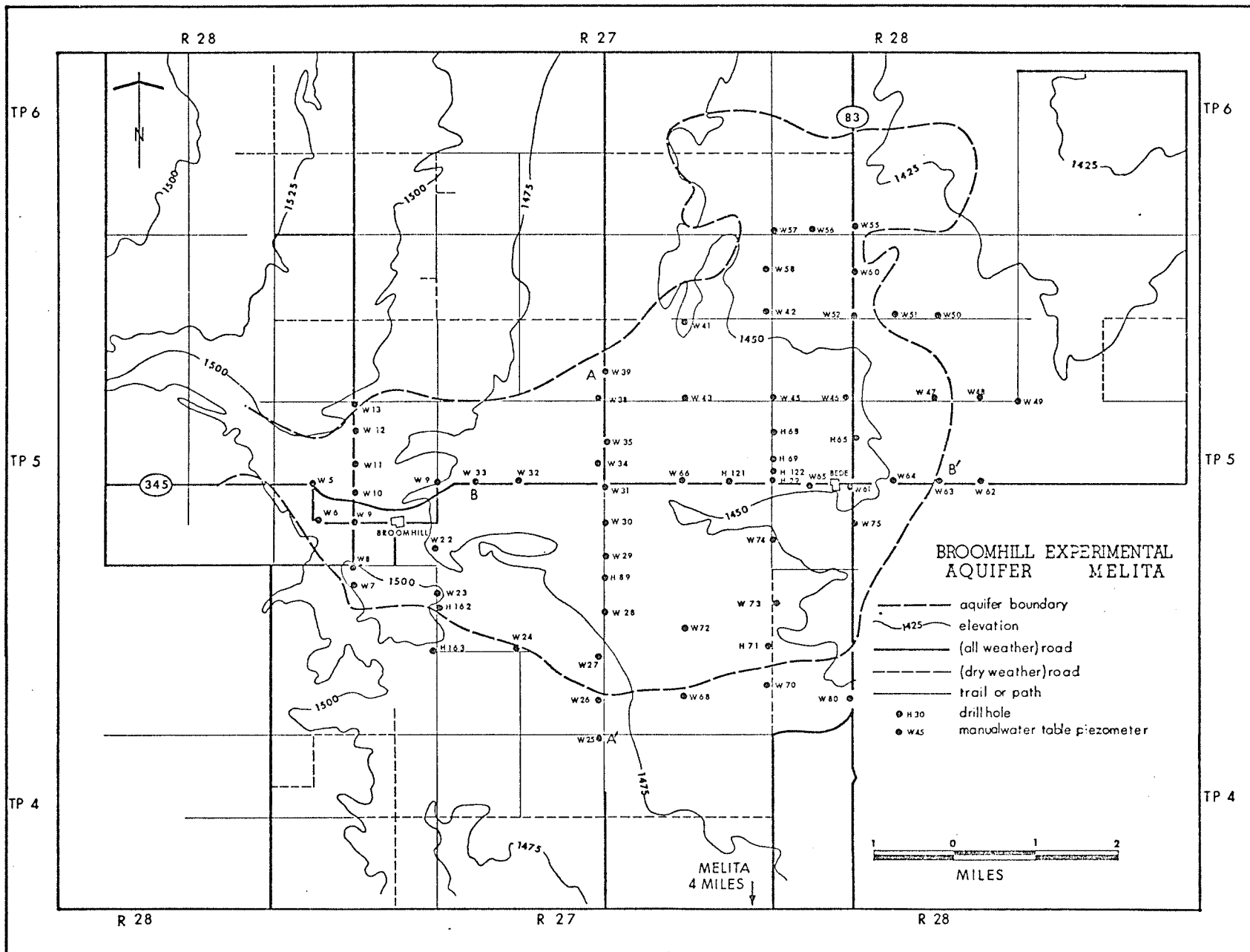


Fig. 8. Some of the piezometer and drill hole locations.

of interest is the outwash till interface in the study area.

Resistivity Results

The location of the resistivity soundings with identification numbers are shown in Fig. 9. Most of the soundings are located at test-well or test-hole sites where the depth to the till interface is known. Thirty-four soundings were done in this area.

The best fits to the data are obtained using Mooney and Wetzel four-layer curves. There is a deviation in apparent resistivity values from the theoretical curve at longer electrode separations ($a \geq 150$ ft.) on almost all the curves selected. Five layer master curves for small resistivity contrasts would be necessary to completely interpret the data and these are not available. Two typical resistivity soundings for this area are shown in Figs. 10 and 11 with the interpretations obtained from master curves and the information from known geology. The fits obtained for spacing less than 150 ft. are quite reasonable and the depths calculated are in very good agreement with the available information. The depth to the outwash-till interface are given in Fig. 12 along with the known depths. The depth to all the layers encountered and their resistivity values are given in Table I.

All the resistivity values encountered in the first layer are less than 200 ohm.m. with nearly 50 percent of the

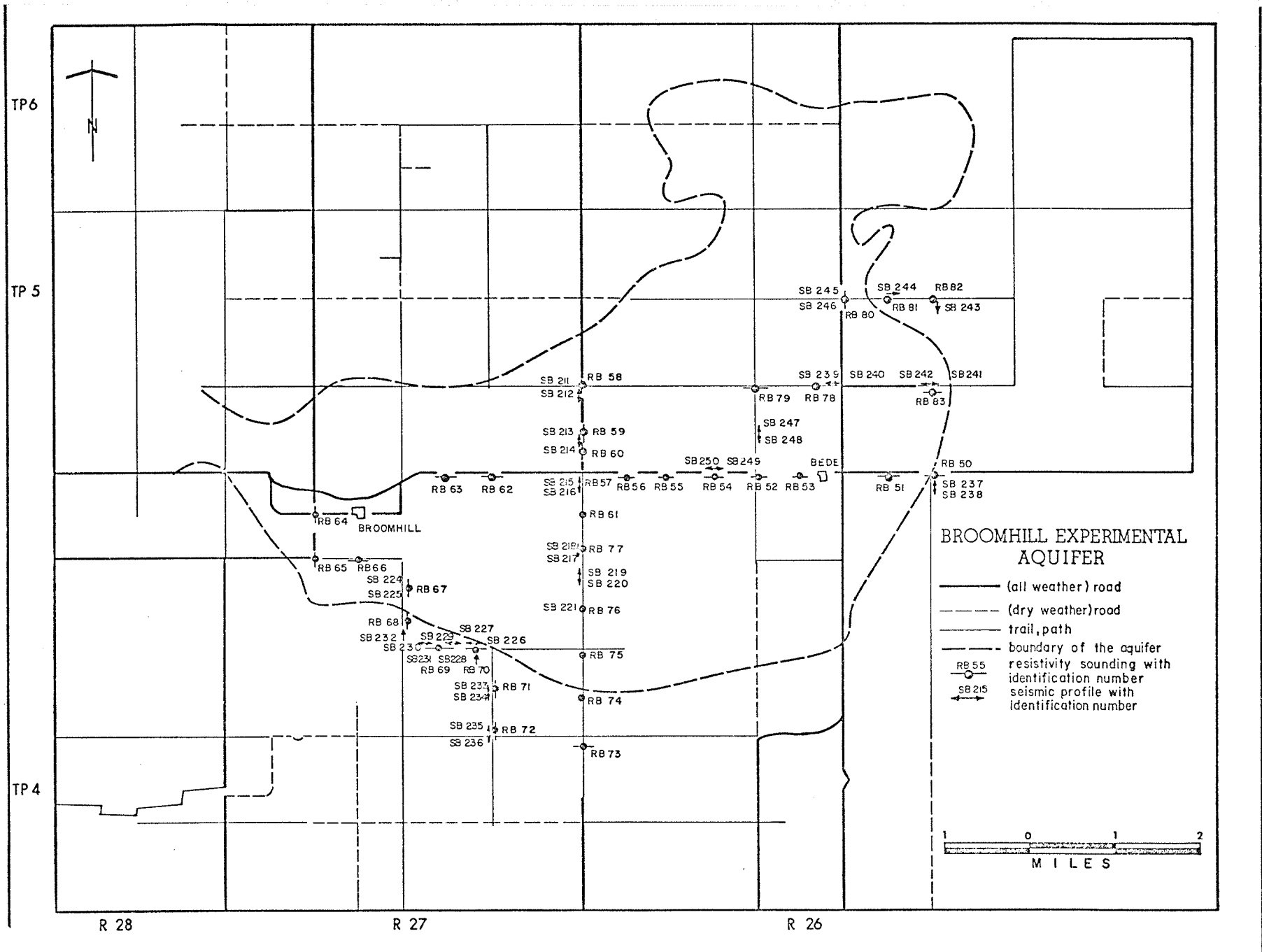


Fig. 9. Map showing resistivity sounding-seismic profile locations.

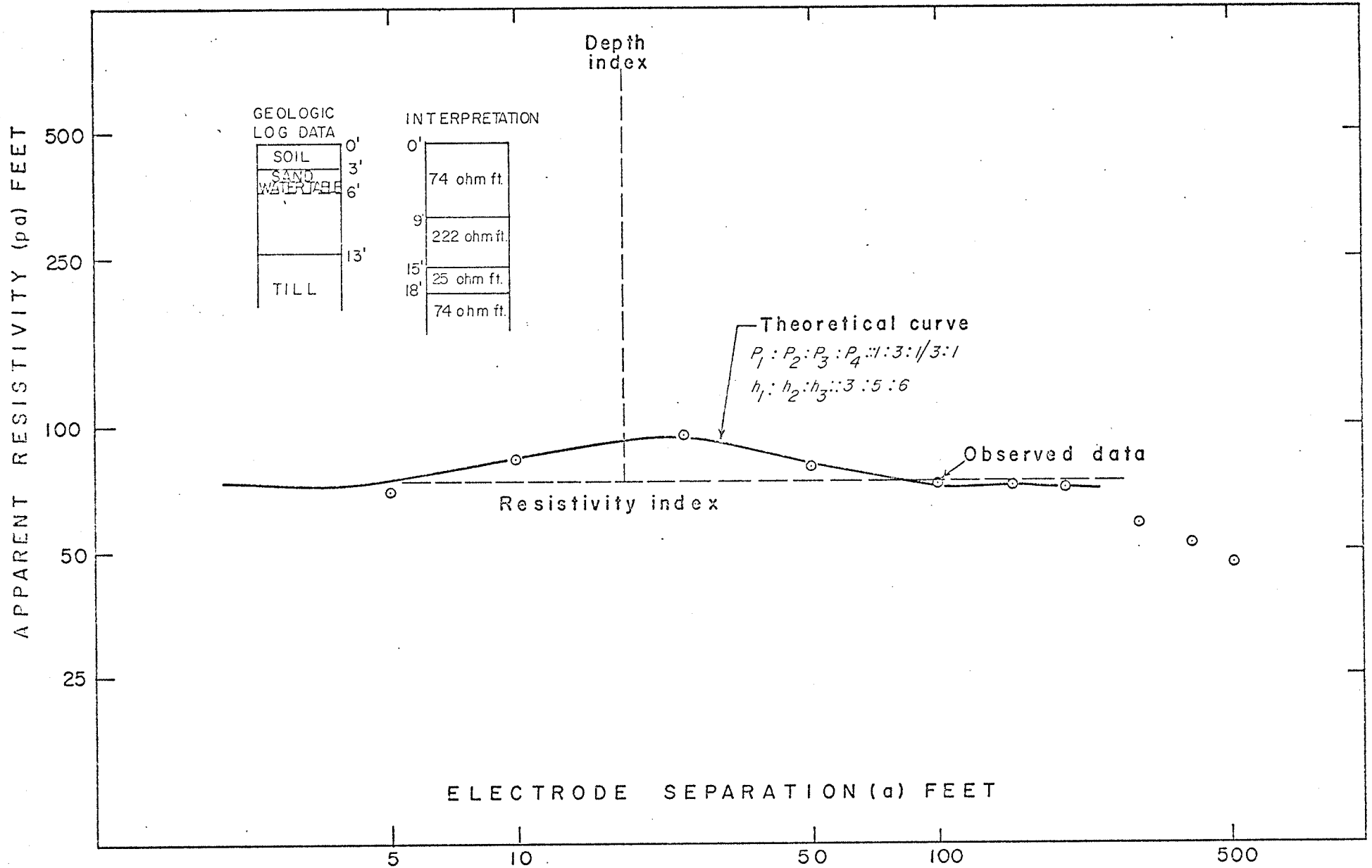


Fig. 10. Resistivity sounding #65, near well 8, curve matching method, Broomhill Experimental Aquifer, Melita.

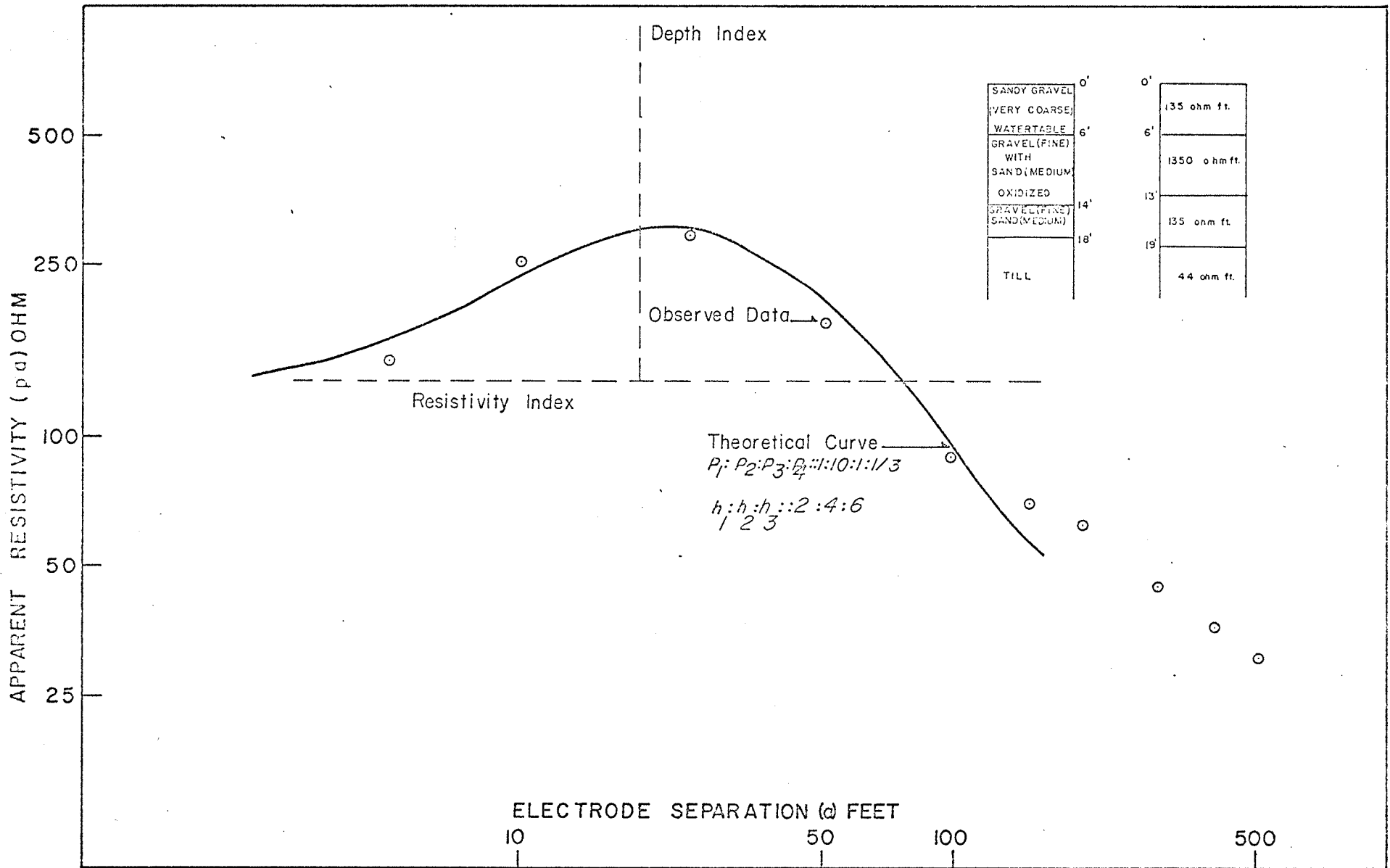


Fig. 11. Resistivity sounding #79, near well 45, curve matching method, Broomhill Experimental Aquifer, Melita.

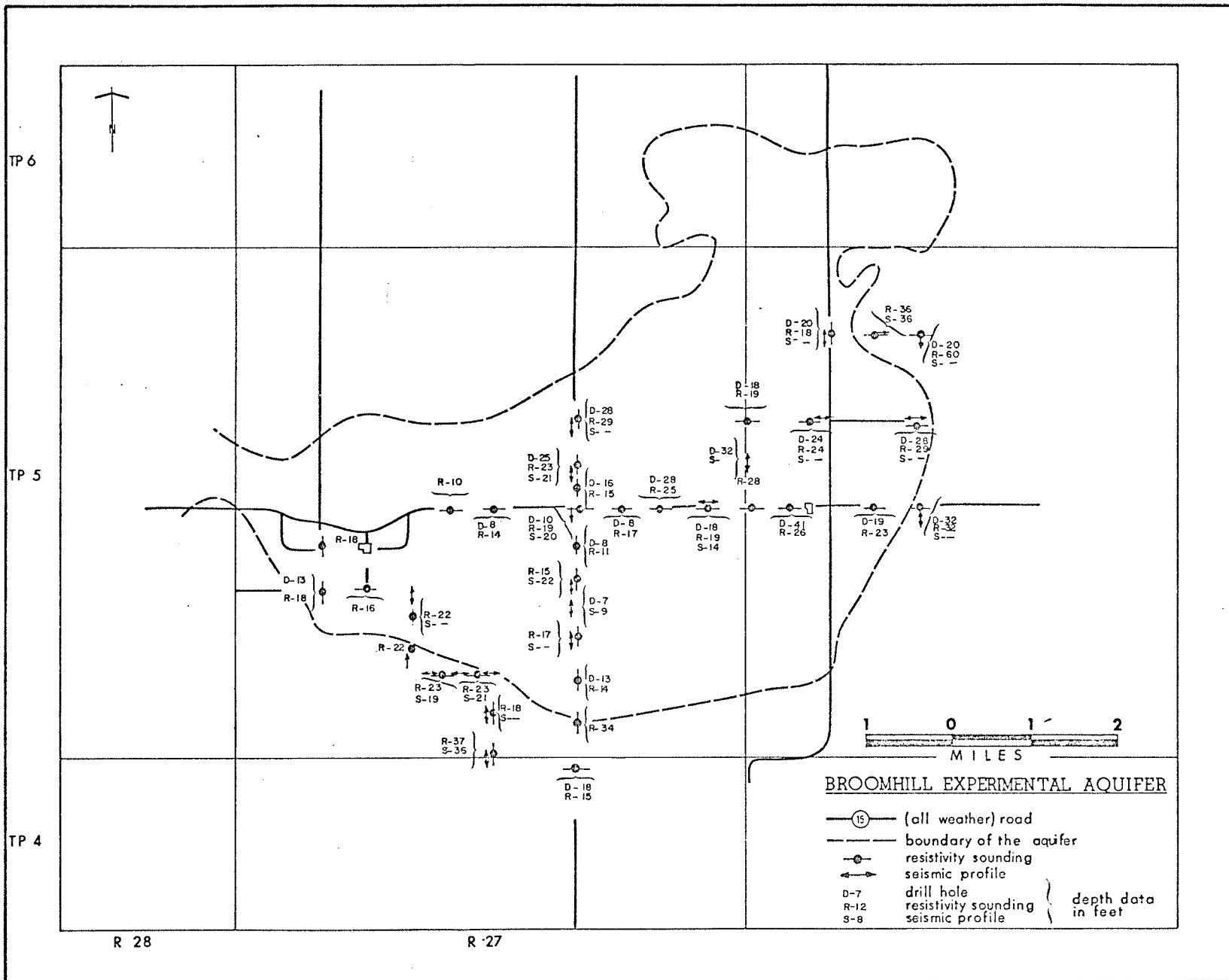


Fig. 12. Map showing depth to till layer.

Table I

Resistivity and Depth Values from Curve Matching Method

<u>Sounding Number</u>	<u>Location</u>	ρ_1 (ohm.m.)	ρ_2 (ohm.m.)	ρ_3 (ohm.m.)	ρ_4 (ohm.m.)	h_1 (ft)	h_2 (ft)	h_3 (ft)
50	At Well 63	45.7	457.0	45.7	4.6	10	16	32
51	At Well 64	56.3	563.0	56.3	18.9	12	16	23
52	At Hole 29	57.9	579.0	57.9	19.2	10	14	28
53	At Well 65	64.0	640.0	64.0	21.3	4	8	26
54	At Hole 121	71.6	214.7	71.6	22.8	6	12	19
55	At Well 66	60.9	609.0	60.9	20.4	4	8	25
56	At Hole 131	70.0	23.3	210.0	23.3	5	8	17
57	At Well 31	51.8	155.3	51.8	17.4	7	10	19
58	At Well 38	64.0	191.9	64.0	21.3	5	24	29
59	At Well 35	68.5	685.0	22.8	6.9	4	15	23
60	At Well 34	64.0	639.6	6.4	21.3	5	10	15
61	At Well 30	176.7	530.0	1.8	17.7	4	9	11
62	At Well 32	79.2	792.0	79.2	26.5	2	7	14
63	At Well 33	38.0	380.0	0.3	380.0	2	10	12
64	At Well 9	134.0	402.0	1.2	44.8	3	12	18
65	At Well 8	22.5	67.6	7.6	22.5	9	15	18
66	Between Well 8 & Hole 161	23.8	71.5	7.9	23.8	3	14	16
67	At Well 23	195.0	585.0	1949.0	19.5	4	7	22

<u>Sounding Number</u>	<u>Location</u>	ρ_1 (ohm.m.)	ρ_2 (ohm.m.)	ρ_3 (ohm.m.)	ρ_4 (ohm.m.)	h_1 (ft)	h_2 (ft)	h_3 (ft)
68	Between Hole 163 & Hole 162	173.6	521.0	1.8	17.4	4	19	22
69	Between Hole 163 & Well 24	128.0	42.6	12.8	42.6	16	23	46
70	Near Well 24	80.7	242.0	8.2	26.8	12	15	23
71	0.5 mile from Well 24 towards south	74.6	25.0	74.6	7.6	18	88	105
72	1 mile from Well 24 towards south	45.7	15.2	45.7	15.2	37	92	110
73	At Well 25	39.6	396.0	0.3	39.6	7	10	15
74	At Well 26	42.6	14.3	42.6	14.3	12	17	34
75	At Well 27	58.0	579.0	5.8	19.2	9	11	14
76	At Well 28	30.5	91.4	10.0	30.5	8	17	50
77	At Well 29	94.4	944.0	9.4	31.4	5	8	15
78	Near Well 46	47.2	472.0	47.2	15.8	4	12	24
79	At Well 45	41.1	411.0	41.1	13.4	6	13	19
80	At Well 52	74.6	746.0	74.6	25.3	9	12	18
81	At Well 51	134.0	44.8	134.0	13.4	6	12	36
82	At Well 50	27.4	82.2	9.1	27.4	10	20	60
83	At Well 47	45.7	457.0	45.7	15.2	10	15	29

ρ_1 = resistivity of the first layer
 ρ_2 = resistivity of the second layer
 ρ_3 = resistivity of the third layer
 ρ_4 = resistivity of the fourth layer

h_1 = depth to the second layer
 h_2 = depth to the third layer
 h_3 = depth to the fourth layer

values being in the range 50 to 100 ohm.m. This may be correlated to the top sandy soil layer. The resistivity values obtained from the second layer are scattered from 0 to 950 ohm.m., with nearly 50 percent of the values being in the range 350 to 650 ohm.m. The high resistivity values obtained may be correlated with sand and gravel deposits. The scattering of the resistivity values likely are a representation of inhomogeneities, such as variation in permeability, variation in grain size, or inclusion of other materials. The third layer resistivities are between 0 and 250 ohm.m. with 90 percent of the values being below 100 ohm.m. The low resistivity values obtained here are likely due to the presence of water table in some cases and due to the occurrence of till in other cases. The water table in some instances is in the second layer. Nearly 95 percent of the resistivities for the fourth layer are below 50 ohm.m. These can be correlated with the till layer. A normalized histogram of resistivities encountered for each layer is given in Fig. 13.

All the resistivity soundings are interpreted using the inverse slope method. The resistivity and depth values are given in Table II. An example of this method is shown in Fig. 14. In this method a layer with resistivity values in the range of 5 to 12 ohm.m. is encountered at depths ranging from 200 to 350 ft. below the ground level. The resistivity values obtained are consistent with the values

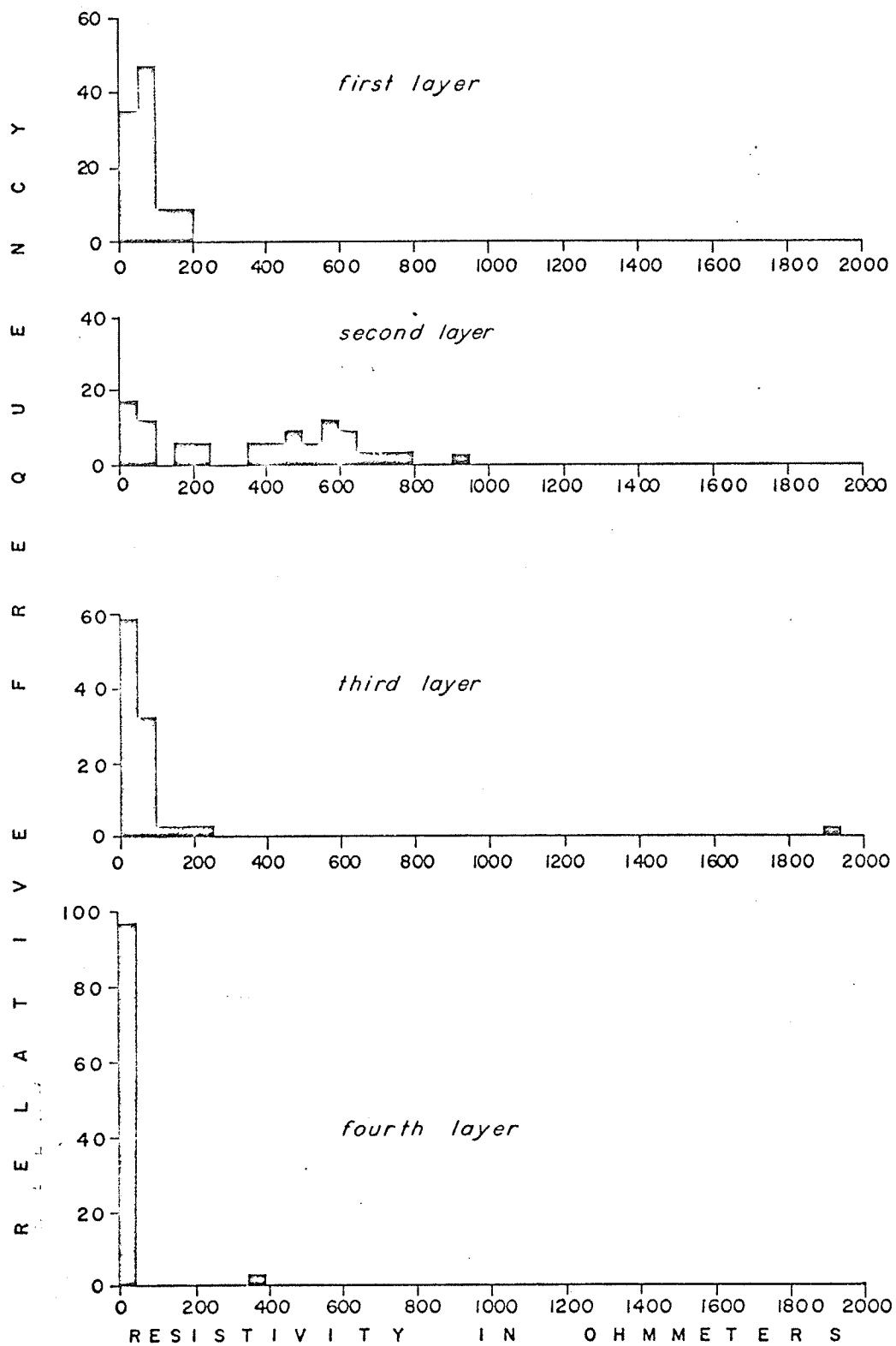


Fig. 13. Broomhill Experimental Aquifer, Melita, histogram of resistivities.

Table II

Resistivity and Depth Values from Inverse Slope Method, Broomhill Experimental Aquifer, Melita

<u>Sounding Number</u>	<u>Location</u>	ρ_1 (ohm.m.)	ρ_2 (ohm.m.)	ρ_3 (ohm.m.)	ρ_4 (ohm.m.)	h_1 (ft)	h_2 (ft)	h_3 (ft)
50	At Well 63	41.7	29.2	7.3	-	41	126	-
51	At Well 64	89.6	53.9	11.0	5.8	23	81	243
52	At Hole 29	160.0	67.0	14.0	6.0	20	77	252
53	At Well 65	137.0	53.3	11.6	5.8	22	72	272
54	At Hole 121	172.1	32.6	13.4	6.7	23	66	268
55	At Well 66	152.3	42.6	13.7	7.0	25	62	285
56	At Hole 131	106.6	34.1	13.7	7.0	17	78	277
57	At Well 31	65.5	18.0	7.6	-	24	242	-
58	At Well 38	124.9	64.0	13.1	7.0	25	70	278
59	At Well 35	222.4	95.0	11.9	6.7	25	67	349
60	At Well 34	195.0	38.7	12.5	6.7	23	70	345
61	At Well 30	152.3	18.0	6.7	-	23	241	-
62	At Well 32	1066.1	35.3	11.9	7.9	22	81	380
63	At Well 33	209.6	32.0	15.2	7.6	23	68	276
64	At Well 9	121.8	44.5	15.5	7.9	27	51	283
65	At Well 8	36.6	21.0	11.3	-	26	240	-
66	Between Well 8 & Hole 161	64.6	25.0	16.4	-	18	369	-
67	At Well 23	533.0	97.5	12.8	-	48	124	-

<u>Sounding Number</u>	<u>Location</u>	ρ_1 (ohm.m.)	ρ_2 (ohm.m.)	ρ_3 (ohm.m.)	ρ_4 (ohm.m.)	h_1 (ft)	h_2 (ft)	h_3 (ft)
68	Between Hole 163 & Hole 162	103.0	12.8	5.2	-	67	288	-
69	Between Hole 163 & Hole 24	155.3	20.7	14.1	5.5	22	78	264
70	Near Well 24	99.3	17.4	9.1				
71	Half mile south of Well 24	79.8	25.9	14.3	8.8	20	73	217
72	One mile south of Well 24	42.9	16.1	8.2	-	46	240	-
73	At Well 25	57.0	25.9	13.7	6.7	20	72	298
74	At Well 26	28.3	20.4	14.3	7.0	23	108	273
75	At Well 27	72.2	14.3	7.0	-	38	278	-
76	At Well 28	33.2	17.3	7.6	-	33	225	
77	At Well 29	134.0	22.8	15.1	7.6	22	58	257
78	Near Well 46	152.3	54.8	11.9	6.1	21	76	260
79	At Well 45	121.8	40.8	14.3	6.4	23	69	248
80	At Well 52	127.9	56.7	12.8	6.1	23	82	252
81	At Well 51	131.0	53.9	12.5	6.1	19	80	244
82	At Well 50	34.1	15.8	5.8	-	39	243	
83	At Well 47	112.7	49.6	12.2	5.8	26	77	227

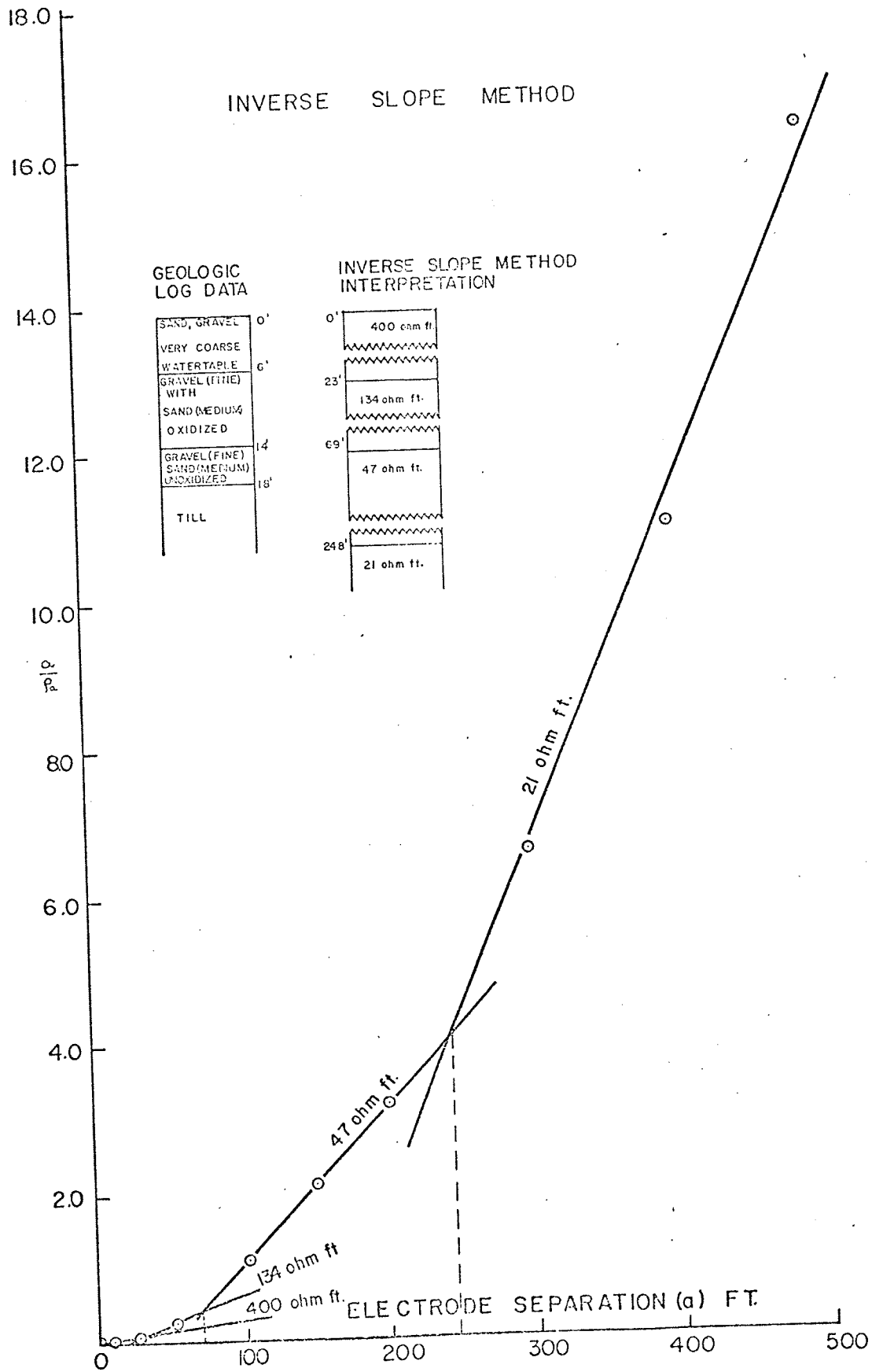


Fig. 14. Resistivity sounding #79 near well 45, Broomhill Experimental Watershed, Melita Inverse slope method

expected for shales (Meidav, 1960). It is known that the bedrock is shale and lies between 200 to 300 ft. below ground level (Groundwater Availability Studies Report No. 1, p. 5). The curve matching method, though indicating a change in resistivity at these depths, could not give the exact depth or resistivity value. The thickness of the first layer obtained from the inverse slope method is in reasonable agreement with the depth to known outwash-till interface. In nearly 70 percent of the cases there exists another layer at about 50 to 100 ft. The resistivity of this layer is in the range of 10 to 15 ohm.m., which is slightly lower than the till resistivity encountered in the layer above and slightly higher than the resistivities encountered for shale below this layer. The slightly lower resistivity layer encountered within the till may be due to the end of the saturated zone in the till, or may be due to changes in composition within the till. Two cross-sections AA' and BB' indicated in Fig. 9 are given in Figs. 15 and 16, respectively. The layers interpreted using the curve matching method along with the known information from drill holes and test wells are represented on these figures. Bedrock depths obtained from inverse slope method are also given along with the resistivity values.

Moore's cumulative method was also tried for all the soundings but only depth values can be obtained in this method. An example of this method is given in Fig. 17 for

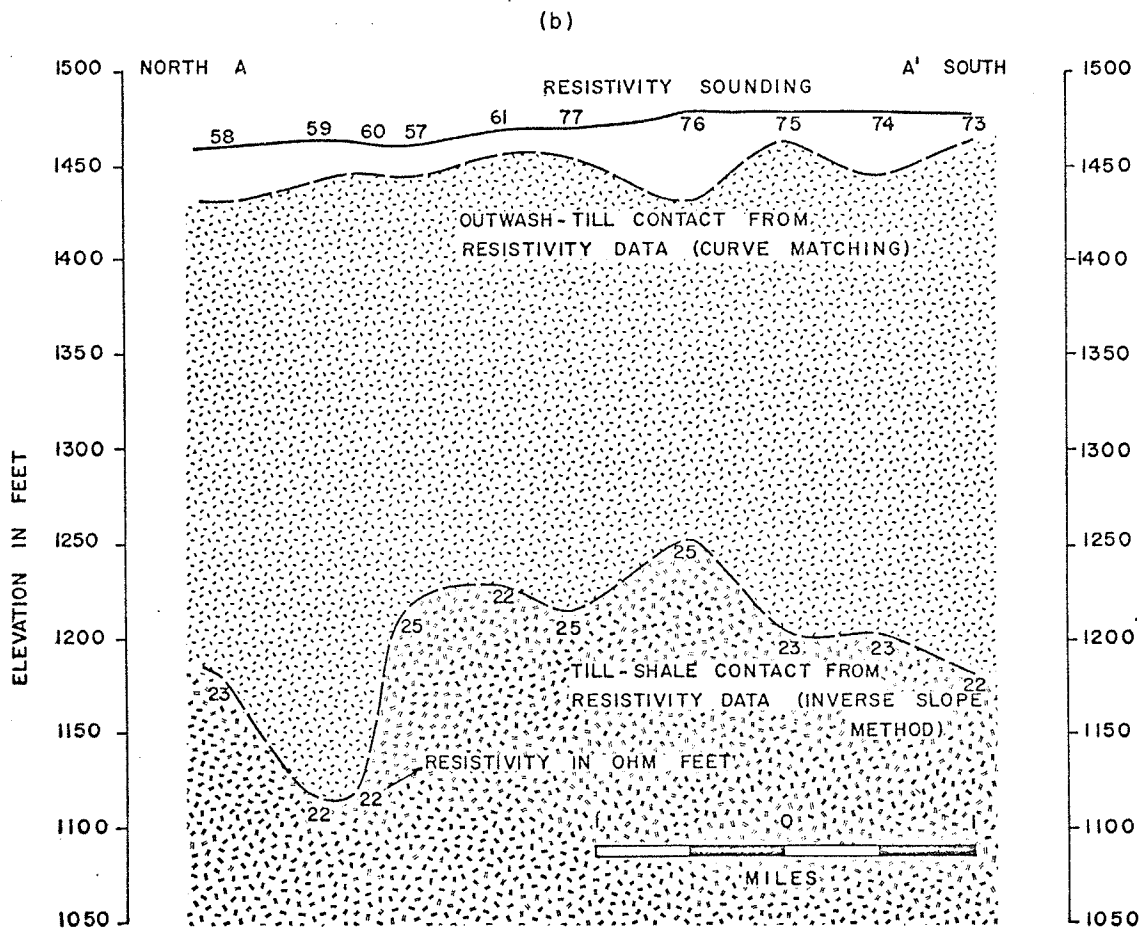
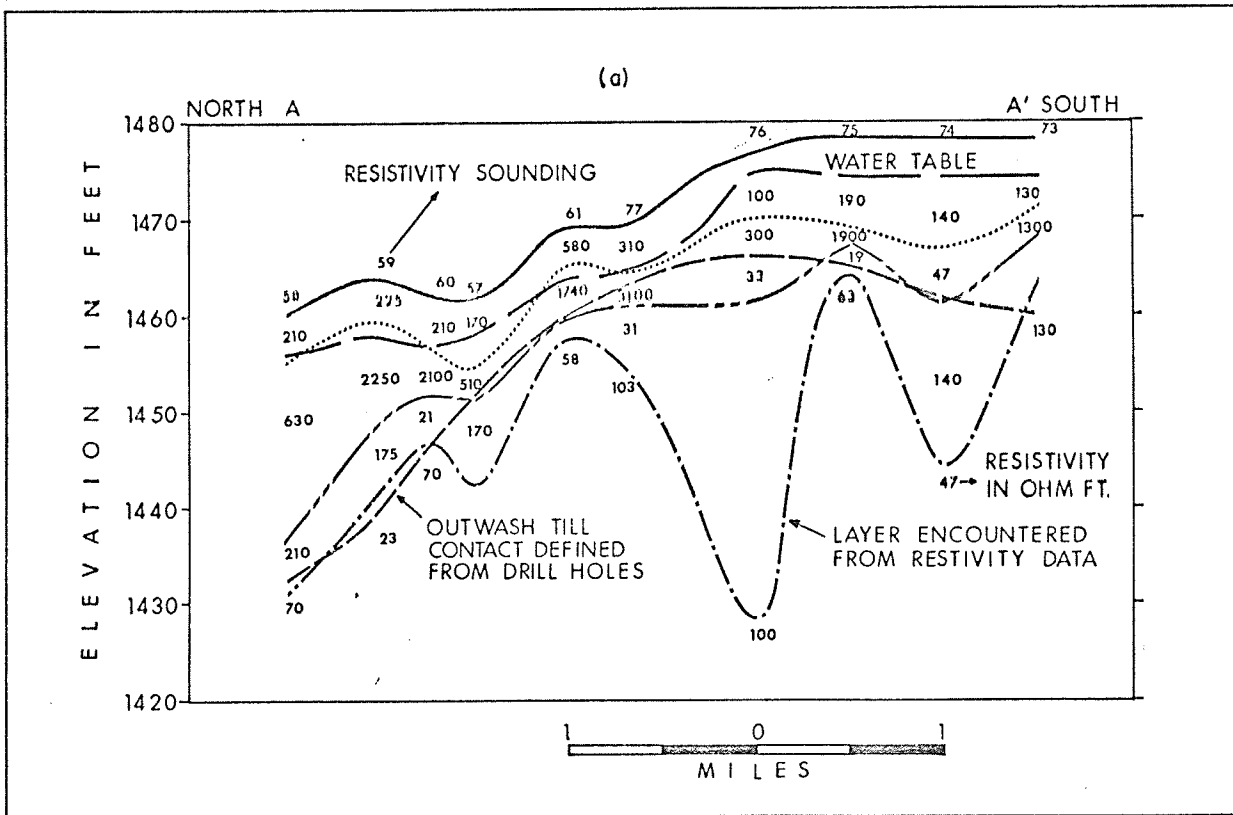


Fig. 15. Cross section AA'
 (a) interpretation from curve matching method
 geologic log data also shown
 (b) outwash-till-shale contacts from
 resistivity data.
 Broomhill Experimental Aquifer, Melita

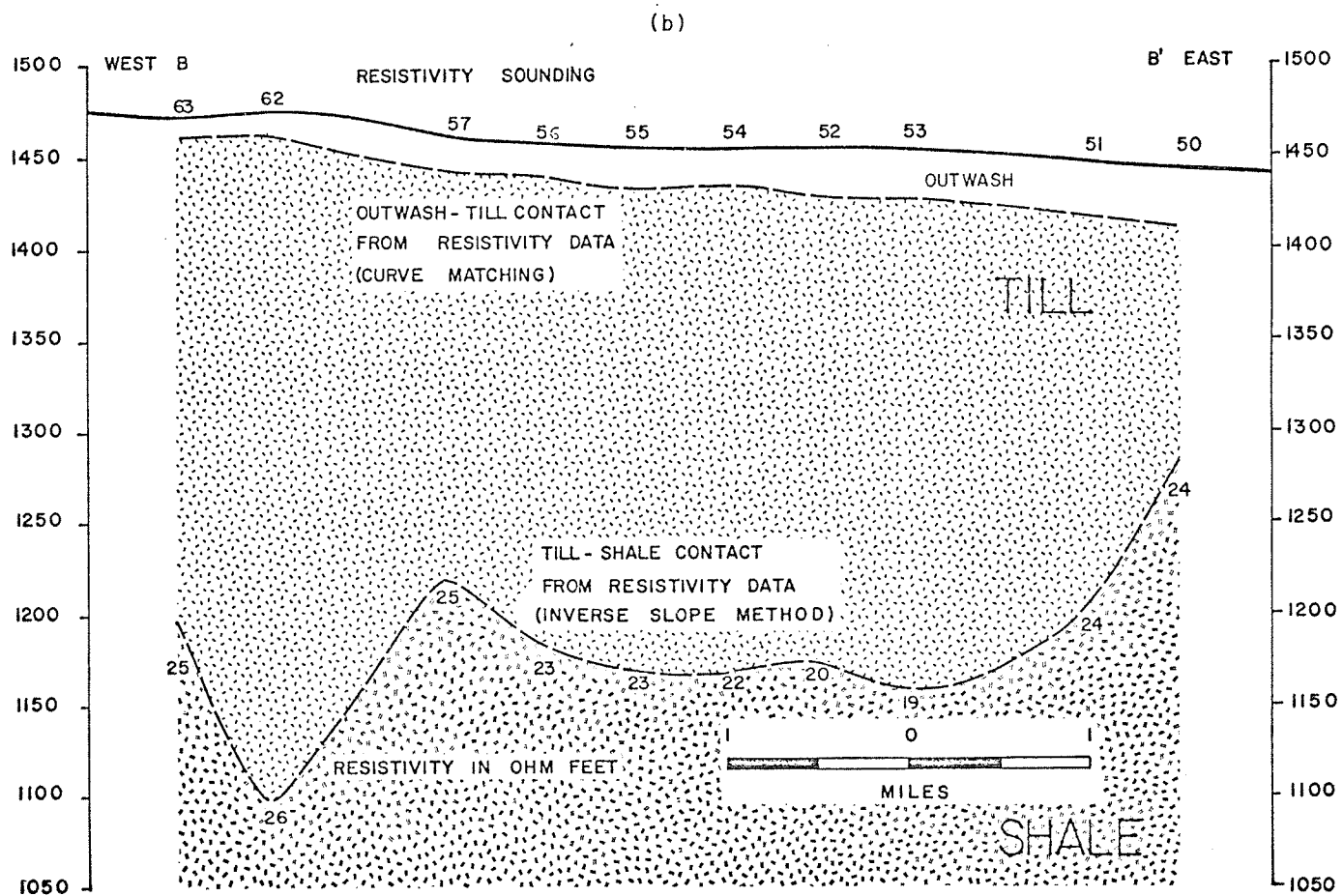
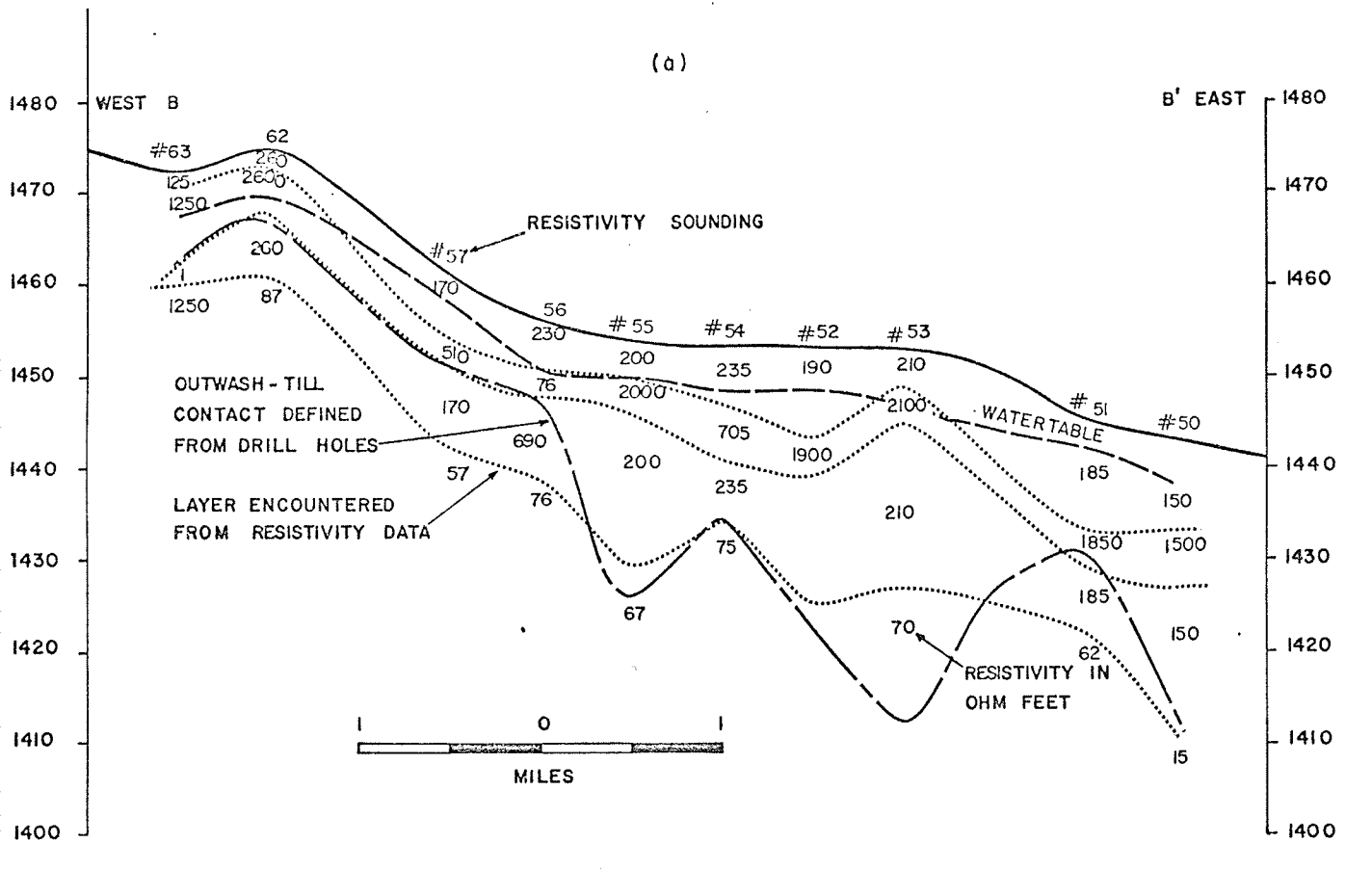


Fig. 16. Cross Section BB'

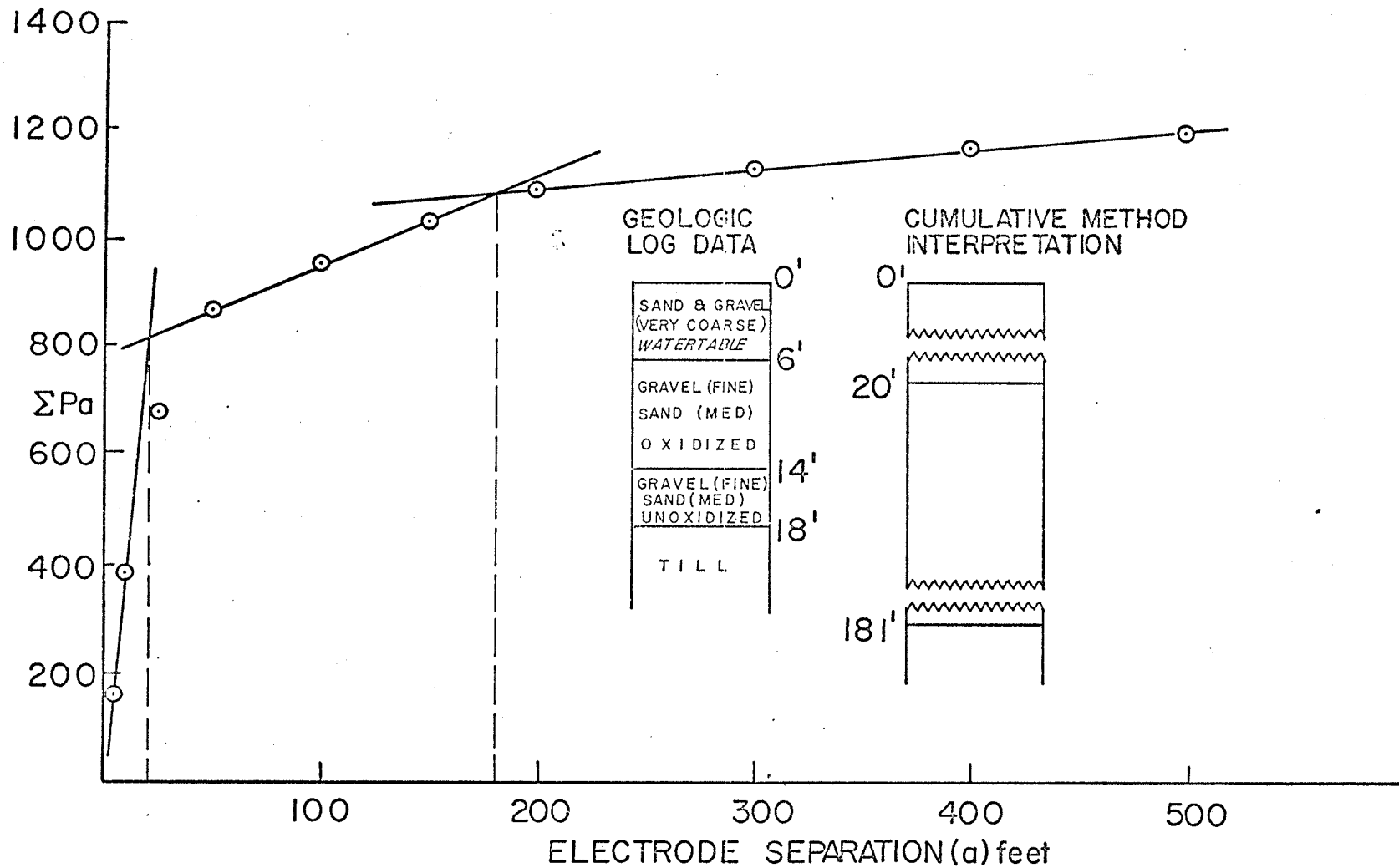


Fig. 17. Resistivity sounding #79, near well 45, cumulative method, Broomhill Experimental Aquifer, Melita.

the same sounding given in the inverse slope method example. The first layer thickness obtained in this method is in good agreement with the known depth to the top of the till layer. The bedrock depths calculated from this method are 3 to 50 percent (on the average 15 percent) less than those calculated from the inverse slope method. The depths obtained from this method are given in Table III.

Tagg's method was tried for six soundings in this area. All the six soundings are treated as two layer cases. The resistivity and depth values obtained are given in Table IV. The depths calculated are in good agreement with the known depth to the top of the till layer.

Seismic Results

Twenty reversed profiles were done in this area and their locations and identification numbers are shown in Fig. 9. In general, the profiles are situated at test-well or drill hole locations.

The depth determinations are carried out using time-distance plots. The time-distance plots obtained in this area are of two types, one with two segments and the other with three segments. In all the cases the top layer velocities are ranging from 900 to 1,500 ft./sec. A segment with velocity range 5,500 to 6,500 ft./sec. is present in all the time-distance plots, except in two in which 8,600 ft./sec. was obtained. In the case of three segment plots

Table III

Depth Values from Cumulative Method
Broomhill Experimental Aquifer, Melita

<u>Sounding Number</u>	<u>Location</u>	<u>h₁ (ft)</u>	<u>h₂ (ft)</u>	<u>h₃ (ft)</u>
50	At Well 63	14	37	175
51	At Well 64	14	57	205
52	At Hole 29	23	208	
53	At Well 65	12	54	210
54	At Hole 121	17	193	
55	At Well 66	10	32	208
56	At Hole 131	13	57	200
57	At Well 31	15	194	
58	At Well 38	31	217	
59	At Well 35	28	198	
60	At Well 34	17	210	
61	At Well 30	12	205	
62	At Well 32	13	177	
63	At Well 33	14	185	
64	At Well 9	15	182	
65	At Well 8	16	206	
66	Between Well 8 and Hole 161	17	187	
67	At Well 23	22	120	

<u>Sounding Number</u>	<u>Location</u>	<u>h₁ (ft)</u>	<u>h₂ (ft)</u>	<u>h₃ (ft)</u>
68	Between Hole 163 and Hole 162	17	182	
69	Between Hole 163 and Well 24	14	196	
70	Near Well 24	15	188	
71	Half mile south of Well 24	15	213	
72	One mile south of Well 24	17	183	
73	At Well 25	18	213	
74	At Well 26	16	210	
75	At Well 27	16	206	
76	At Well 28	12	44	185
77	At Well 29	10	48	197
78	Near Well 46	27	173	
79	At Well 45	20	181	
80	At Well 52	19	207	
81	At Well 51	13	57	206
82	At Well 50	18	217	
83	At Well 47	30	180	

Table IV

Resistivity and Depth Values from Tagg's Method,
Broomhill Experimental Aquifer, Melita

<u>Sounding Number</u>	<u>Location</u>	ρ_1 (ohm.m.)	ρ_2 (ohm.m.)	h_1 (ft)
53	At Well 65	139.2	18.0	34
62	At Well 32	246.7	35.0	19
64	At Well 9	242.2	27.0	21
66	Between Well 8 and Hole 161	44.8	21.6	23
69	Between Hole 163 and Well 24	123.4	17.7	19
71	0.5 mile from Well 24 towards south	71.9	27.4	17

a layer with velocities 3,500 to 5,000 ft./sec. is present in between the two above mentioned segments. A normalized histogram of velocities for this area is given in Fig. 18.

Whenever the time distance plot contains three segments the depths calculated are in reasonable agreement with the known information. When the time distance plot contains only two segments the calculated depths are not correlating with the known depths to till layer. The calculated depths along with the velocities are given in Table V. The depths calculated for three layer cases are shown in Fig. 12 along with the resistivity results and known geologic information.

The velocity range 900 to 1,500 ft./sec. obtained for the top layer may be correlated with the velocities of top sandy soil or loam. The velocity range 5,500 to 6,500 ft./sec. is high for dry sand and gravel (Lennox and Carlson, 1967) and low for semiconsolidated or consolidated till, (Hobson, 1964). An increase of moisture content in unconsolidated sediments gives rise to an increase in seismic velocities (Heiland, p. 475) and a velocity range 5,500 to 6,500 ft./sec. may be expected for saturated sand and gravel (McGinnis, 1961). This same range of velocities is likely for unconsolidated sandy till (McGinnis, 1961). Thus when saturated sand and gravel lies over unconsolidated sandy till, there may not be enough velocity contrast to delineate the two layers by seismic velocities. This seems to be the reason-

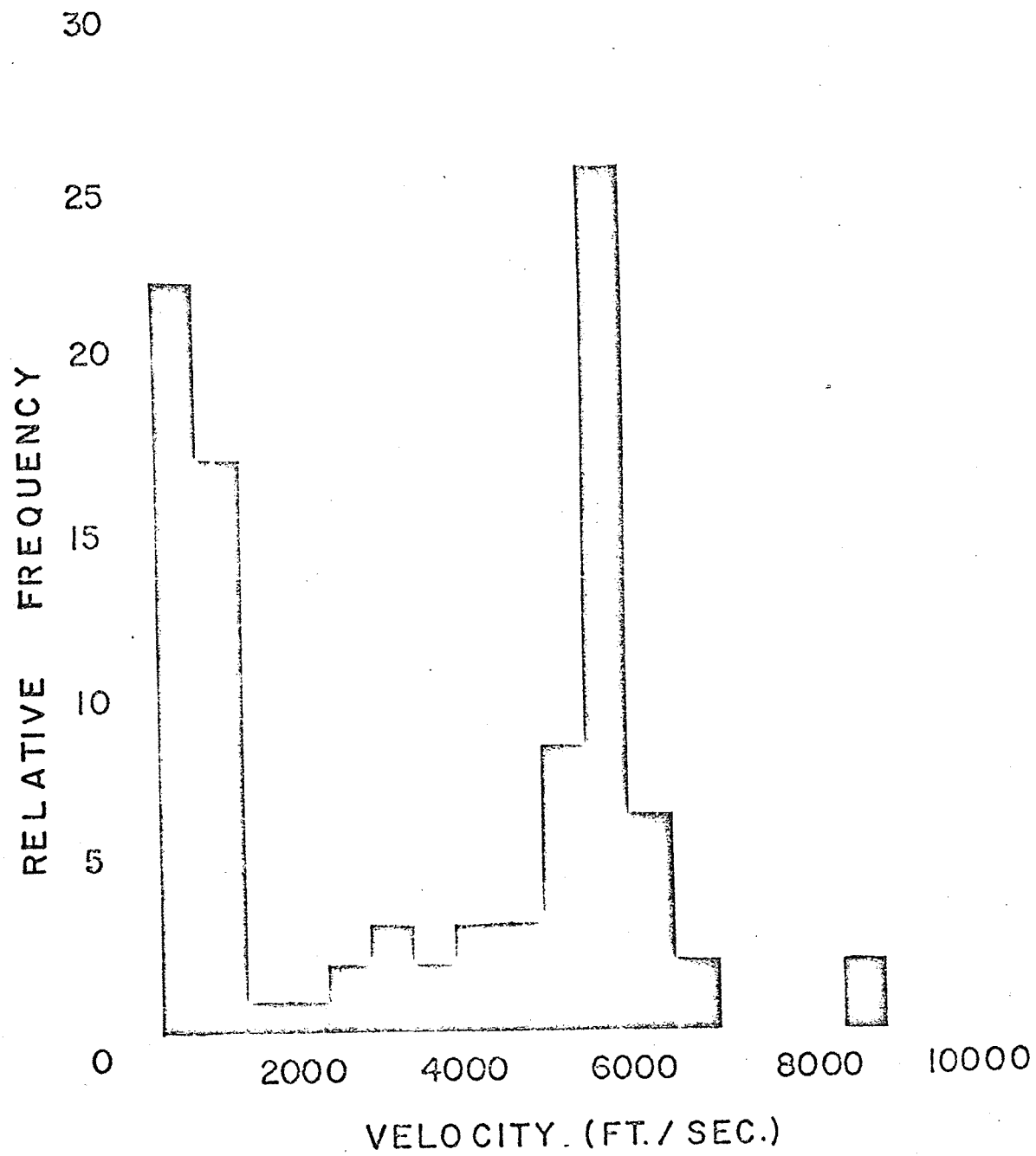


Fig. 18. Normalized histogram of velocities, Broomhill Experimental Aquifer, Melita.

Table V

Seismic Velocities and Calculated Depths, Broomhill Experimental Aquifer, Melita

<u>Seismic Profile Number</u>	<u>Velocity (V₁ in ft/sec)</u>	<u>Velocity (V₂ in ft/sec)</u>	<u>Velocity (V₃ in ft/sec)</u>	<u>h₁ (ft)</u>	<u>h₂ (ft)</u>
211	1500	4000		11	
212	900	6850		7	
213	1300	5900		10	
214	1000	3900	6100	6	21
215	1200	4100	6100	5	16
216	800	5400	7000	4	23
217	900	5100	8600	5	27
218	700	5600		4	
219	1700	5600		9	
220	1100	5500		12	
221	1450	5500		12	
222	700	5700		6	
223	700	4200	6200	5	27
224	1100	4900	5800	15	28
225	1100	5000	5600	12	30
226	1000	3400	5900	7	22
227	700	4100	5800	3	20
228	700	3500	5800	3	19

Table V

Seismic Velocities and Calculated Depths, Broomhill Experimental Aquifer, Melita

<u>Seismic Profile Number</u>	<u>Velocity (V₁ in ft/sec)</u>	<u>Velocity (V₂ in ft/sec)</u>	<u>Velocity (V₃ in ft/sec)</u>	<u>h₁ (ft)</u>	<u>h₂ (ft)</u>
211	1500	4000		11	
212	900	6850		7	
213	1300	5900		10	
214	1000	3900	6100	6	21
215	1200	4100	6100	5	16
216	800	5400	7000	4	23
217	900	5100	8600	5	27
218	700	5600		4	
219	1700	5600		9	
220	1100	5500		12	
221	1450	5500		12	
222	700	5700		6	
223	700	4200	6200	5	27
224	1100	4900	5800	15	28
225	1100	5000	5600	12	30
226	1000	3400	5900	7	22
227	700	4100	5800	3	20
228	700	3500	5800	3	19

able explanation for obtaining only two segments on the time-distance plots. The depths calculated from the data does not necessarily represent the depth to the till layer but may represent the depth to the water saturated layer. An example of this type of data is given in Fig. 19.

Where the velocity range of 3,500 to 5,000 ft./sec. is present on the time-distance plot, it may be concluded that the sand and gravel deposit at these places is not saturated or has a lower moisture content than at other locations where the deposits have a higher velocity range. An example of this type of data is given in Fig. 20. Though the seismic velocities could not be used to differentiate the outwash and till layers in this area it is interesting to note that the seismic velocities may be used to find the depth to the saturated layer and may give a qualitative idea on the moisture content.

Conclusions

The resistivity method in this area was quite successful and there is good correlation between the interpretation techniques used. The disagreement in few cases with the known information is suspected to be due to the invalidity of the approximation of a layered earth in resistivity interpretation techniques. In general the bed-rock shale resistivities in this area are between 5.5 and 9.0 ohm.m. The resistivity of the superficial deposit, till

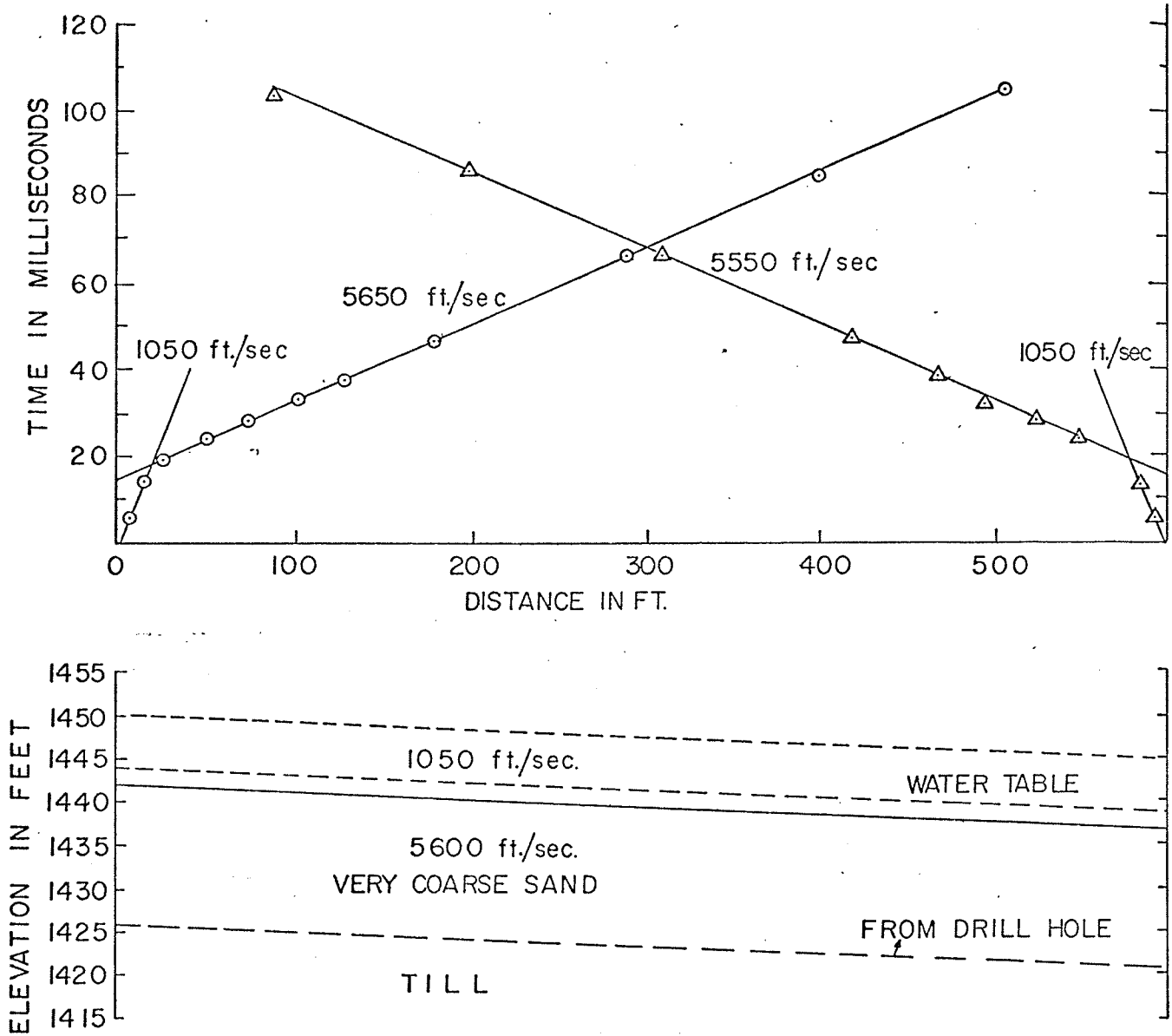


Fig. 19. Seismic profile 239-240, near well 46, drill hole information also shown Broomhill Experimental Aquifer, Melita.

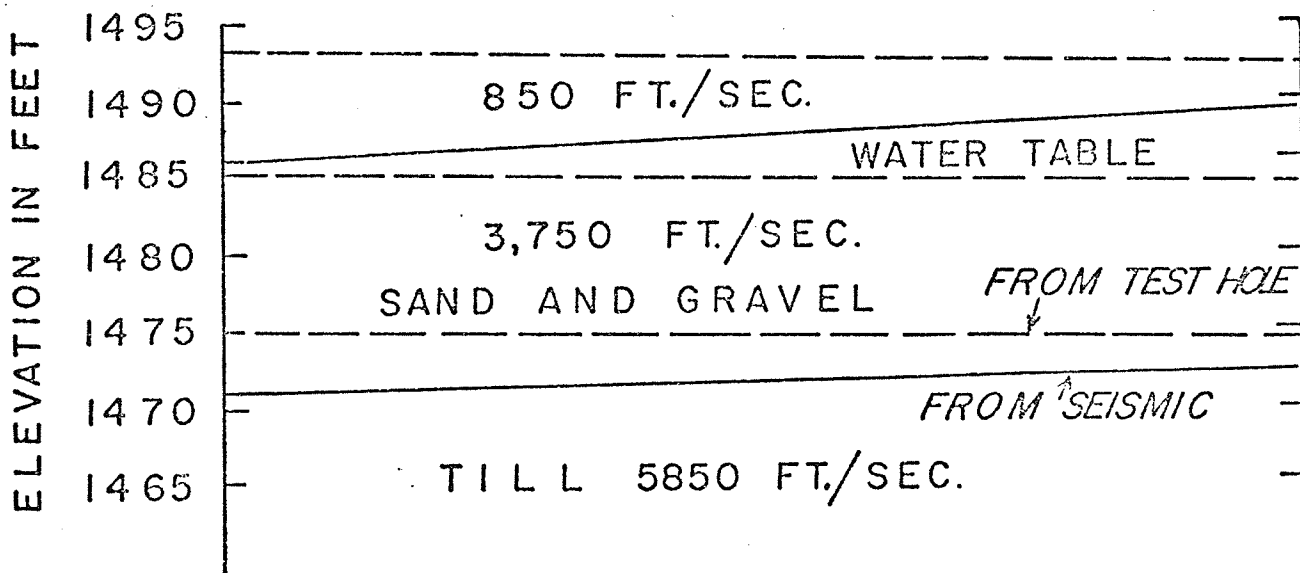
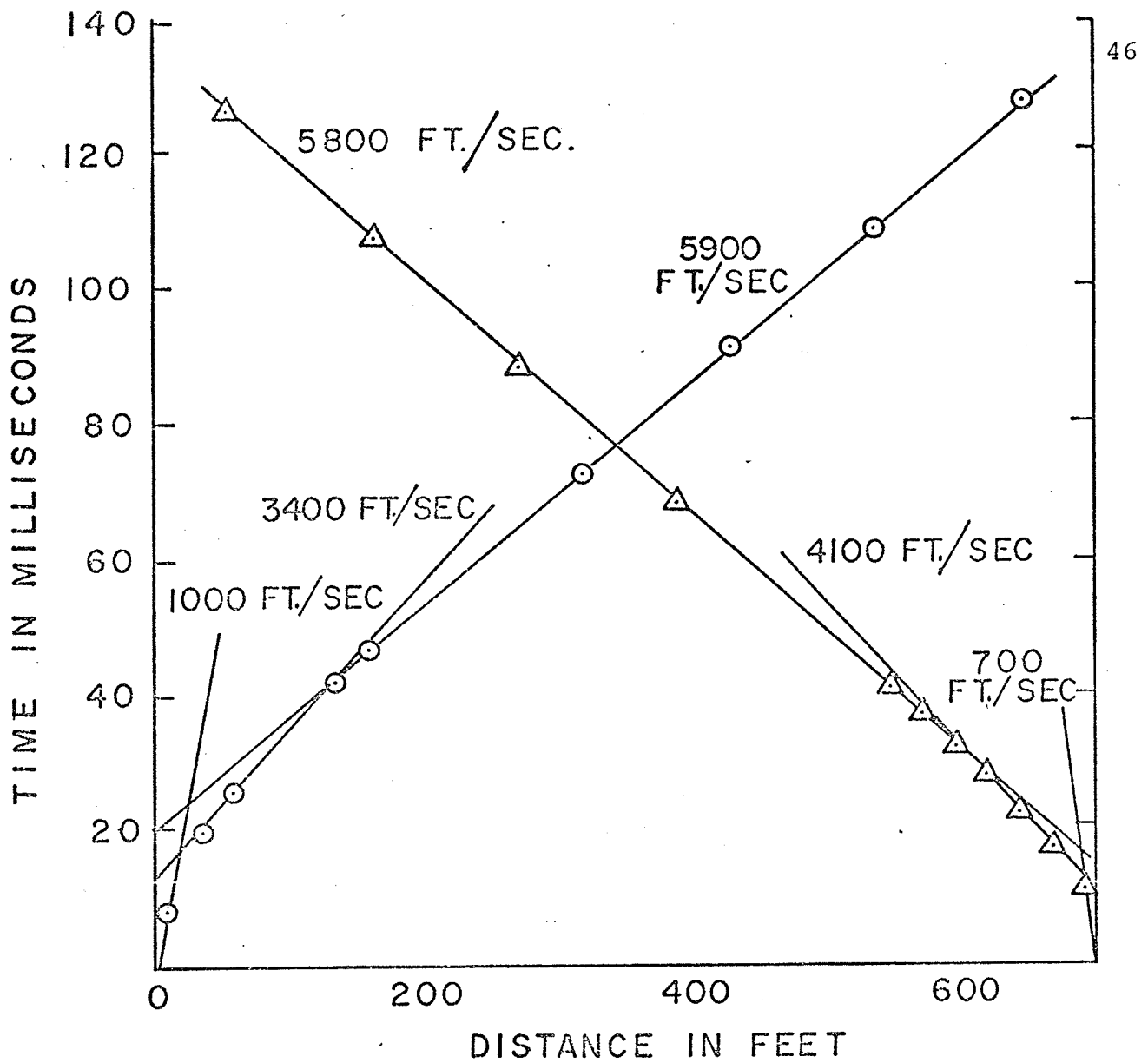


Fig. 20. Seismic profile 226-227, near well 24, Broomhill Experimental Aquifer, Melita.

is varying from 10.0 to 60.0 ohm.m. From inverse slope method interpretations, resistivity range of 10.0 to 16.0 ohm.m. is obtained for till on the average below 50 feet from the ground surface. The superficial till deposit is slightly more resistive than the bedrock shale in this area. Similar observations were quoted by (Lennox and Carlson, 1967). Resistivities as high as 1000 ohm.m. were observed for the outwash deposit of sand and gravel. The study in this area proves that the resistivity surveys are quite useful and economical to use for depth determinations where enough resistivity contrast exists.

The seismic refraction surveys in this area indicates it is not possible to find the depth to the top of the till layer due to a lack of a suitable velocity contrast between the saturated sand and gravel deposit and the underlying till. The seismic velocities indicates that the outwash deposit is saturated in most places and that the till is likely unconsolidated sandy till in the study area.

Whiteshell Nuclear Research Establishment Plant Site

Geology of the Area

The Whiteshell Nuclear Research Establishment is situated on the western edge of the Canadian Pre-Cambrian shield approximately 75 miles northeast of Winnipeg (Fig. 1). The geology of the area is described by McPherson (1968). Sedimentary terrain overlying the granite bedrock in the area originated from Wisconsinian glaciations of the Pleistocene epoch and associated phases of glacial Lake Agassiz. The major superficial deposits which underline the soil zone in the study area are lacustrine clay and silty clay, lacustrine sand and gravel, sandy till and associated poorly sorted sandy deposits. The total thickness of glacial deposits overlying the granite bedrock ranges between 30 and 70 ft. (Cherry *et al.*, 1970). The geological contacts of interest for hydrogeological purposes in this area are a) the clay unit - glacial till unit contact, and b) the till - basal sandy unit contact, and c) the bedrock contact with the superficial deposits.

Resistivity Results

Thirteen resistivity soundings were done in this area and their location and identification numbers are shown in Fig. 21. Except sounding #22, all the soundings were situated where drill hole information is available. Some piezometer and drill hole locations are also shown

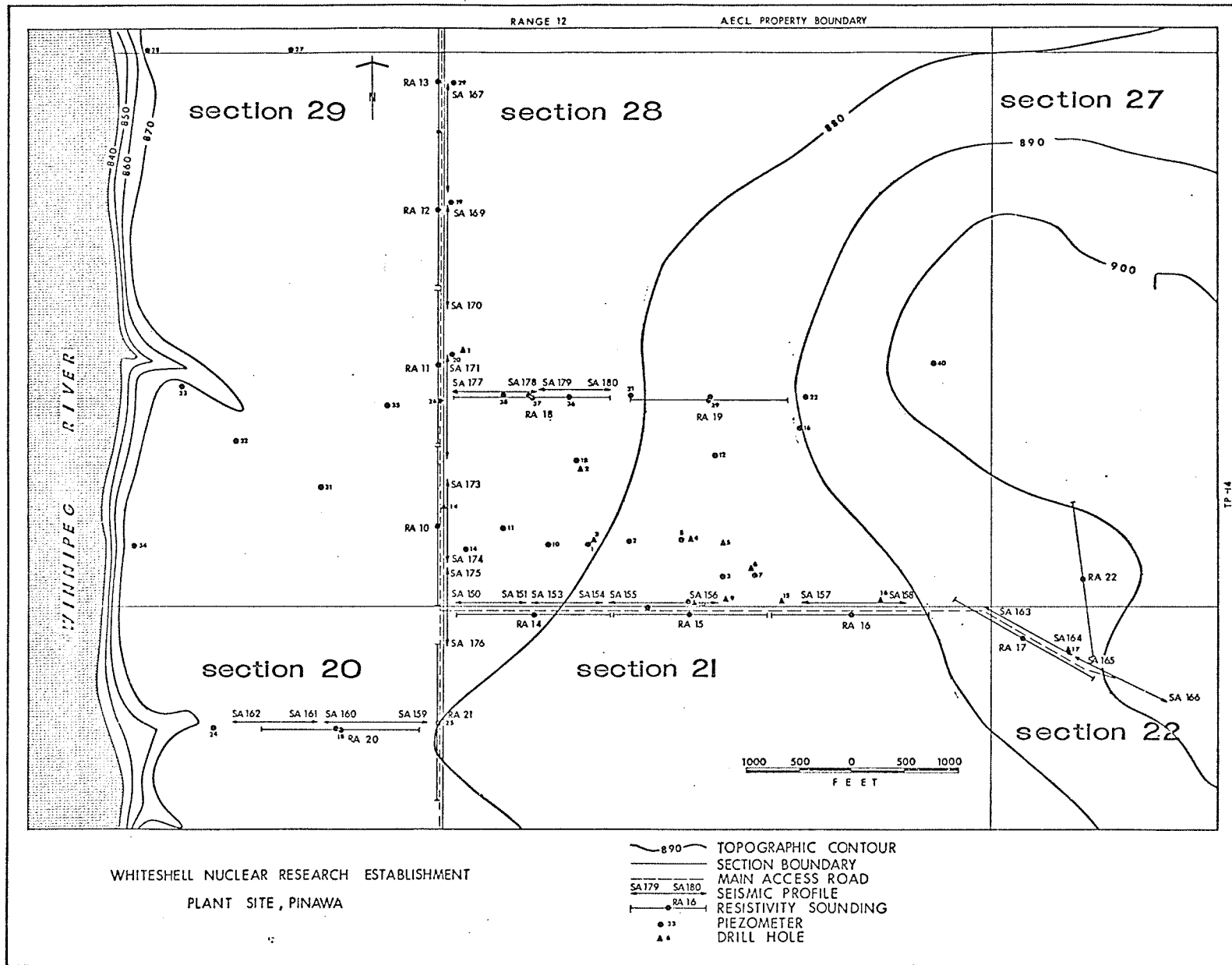


Fig. 21. Map showing resistivity sounding-seismic profile, piezometer and drill hole locations.

in Fig. 21.

Mooney and Wetzel four-layer master curves give the best fits in all the cases. The depth to bedrock calculated using this method plus the known geologic information is given in Fig. 22, and are in very good agreement. A typical resistivity sounding from the area along with interpretation is shown in Fig. 23. Geologic information from the same location is also given. More than 90 percent of the resistivities encountered in the first layer are less than 50 ohm.m. The resistivities encountered in the second layer are between 0 and 200 ohm.m. Nearly 75 percent of the resistivities encountered in the third layer are less than 250 ohm.m. and the rest are scattered above 4,000 ohm.m. Nearly 85 percent of the resistivities encountered in the fourth layer are between 1,150 and 2,100 ohm.m. A normalized histogram of resistivities of each layer is given in Fig. 24. The resistivities and depth to various layers encountered are given in Table VI. The resistivity values correlates quite well with the expected values for the superficial deposits.

The depths and resistivities calculated from inverse slope method are given in Table VII. The bedrock depths calculated from this method are in good agreement with the known information. In Fig. 25 an example of this method is given for the same resistivity sounding as given for the curve matching method. An interesting feature

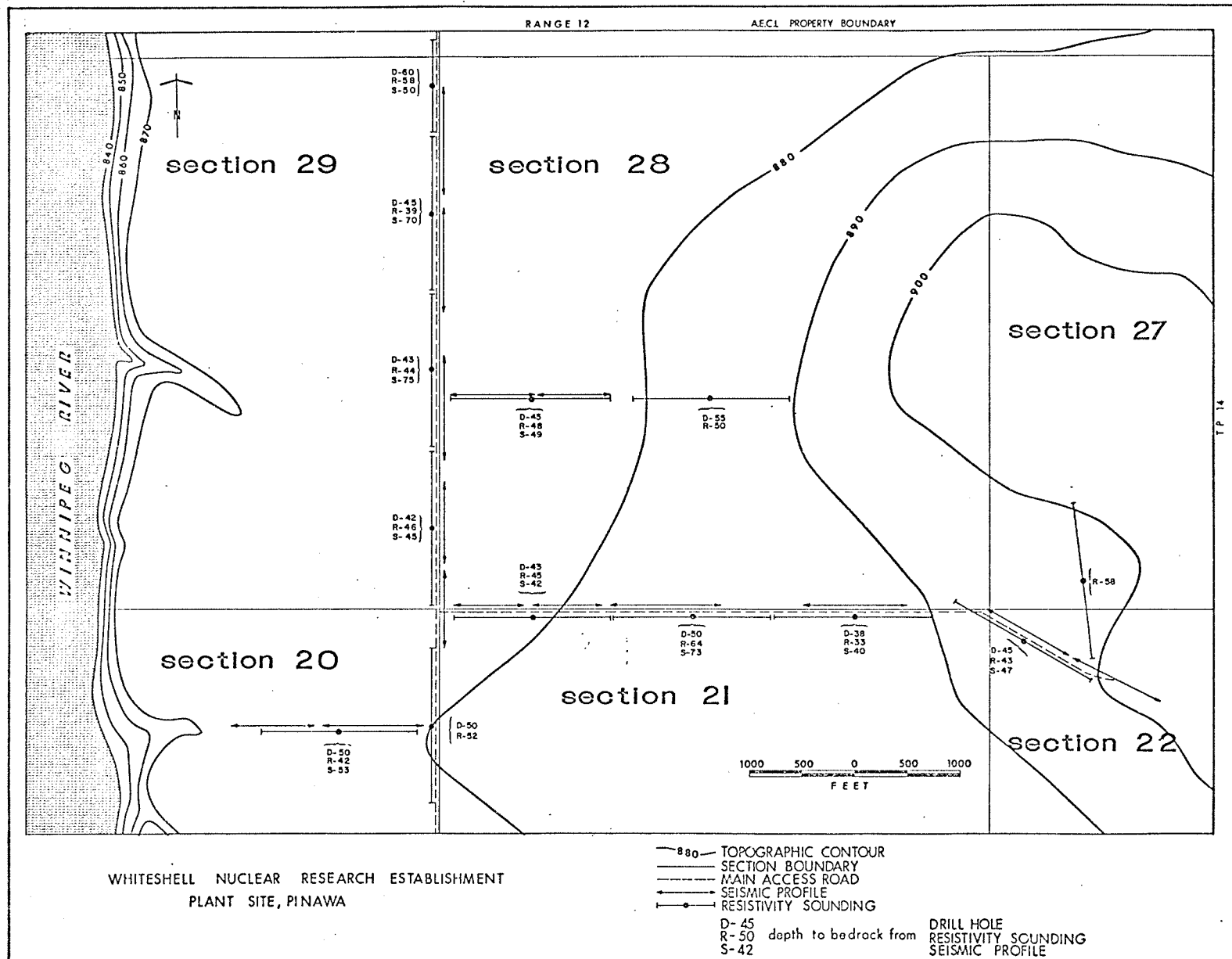


Fig. 22. Map showing depth to bedrock.

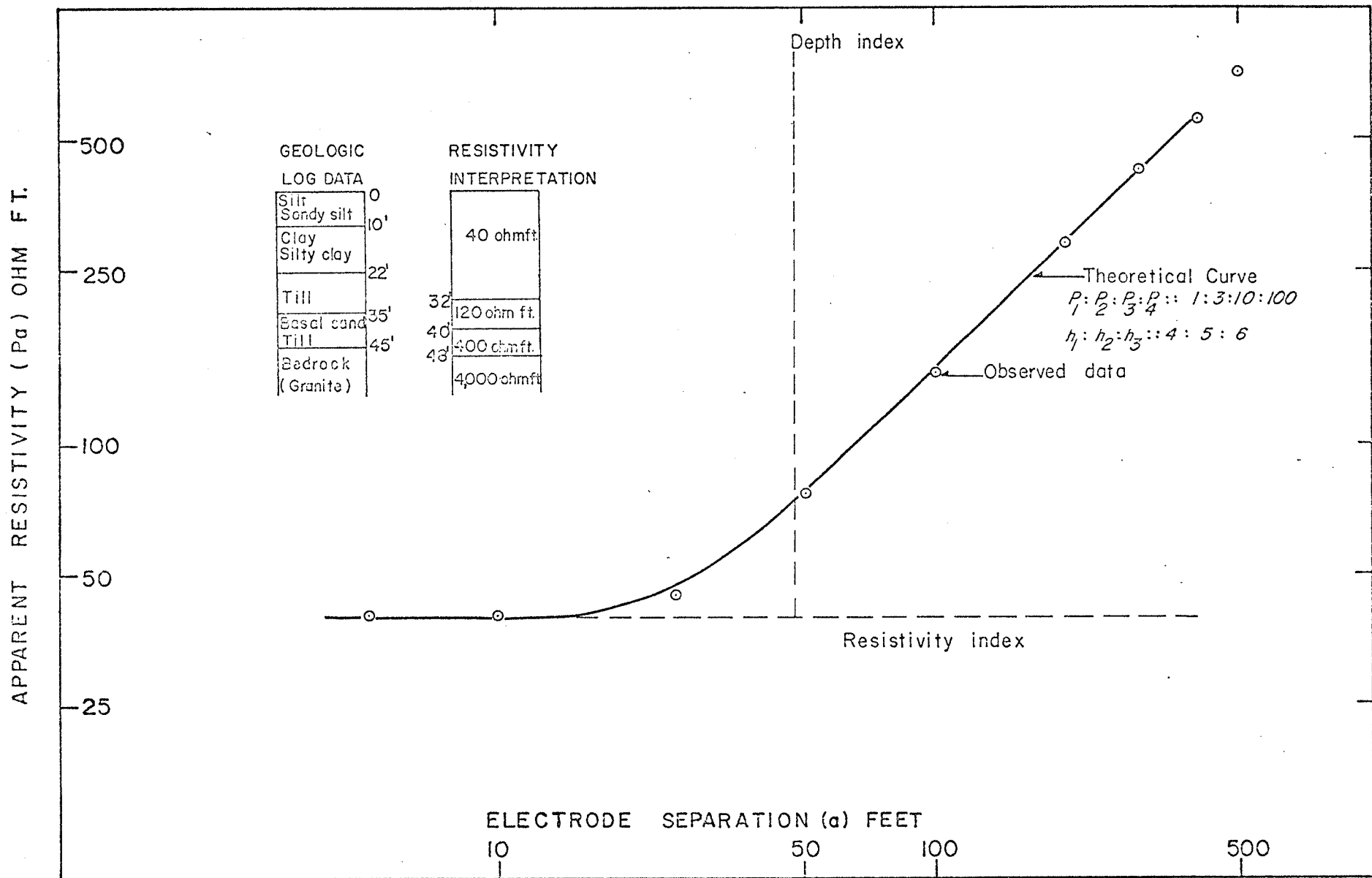


Fig. 23. Resistivity sounding #18, near piezometer 37, curve matching - WNRE Plant Site, Pinawa.

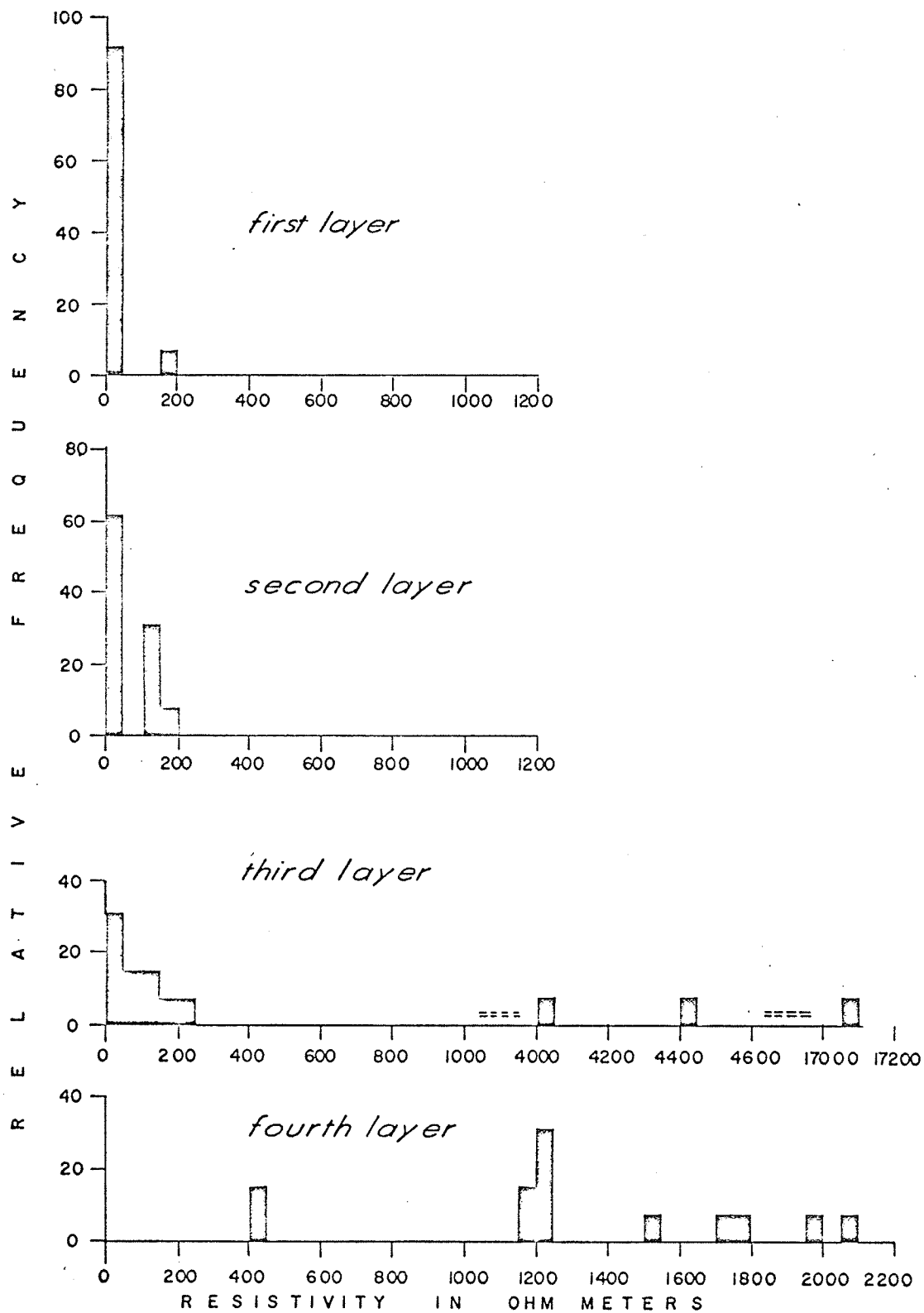


Fig. 24. Normalized histogram of resistivities, Whiteshell Nuclear Research Establishment Plant Site, Pinawa.

Table VI

Resistivity and Depth Data from Curve Matching Method, Whiteshell Nuclear Research Establishment Plant Site Pinawa

<u>Sounding Number</u>	<u>Location</u>	ρ_1 (ohm.m.)	ρ_2 (ohm.m.)	ρ_3 (ohm.m.)	ρ_4 (ohm.m.)	h_1 (ft)	h_2 (ft)	h_3 (ft)
10	Near Piezometer #14	20.7	7.0	207.1	2071.3	23	39	46
11	Near Piezometer #20	12.5	3.3	124.9	1248.8	22	37	44
12	Near Piezometer #19	41.5	3.3	4112.1	411.2	20	33	39
13	Near Piezometer #29	11.6	115.7	11.6	1157.4	29	49	58
14	500 ft south of Piezometer #10	12.5	124.8	12.5	1248.0	23	38	45
15	Near Piezometer #4	12.2	121.8	36.6	1218.4	11	43	64
16	500 ft east of Drill Hole #15	11.6	115.7	35.0	1157.5	11	17	33
17	400 ft NW of Drill Hole #17	19.8	198.0	59.4	1979.9	29	36	43
18	Near Piezometer #37	12.2	36.6	121.8	1218.4	32	40	48
19	Near Piezometer #39	15.2	45.6	152.3	1523.0	8	33	50
20	Near Piezometer #18	17.7	5.8	53.3	1766.7	21	35	42
21	Near Piezometer #25	44.2	4.6	4416.7	441.7	9	18	52
22	600 ft north of Drill Hole #17	170.6	17.1	17057.0	1705.8	10	29	58

Table VII

Resistivity and Depth Data from Inverse Slope Method, Whiteshell Nuclear Research Establishment Plant Site, Pinawa

<u>Sounding Number</u>	<u>Location</u>	ρ_1 (ohm.m.)	ρ_2 (ohm.m.)	ρ_3 (ohm.m.)	ρ_4 (ohm.m.)	h_1 (ft)	h_2 (ft)	h_3 (ft)
10	Near Piezometer #14							
11	Near Piezometer #20	12.2	1523.0	865.0		30	200	
12	Near Piezometer #19	39.6	16.5	1870.2		17	54	
13	Near Piezometer #29	13.1	35.3	376.2	3289.7	19	58	143
14	500 ft south of Piezometer #10	12.2	21.0	388.4	8833.0	9	28	123
15	Near Piezometer #4	11.0	70.1	199.5	6152.9	7	33	108
16	500 ft east of Test Hole #15	7.6	895.5	2741.4		5	39	
17	400 ft northwest of Test Hole #17	20.4	83.8	4148.6		17	51	
18	Near Piezometer #37	14.0	85.6			24	63	
19	Near Piezometer #39	17.7	197.1	9320.7		12	52	
20	Near Piezometer #18	14.3	254.3	965.6		39	98	
21	Near Piezometer #25	11.6	42.9	527.0	1181.0	13	56	169
22	600 ft north of Test Hole #17	50.9	4447.0			57		

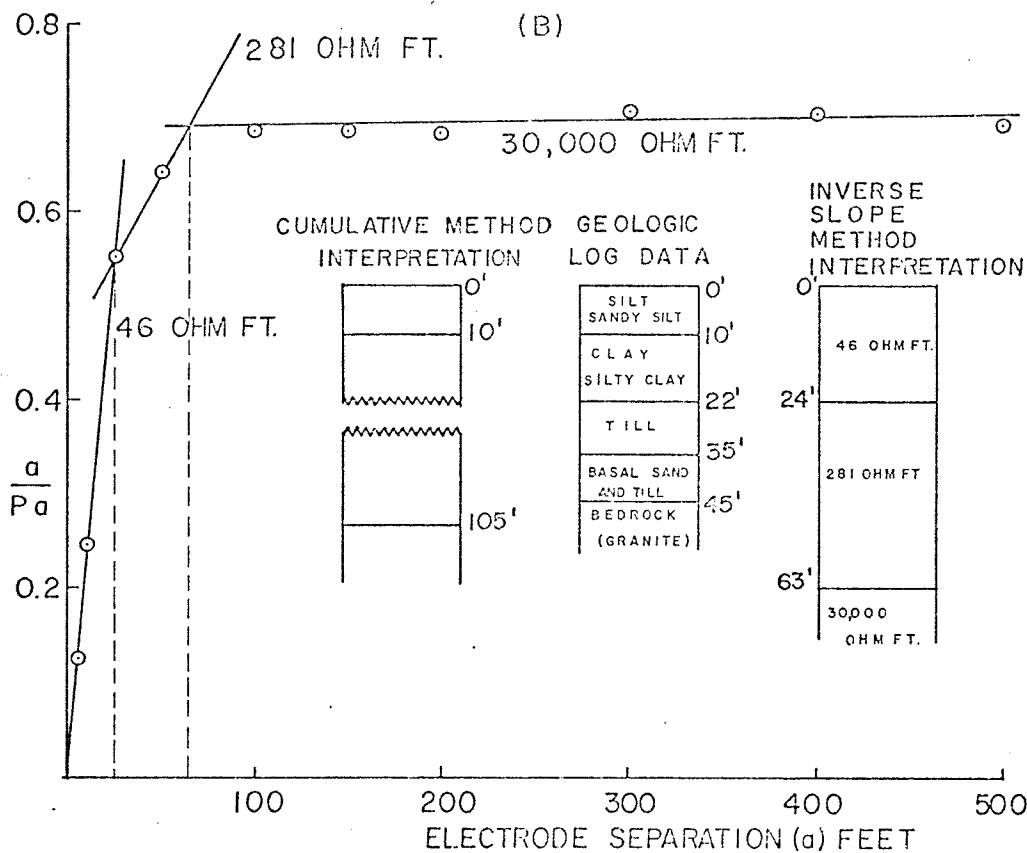
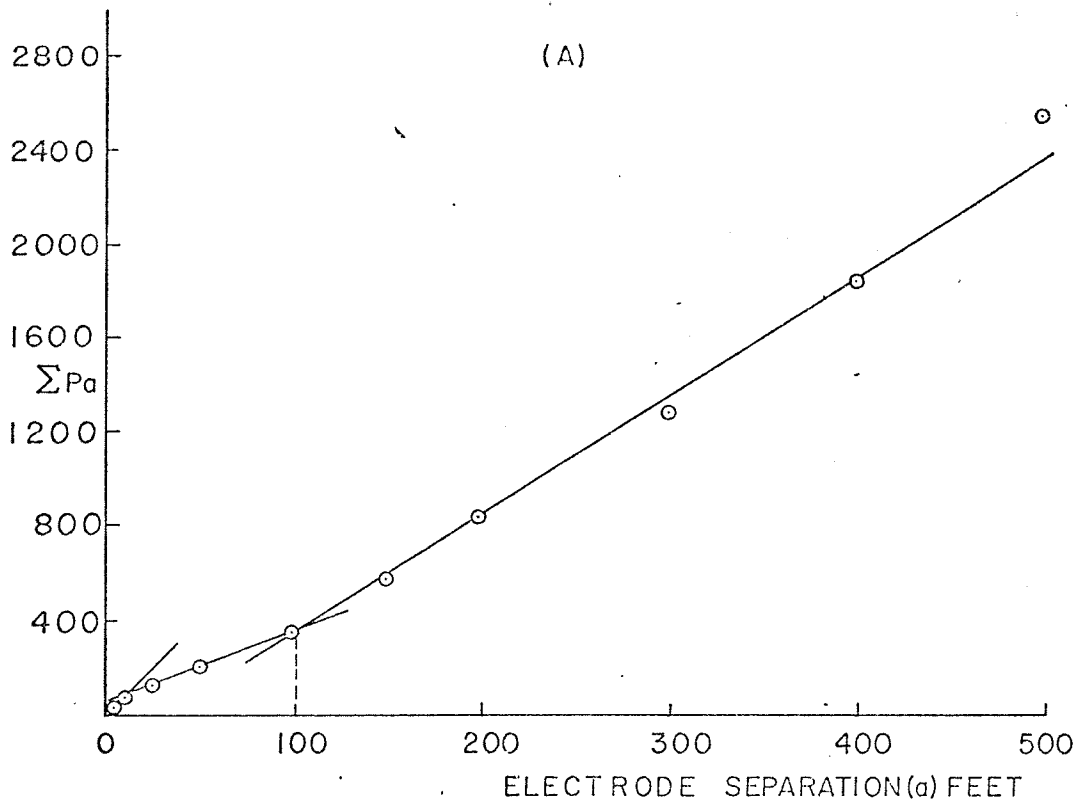


Fig. 25. Resistivity sounding #18, near piezometer 37
 (a) cumulative method
 (b) inverse slope method

Whiteshell Nuclear Research Establishment Plant Site

of the interpretation in this area is that a change in resistivity has been observed in many instances within the bedrock, normally below 100 ft. from the ground surface. In some cases the interpretation in these situations has become critical as negative slopes are possible. No mention has been made by the authors of the inverse slope method (Sankernarain, Ramanujachary, 1967) for this type of situation. An example showing this ambiguity is given in Fig. 26.

The depths calculated from Moore's cumulative method are given in Table VIII. The depths obtained from this interpretation are not in good agreement with the known information except the depths to the second layer. In all the cases a change in resistivity has occurred at depths much greater than the known depth to bedrock. The interpretation from cumulative method is given in Fig. 25 for the same sounding used in illustrating the other two methods. An interesting feature is that the depths obtained from inverse slope method below 100 ft. are roughly in the same range as from cumulative method. The cumulative method interpretation is also given in Fig. 26 where the ambiguity in Sankernarain's method is shown.

Seismic Results

Fifteen reversed profiles were done in this area and their location with identification numbers are shown

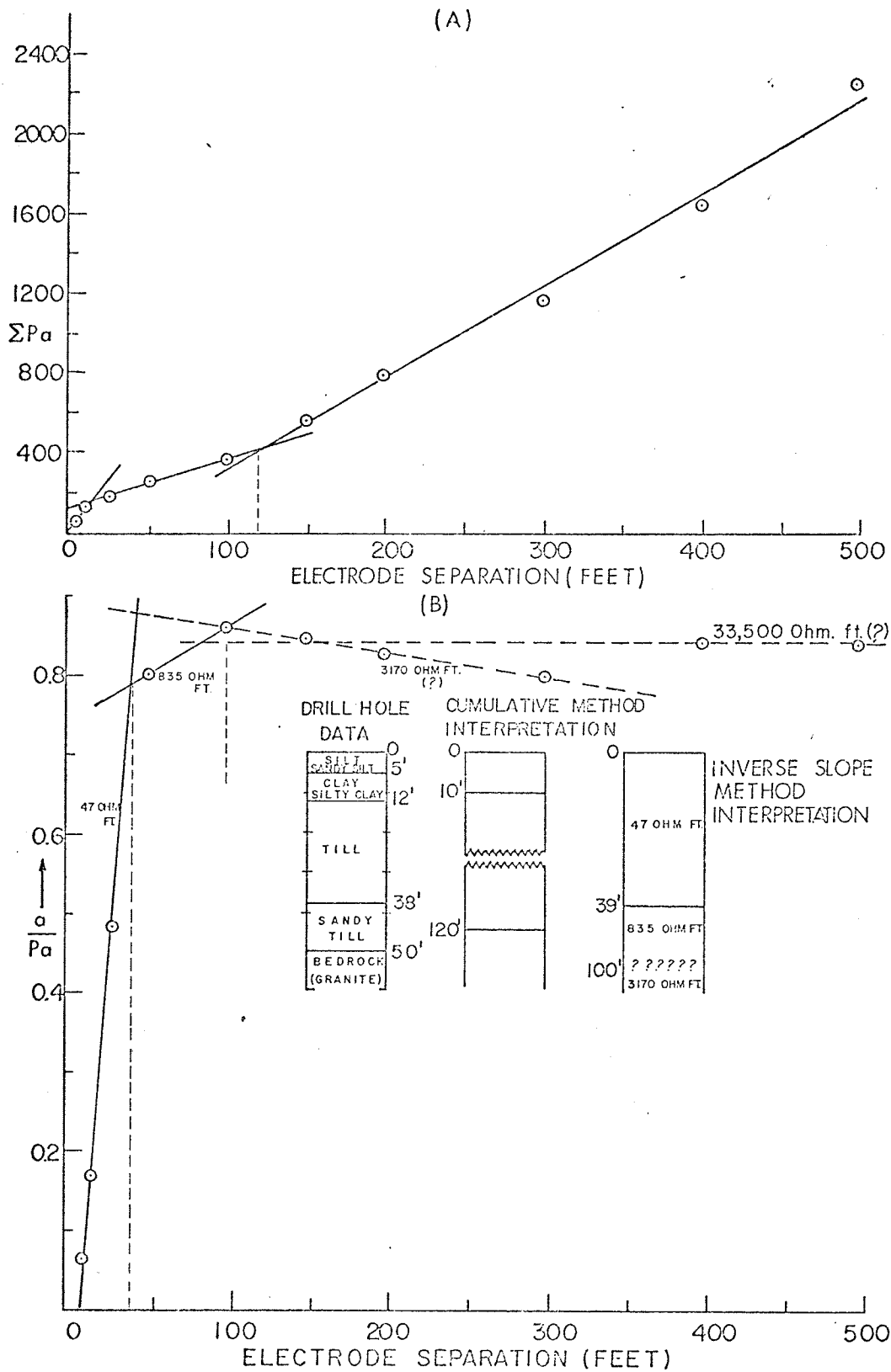


Fig. 26. Resistivity sounding #20, near piezometer 18
 (a) cumulative method
 (b) inverse slope method
 Whiteshell Nuclear Research Establishment
 Plant Site

Table VIII

Depth Data from Cumulative Method,
Whiteshell Nuclear Research Establishment Plant Site, Pinawa

<u>Sounding Number</u>	<u>Location</u>	<u>h₁ (ft)</u>	<u>h₂ (ft)</u>
10	Near Piezometer #14	12	100
11	Near Piezometer #20	17	115
12	Near Piezometer #19	12	123
13	Near Piezometer #29	14	105
14	500 ft. south of Piezometer #10	10	135
15	Near Piezometer #4	13	120
16	500 ft. east of Test hole #15	10	90
17	400 ft. northwest of Test hole #17	10	117
18	Near Piezometer #37	10	110
19	Near Piezometer #39	9	88
20	Near Piezometer #18	13	120
21	Near Piezometer #25	15	122
22	600 ft north of Test hole #17	11	129

in Fig. 21. In general, the locations were so selected as to compare the results with the known drill hole information.

Depth determinations are carried out using the time-distance plots with dip determinations made whenever necessary. The calculated depths and velocities are given in Table IX. In general, only two segments are present on the time-distance plot. The first layer velocities range from 3,500 to 8,000 ft./sec. The velocities encountered in the second layer range from 14,000 to 22,000 ft./sec., with the major concentration being at 18,000 to 19,000 ft./sec. A normalized histogram of the velocities encountered in this area is given in Fig. 27. The velocities encountered in the second layer correlate with the bedrock (granite) velocities. As mentioned in the description of the geology of the area, layers of silty clay, clay, till and sandy till overlies the bedrock. In spite of using close geophone spacing, no individual segments were obtained for these formations on the time-distance plot. An average velocity of these thin superficial formations is obtained in the first segment of the time-distance plot. A typical example of the time-distance plot along with interpretation and drill hole information is given in Fig. 28. The depths calculated are in good agreement in most of the cases. Average depths are given at each resistivity sounding location in Fig. 22 along with depth to bedrock obtained from resistivity interpretation and from drill hole. In a few

Table IX

Seismic Velocities and Calculated Depths, Whiteshell Nuclear Research Establishment Plant Site, Pinawa

<u>Seismic Profile Number</u>	<u>Velocity (V₁ in ft/sec)</u>	<u>Velocity (V₂ in ft/sec)</u>	<u>Velocity (V₃ in ft/sec)</u>	<u>h₁ (ft)</u>	<u>h₂ (ft)</u>
150	5500	20400		69	
151	5000	18500		56	
153	5300	19000		47	
154	4150	16000		35	
155	5000	13000	22000	34	73
156	5000	11500	22000	27	74
157	4800	18500		40	
158	4900	17500		40	
159	7900	14600		81	
160	6400	15100		89	
161	4700	17400		53	
162	4200	21000		59	
163	3900	19800		48	
164	5100	18200		46	
165	4850	16800		51	
166	3900	20000		82	

<u>Seismic Profile Numbers</u>	<u>Velocity (V₁ in ft/sec)</u>	<u>Velocity (V₂ in ft/sec)</u>	<u>Velocity (V₃ in ft/sec)</u>	<u>h₁ (ft)</u>	<u>h₂ (ft)</u>
167	3600	14600		50	
169	7650	12800		51	
170	4000	17800		91	
171	7500	19000		75	
173	1800	5200	17200	10	50
174	2900	14400		28	
175	5300	22000		63	
176	4300	16000		52	
177	4000	18600		47	
178	5600	19000		50	
179	3750	18600		39	
180	4500	19700		46	

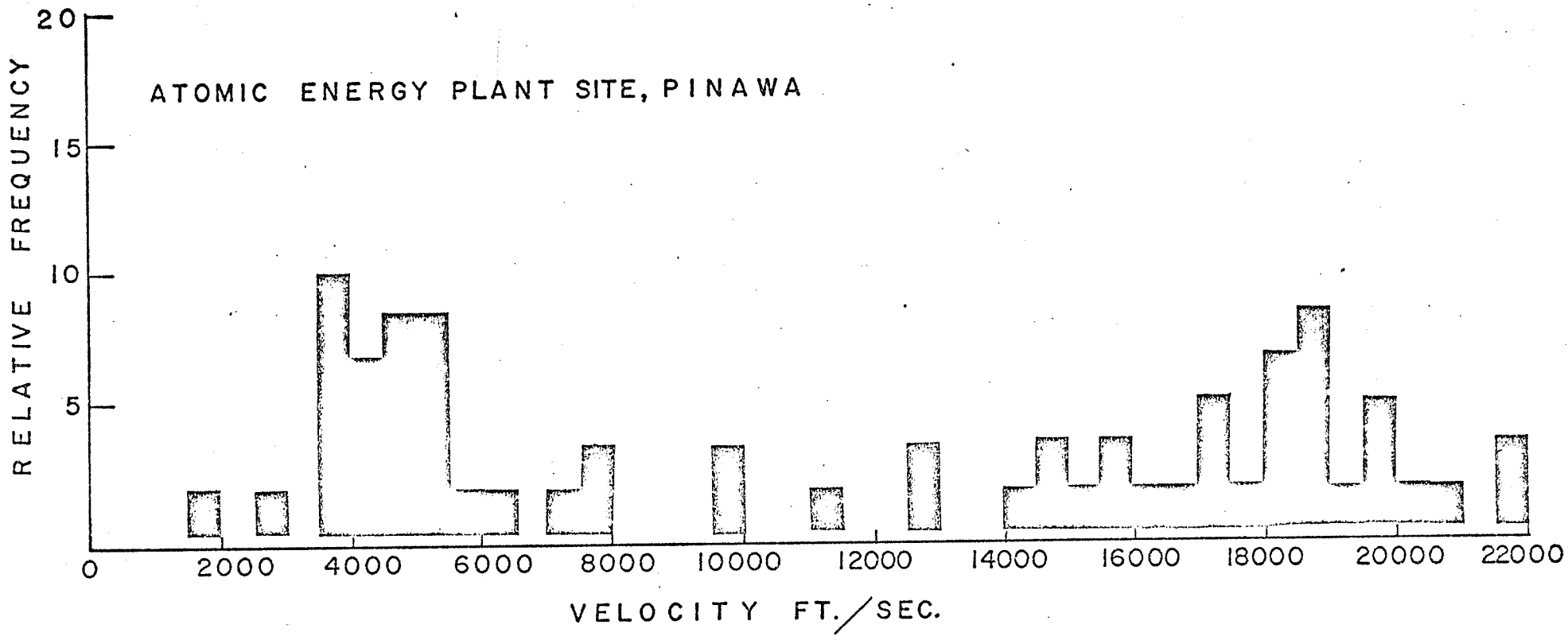


Fig. 27. Normalized histogram of velocities.

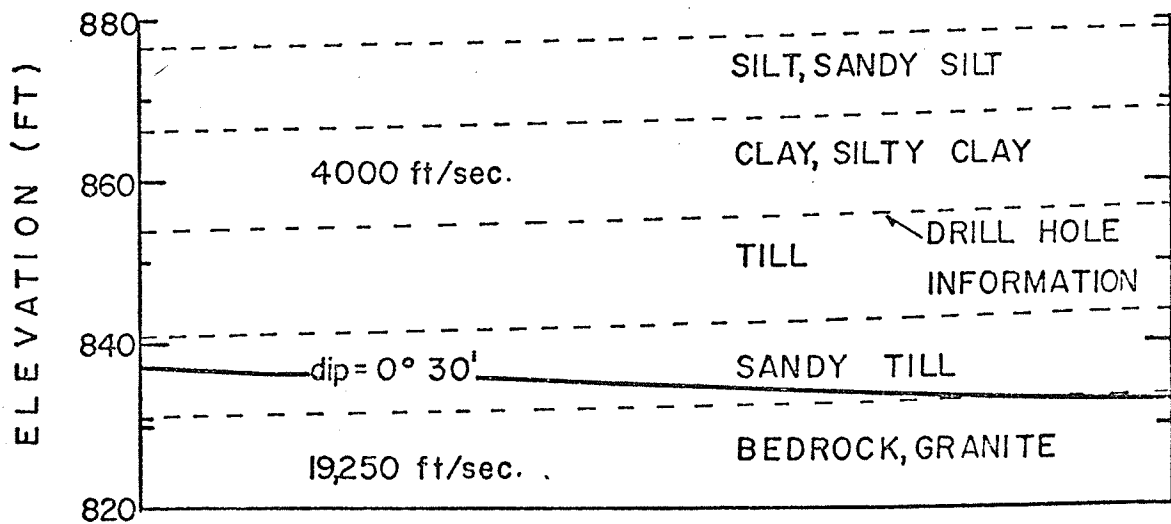
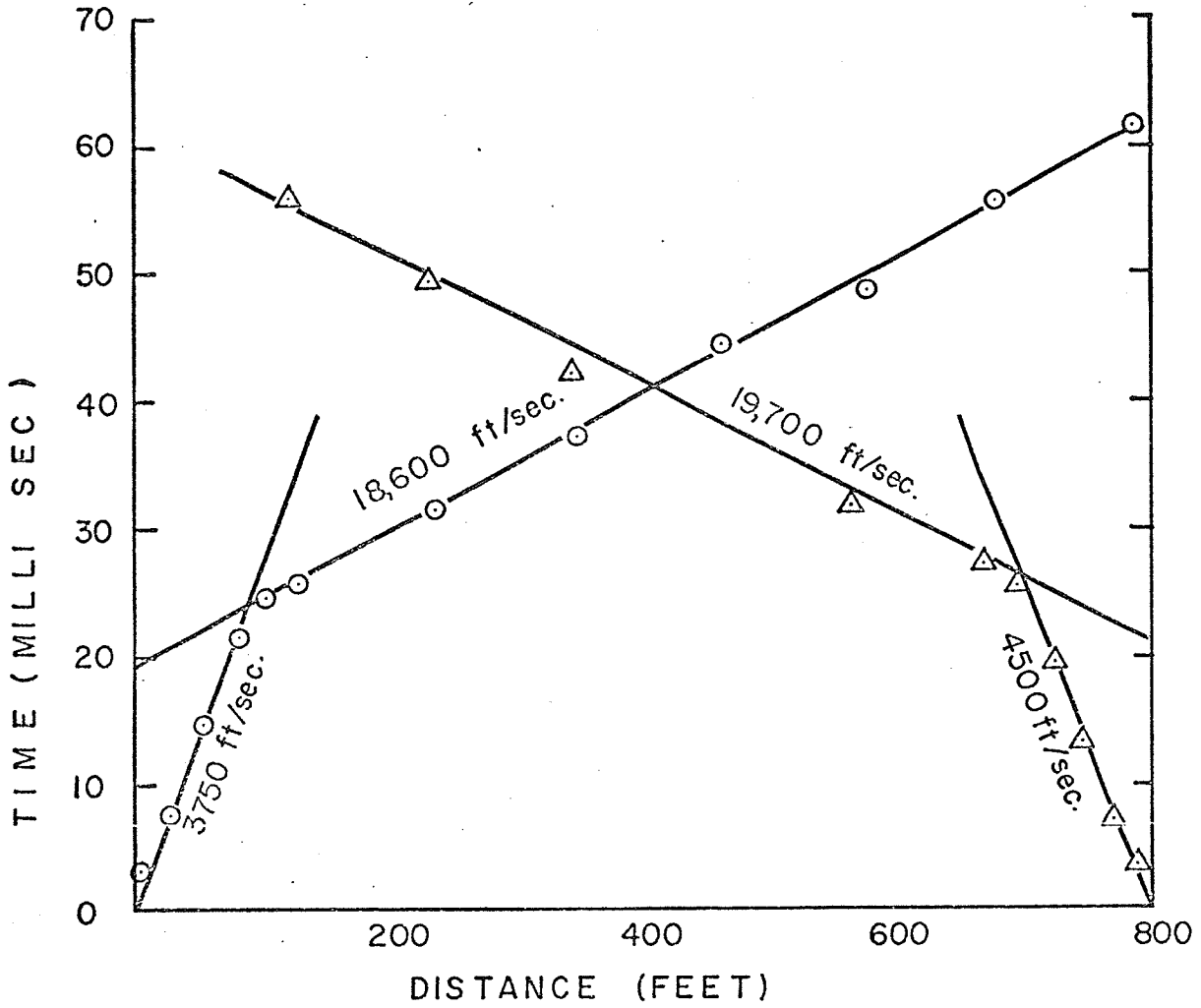


Fig. 28. Seismic profile 179-180, near piezometer 37, Whiteshell Nuclear Research Establishment Plant Site, Drill hole information given along with seismic interpretation.

instances the depths obtained from seismic interpretation are higher than the known depth.

Conclusions

The resistivity method is quite useful to map the bedrock topography and to differentiate the superficial deposits in this area. It seems that the inverse slope method and cumulative method are not suitable methods of interpretation in this area. The curve matching method is applicable in this area and gives good results. The observed resistivities of the various units in this area are shown in Fig. 24. In general, the clay unit resistivity is 10.0 to 20.0 ohm.m., the till unit resistivity is 5.0 to 60.0 ohm.m., and the sand unit resistivity is 100.0 to 200.0 ohm.m. The resistivity of the sand unit in this area is much less than observed elsewhere and is possibly due to the moisture content and till fraction contained in the sand unit. In general, the bedrock granite gives resistivities over 1,000 ohm.m.

The seismic refraction method in this area is not sensitive enough to differentiate the superficial deposits. This may be due to the fact that the different superficial units are not thick enough to be represented on the time-distance plot. It is equally possible there is not enough velocity contrast within the superficial deposits. In situations where more than 20 ft. of till is present, the velocities encountered in the first layer are considerably

higher than in the other parts. Nevertheless, the seismic method is quite useful to map the bedrock topography in this area.

Metro Winnipeg Area

Geology

The location of the study area is shown in Fig. 1. The geology of the area is described by Davies *et al.* (1962) and by Render (1970) in relation to the geohydrology of the area.

The bedrock in the study area is characterized by Paleozoic carbonate formations of limestones and dolomites which range in thickness from 250 to 750 ft. The bedrock surface has a number of closed depressions or large solution cavities which suggest a Karst topography. A mantle of Pleistocene drift overlies the bedrock and has a maximum thickness approximately 200 ft. The average thickness in the area is about 60 ft. The drift comprises Glacial Lake Agassiz clay and recent fluvial deposits overlying till. Alluvium occurs over the drift near rivers and streams.

The lower portion of the drift consists of boulder till and associated glaciofluvial deposits. The bouldery till consists of carbonate rock fragments in a clay silt matrix. The till thickness under Metropolitan Winnipeg averages 20 ft and ranges up to 40 ft. Deposits consisting primarily of outwash sand and gravel occur in the Bird's Hill area northeast of Winnipeg.

Lake Agassiz deposits which underline the study area in general consists of two units. The upper unit consists

of 5 to 15 ft. of silt and very fine sand interbedded with thin beds of clay. The lower unit consists of clay. Under Winnipeg the Agassiz sediments have a maximum thickness of 80 ft. and an average thickness of 40 ft.

Resistivity Surveys

Twenty-five resistivity soundings were done in Metro Winnipeg area. All the soundings were situated near test wells where geologic logs are available to compare the results. The location of the test wells where resistivity soundings were conducted are shown in Fig. 29.

Since the drift in the study area is comprised of three or four different lithologic units additional potential measurements are taken at electrode separations of 40 ft., 75 ft. and 125 ft. for increased resolution of these units. The location of the resistivity soundings are shown in Fig. 30.

The best fits are obtained for all the soundings using Mooney and Wetzel four-layer master curves. The depths determined from this interpretation are in very good agreement with the known information. A typical resistivity sounding from the area is given in Fig. 31. In many instances a distinct resistivity change has occurred within the bedrock. This is suspected to be due to a decrease in porosity at these depths. An example of this is shown in Fig. 32. The resistivity and depths values obtained from

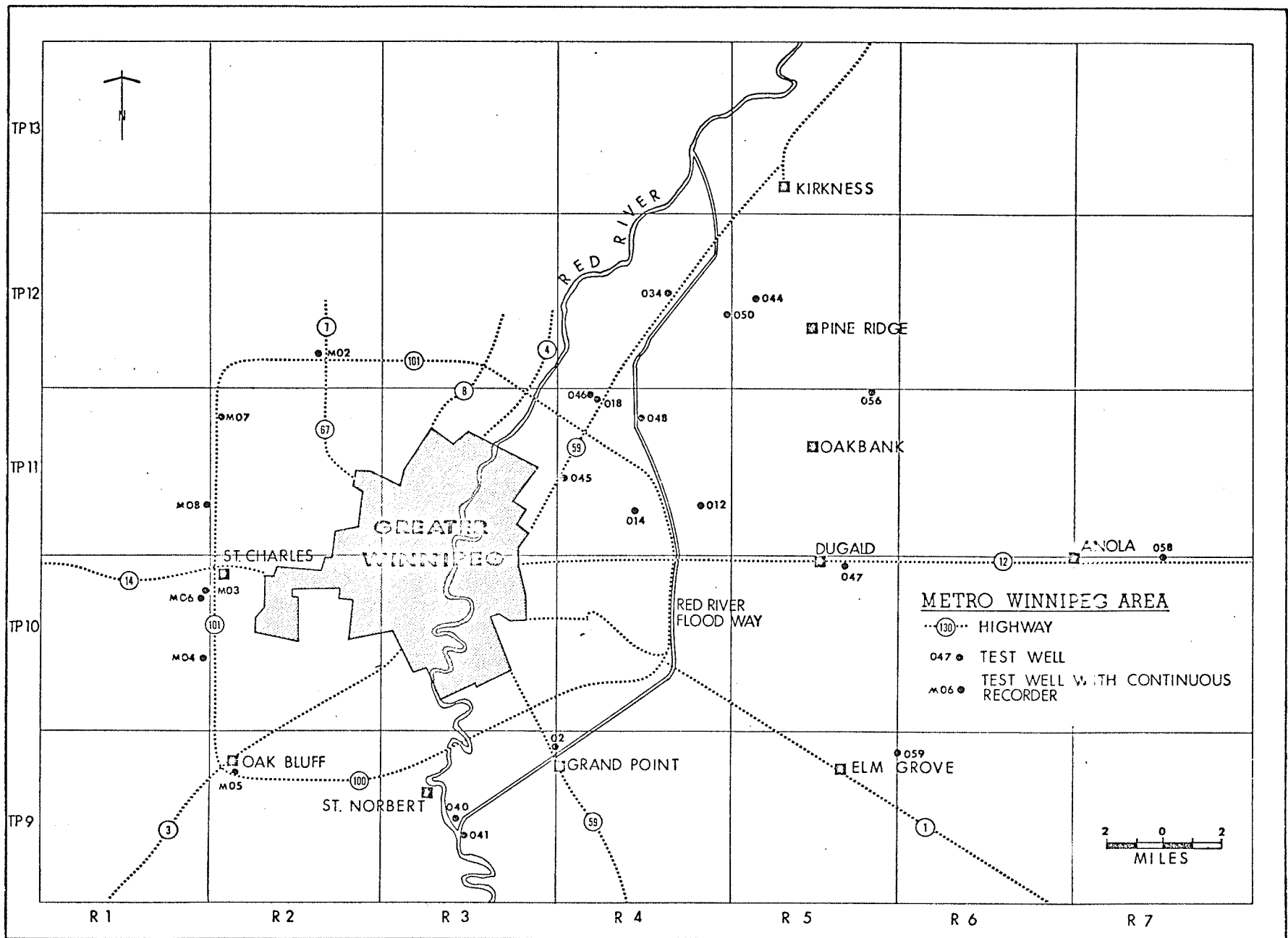


Fig. 29. Map showing well locations.

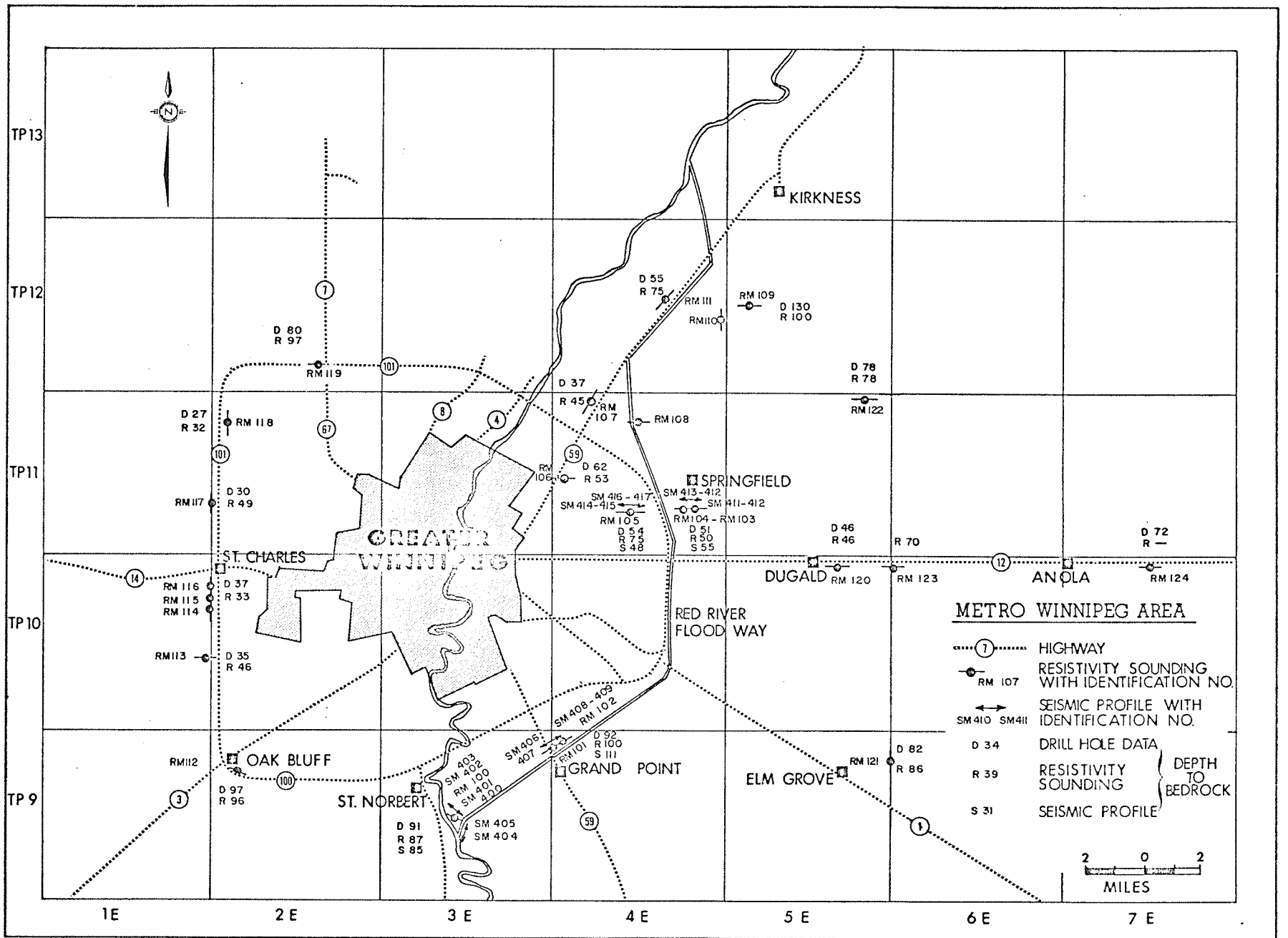


Fig. 30. Map showing resistivity sounding-seismic profile locations, depth information also shown.

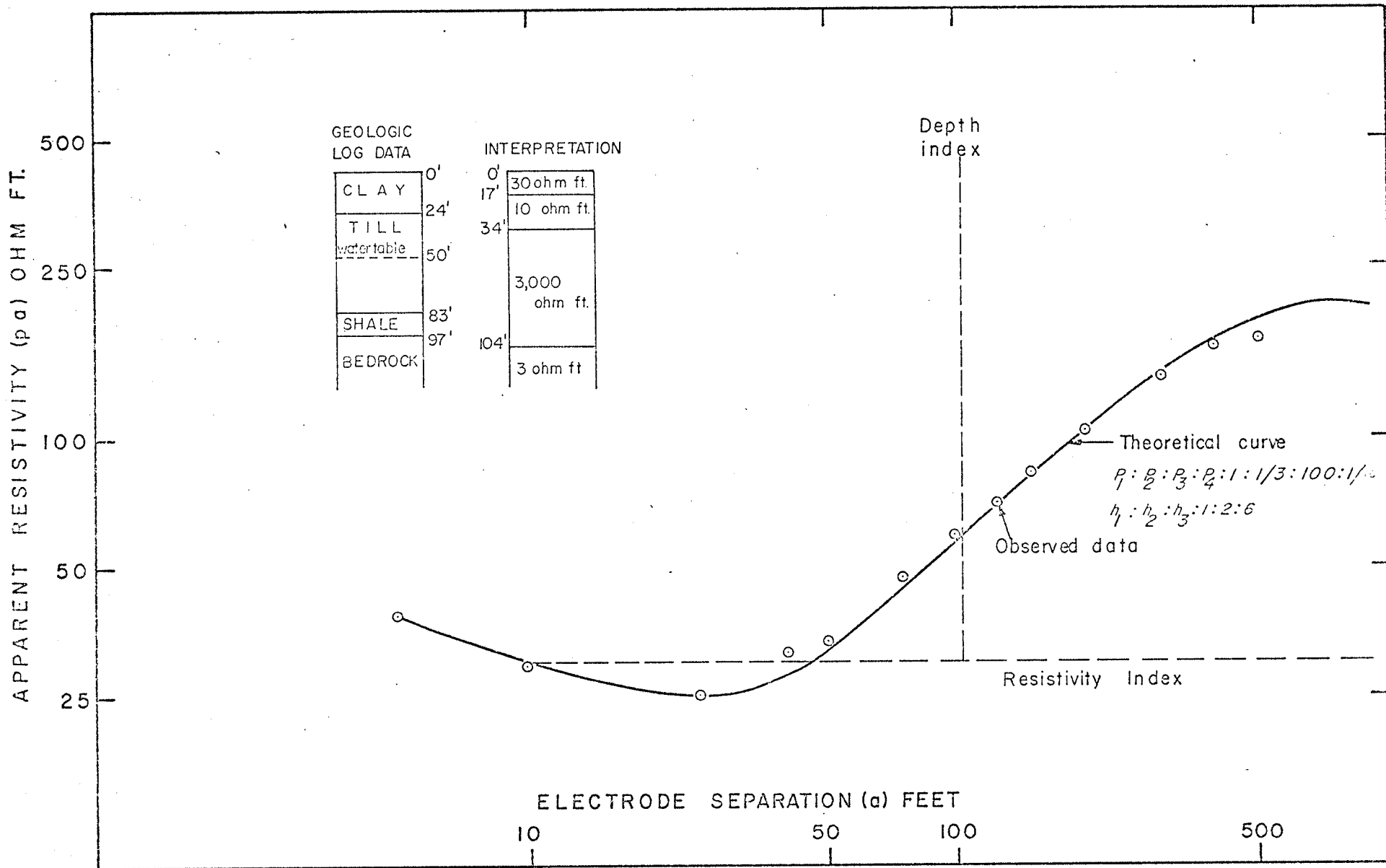


Fig. 31. Resistivity sounding #112, near MO-5, curve matching method - Metro Winnipeg Area.

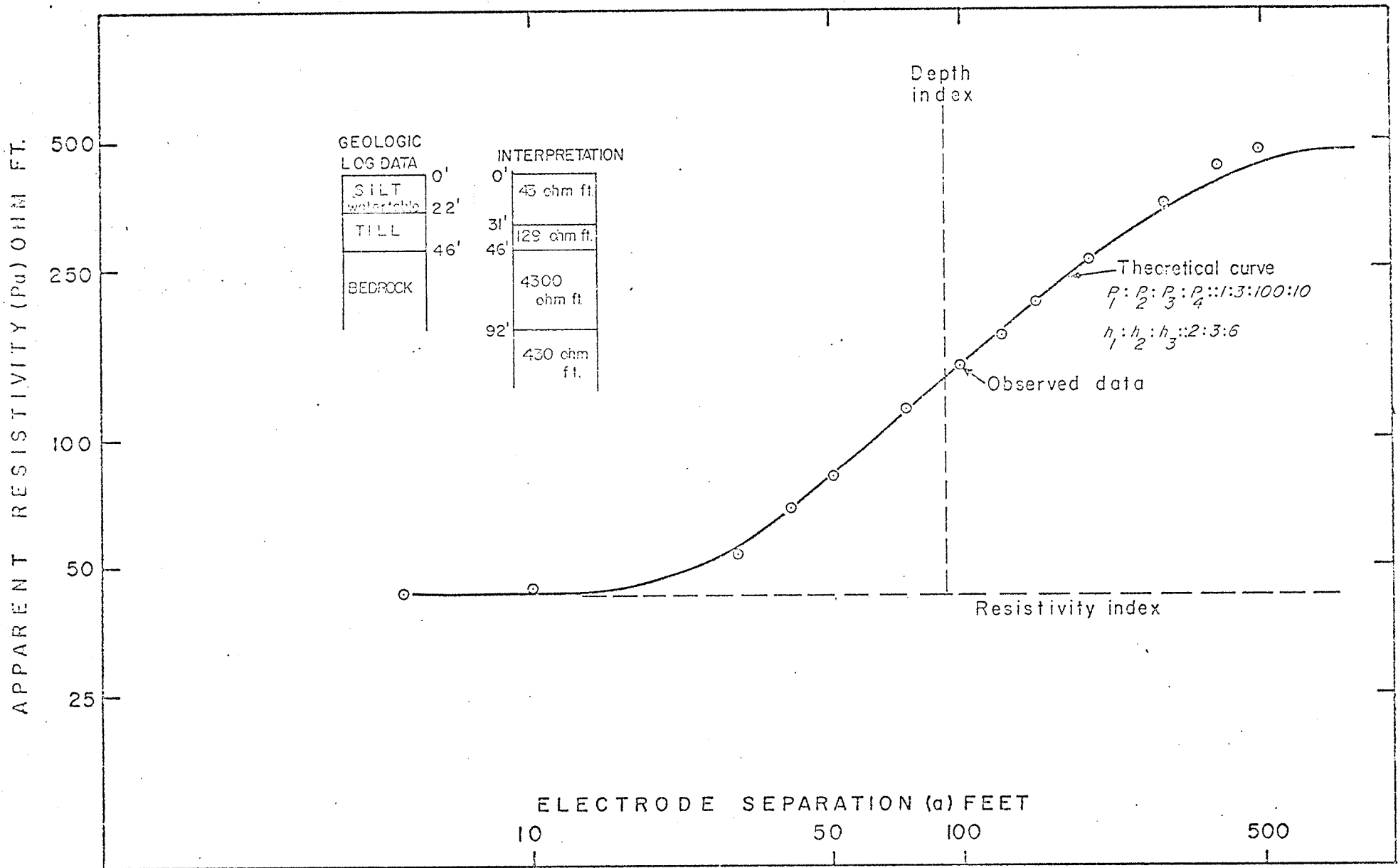


Fig. 32. Resistivity sounding #120, near well , curve matching method - Metro Winnipeg Area.

this interpretation is given in Table X. A normalized histogram of the resistivities encountered in each layer is given in Fig. 33. Nearly 90 percent of the resistivity values encountered in the first layer are in the range 0-50 ohm.m. In the second layer nearly 80 percent of the resistivities are below 50 ohm.m. In the third layer 55 percent of the values are distributed from 700-1950 ohm.m. with a peak at 950-1000 ohm.m. range and the remaining 45 percent are below 100 ohm.m. Nearly 75 percent of the values encountered in the fourth layer are between 0-200 ohm.m. and the remaining 25 percent are scattered from 500-2100 ohm.m.

Two resistivity soundings in the area (#108, #124) could not be interpreted using curve matching method. Also the potential measurement at these two locations are questionable as the measurements were not repeatable. At both these locations it has become hard to drive the current electrodes well into the ground. The lack of a good ground contact and hence low source current seems to be the major reason for not being able to repeat the observations.

The depths obtained from curve matching at two other locations (Soundings #109 and #110) are not in agreement with known information, though the fits obtained are reasonable. An example of this (Sounding #109) is shown in Fig. 34. From drill hole information it is known

Table X

Resistivity and Depth Data from Curve Matching Method, Metro Winnipeg Area

<u>Resistivity Sounding</u>	<u>Location</u>	ρ_1 (ohm.m.)	ρ_2 (ohm.m.)	ρ_3 (ohm.m.)	ρ_4 (ohm.m.)	h_1 (ft)	h_2 (ft)	h_3 (ft)
100	Near Well 040	7.9	23.8	791.0	79.1	58	87	175
101	Near Well 02	6.7	20.1	68.5	685.0	40	90	120
102	Near Well 02	9.7	3.4	974.7	97.4	20	39	116
103	Near Well 012	17.0	3.3	17.0	170.6	5	11	32
104	Near Well 012	9.7	29.2	974.7	97.4	42	84	252
105	Near Well 014	9.7	29.2	974.7	97.4	50	75	150
106	Near Well 045	10.4	4.0	1035.0	31.0	40	53	80
107	Near Well 046	14.3	4.9	1431.0	4.9	30	45	91
108	Near Well 068	-	-	-	-	-	-	-
109	Near Well 044	53.3	160.0	17.7	533.0	6	12	36
110	Near Well 050	228.5	22845.0	23.0	2284.0	5	10	30
111	Near Well 034	8.8	883.3	26.5	88.3	30	75	91
112	Near Well MO-5	9.1	3.0	913.7	0.9	17	34	104
113	Near Well MO-4	8.5	2.7	852.8	25.6	15	23	46
114	Near Well MO-6	7.0	2.4	700.5	7.0	21	28	41
115	1000 ft south of Well MO-3	6.7	2.1	67.0	6.7	6	11	33

<u>Resistivity Sounding</u>	<u>Location</u>	ρ_1 (ohm.m.)	ρ_2 (ohm.m.)	ρ_3 (ohm.m.)	ρ_4 (ohm.m.)	h_1 (ft)	h_2 (ft)	h_3 (ft)
116	Near Well MO-3	5.8	1.8	57.9	17.4	7	11	21
117	Near Well MO-8	15.5	5.2	1553.4	46.6	16	49	98
118	Near Well MO-7	12.5	4.3	1248.8	124.8	6	11	32
119	Near Well MO-2	11.6	115.7	11.6	1157.0	16	80	97
120	Near Well 047	13.1	39.3	1309.7	131.0	31	46	92
121	Near Well 059	7.6	22.8	76.2	761.5	29	43	86
122	Near Well 056	19.2	57.6	1919.0	191.9	13	65	78
123	2 miles east of 047	7.3	21.6	71.6	715.8	24	35	70
124	Near Well 058	-	-	-	-	-	-	-

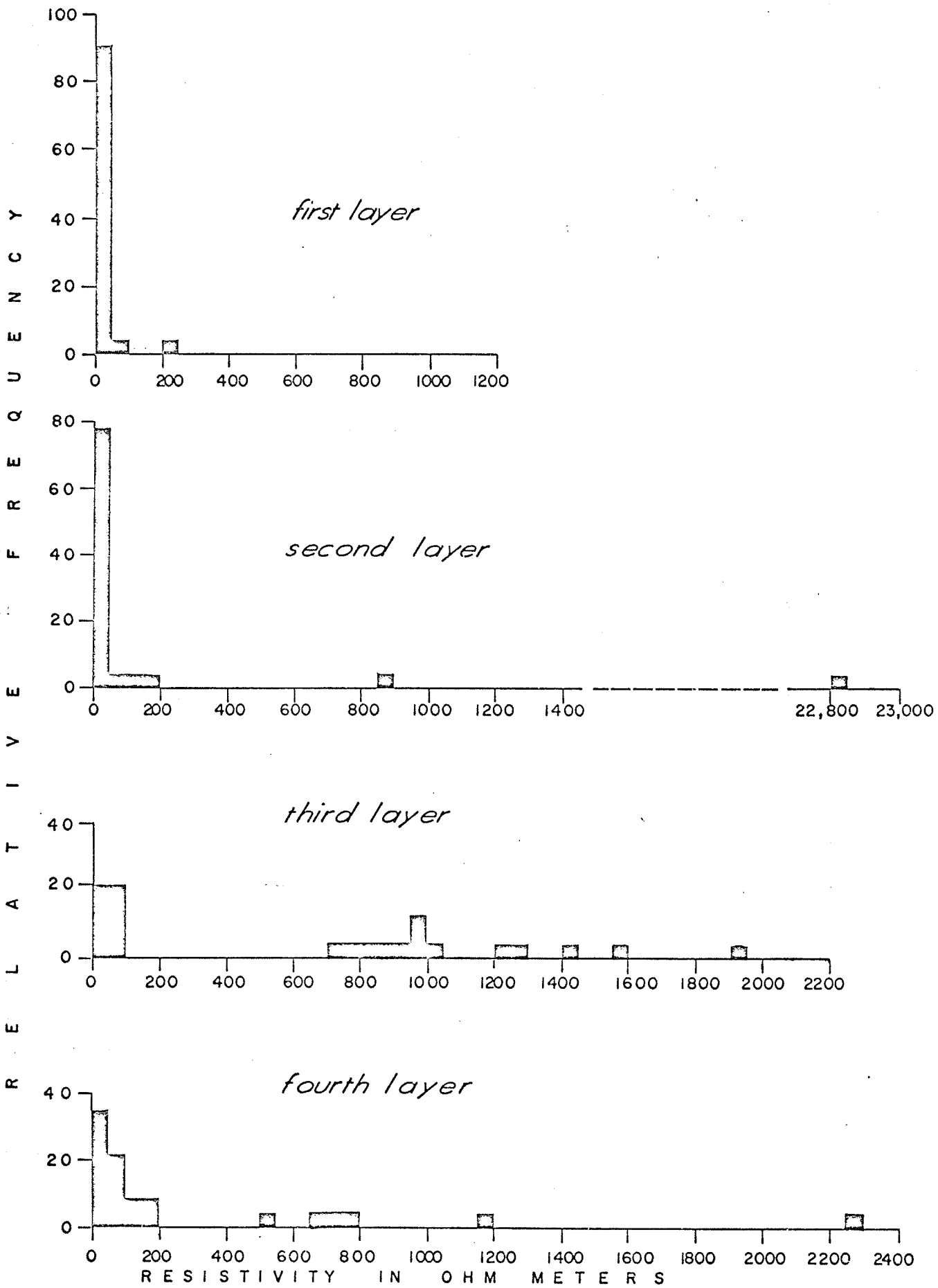


Fig. 33. Normalized histogram of resistivities - Metro Winnipeg Area.

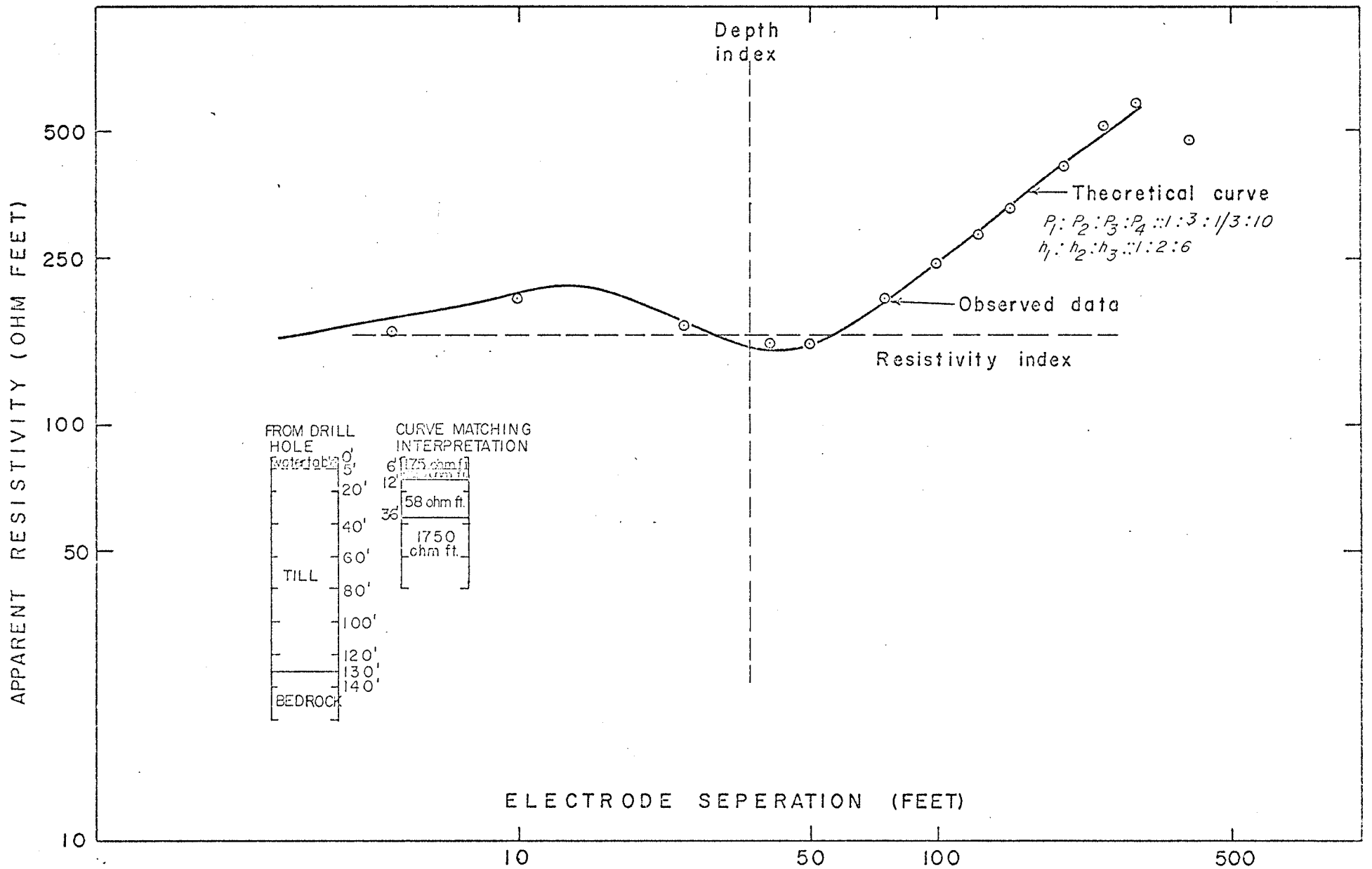


Fig. 34. Resistivity sounding #109, near well 044, curve matching method, Metro Winnipeg Area.

that 130 ft. of till lies over the bedrock. But the depth obtained from curve matching is only 36 ft. At well 050 (sounding #110) it is known that the thickness of sand and gravel deposit lying above till is 124 ft. The interpreted depth from curve matching in this case is only 30 ft. Limit on depth of penetration does not seem to be the explanation for this ambiguity as the interpreted depth from inverse slope method and cumulative method (Table XI and XII) for these two soundings are in rough agreement with the known depths. Thus it seems to be useful to compliment the main interpretation technique with other methods.

The resistivity and depth values obtained from inverse slope method are given in Table XI. The interpreted depths are in very good agreement with the known information. An example of this method is given in Fig. 35 for sounding #112, which was given for curve matching method also. Distinct changes in resistivity within the bedrock are found in this interpretation also for some soundings. The inverse slope method interpretation is shown in Fig. 36 for the same sounding (#120) as given in curve matching method. The change in resistivity due to the water table is clearly defined in this interpretation for the example in Fig. 35. In several other instances the known depth to the water table agrees with this interpretation. It may be pointed out that whenever the table is distinctly separated from a

Table XI

Resistivity and Depth Data from Inverse Slope Method, Metro Winnipeg Area

<u>Resistivity Sounding</u>	<u>Location</u>	ρ_1 (ohm.m.)	ρ_2 (ohm.m.)	ρ_3 (ohm.m.)	ρ_4 (ohm.m.)	ρ_5 (ohm.m.)	h_1 (ft)	h_2 (ft)	h_3 (ft)	h_4 (ft)
100	Near Well 040	8.2	11.0	76.8	2040.8		17	57	107	
101	Near Well 020	6.1	13.1	39.9	89.6	609.2	18	46	100	153
102	Near Well 020	7.0	10.4	103.5	167.5	371.6	33	54	100	
103	Near Well 012	7.6	35.0	129.8	1090.5		30	54	151	
104	Near Well 012	10.0	16.1	132.5	319.0		20	47	86	
105	Near Well 014	6.7	39.6	792.0	274.1		28	87	170	
106	Near Well 045	11.0	43.2	120.3	70.0		54	95	318	
107	Near Well 046	10.7	24.7	93.2	153.8	100.5	25	55	150	300
108	Near Well 068	354.2	400.5	682.6	354.0		68	77	253	
109	Near Well 044	46.0	158.4	350.3			50	100		
110	Near Well 050	1538.2	688.4	269.6			58	109		
111	Near Well 034	8.2	16.7	116.7	539.1		8	29	74	
112	Near Well MO-5	7.0	15.2	84.1	118.8		25	50	110	
113	Near Well MO-4	8.8	64.6	118.5			26	130		
114	Near Well MO-6	5.2	20.2	65.2			16	58		
115	1000' south of Well MO-3	5.2	18.9	13.1			11	91		

<u>Resistivity Sounding</u>	<u>Location</u>	<u>ρ_1 (ohm.m.)</u>	<u>ρ_2 (ohm.m.)</u>	<u>ρ_3 (ohm.m.)</u>	<u>ρ_4 (ohm.m.)</u>	<u>ρ_5 (ohm.m.)</u>	<u>h_1 (ft)</u>	<u>h_2 (ft)</u>	<u>h_3 (ft)</u>	<u>h_4 (ft)</u>
116	Near Well MO-3	4.9	20.7				18			
117	Near Well MO-8	8.2	27.7	237.6			16	52		
118	Near Well MO-7	10.7	252.8	627.5	266.5		13	73	206	
119	Near Well MO-2	13.1	104.5	313.1			13	90		
120	Near Well 047	15.2	54.8	192.8	365.5		22	48	100	
121	Near Well 059	7.3	28.0	240.6	411.2		21	49	85	
122	Near Well 056	18.6	130.0	236.4			12	79		
123	2 miles east of 047	7.6	61.5	1248.8	438.6		19	53	183	
124	Near Well 058	103.3	250.7				20			

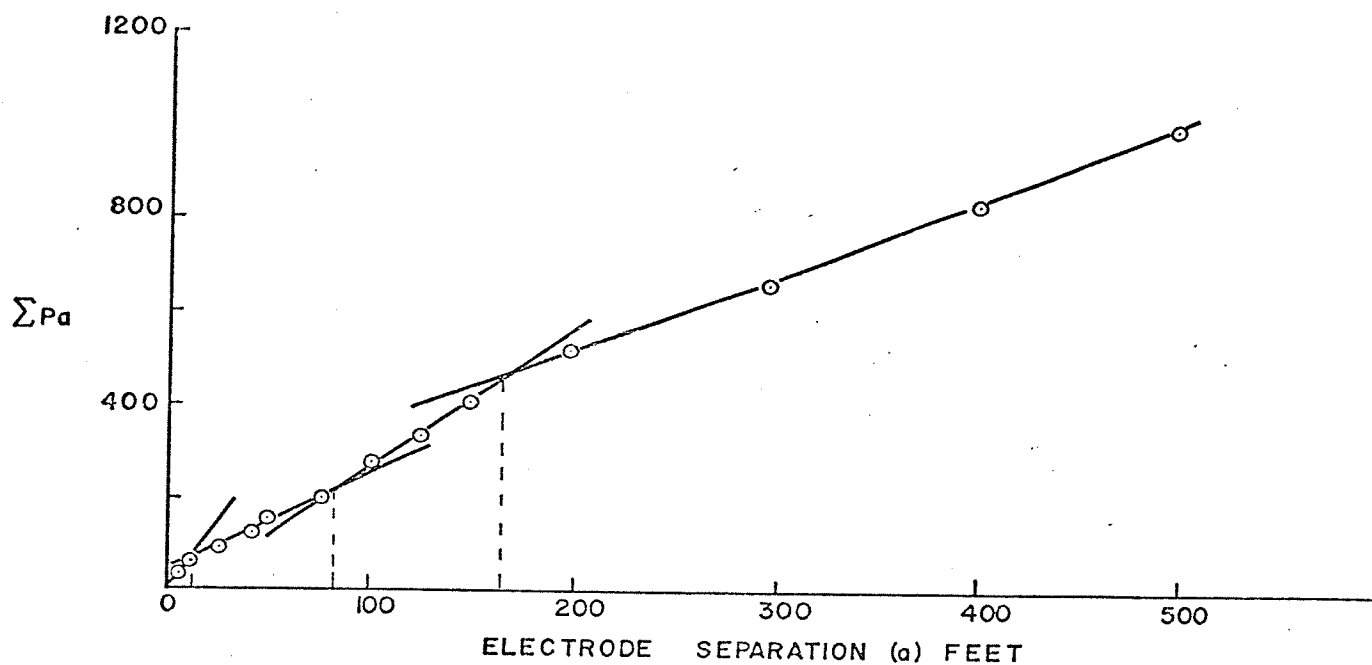
Table XII

Depth Data from Cumulative Method, Metro Winnipeg Area

<u>Resistivity Sounding</u>	<u>Location</u>	<u>h₁ (ft)</u>	<u>h₂ (ft)</u>	<u>h₃ (ft)</u>
100	Near Well 040	10	55	187
101	Near Well 020	90	161	
102	Near Well 020	7	87	170
103	Near Well 012	9	48	180
104	Near Well 012	5	52	
105	Near Well 014	180		
106	Near Well 045	10	35	177
107	Near Well 046	185		
108	Near Well 068	15	169	
109	Near Well 044	30	163	
110	Near Well 050	57	147	
111	Near Well 034	2	94	147
112	Near Well MO-5	10	88	160
113	Near Well MO-4	180		
114	Near Well MO-6	48	165	
115	1000' south of Well MO-3	80	163	
116	Near Well MO-3	78	167	

<u>Resistivity Sounding</u>	<u>Location</u>	<u>h₁ (ft)</u>	<u>h₂ (ft)</u>	<u>h₃ (ft)</u>
118	Near Well MO-7	45	176	
119	Near Well MO-2	40	142	
120	Near Well 047	12	55	138
121	Near Well 059	9	56	92
122	Near Well 056	180		
123	2 miles east of 047	83		
124	Near Well 058	7	57	143

(A) CUMULATIVE METHOD



(B) INVERSE SLOPE METHOD

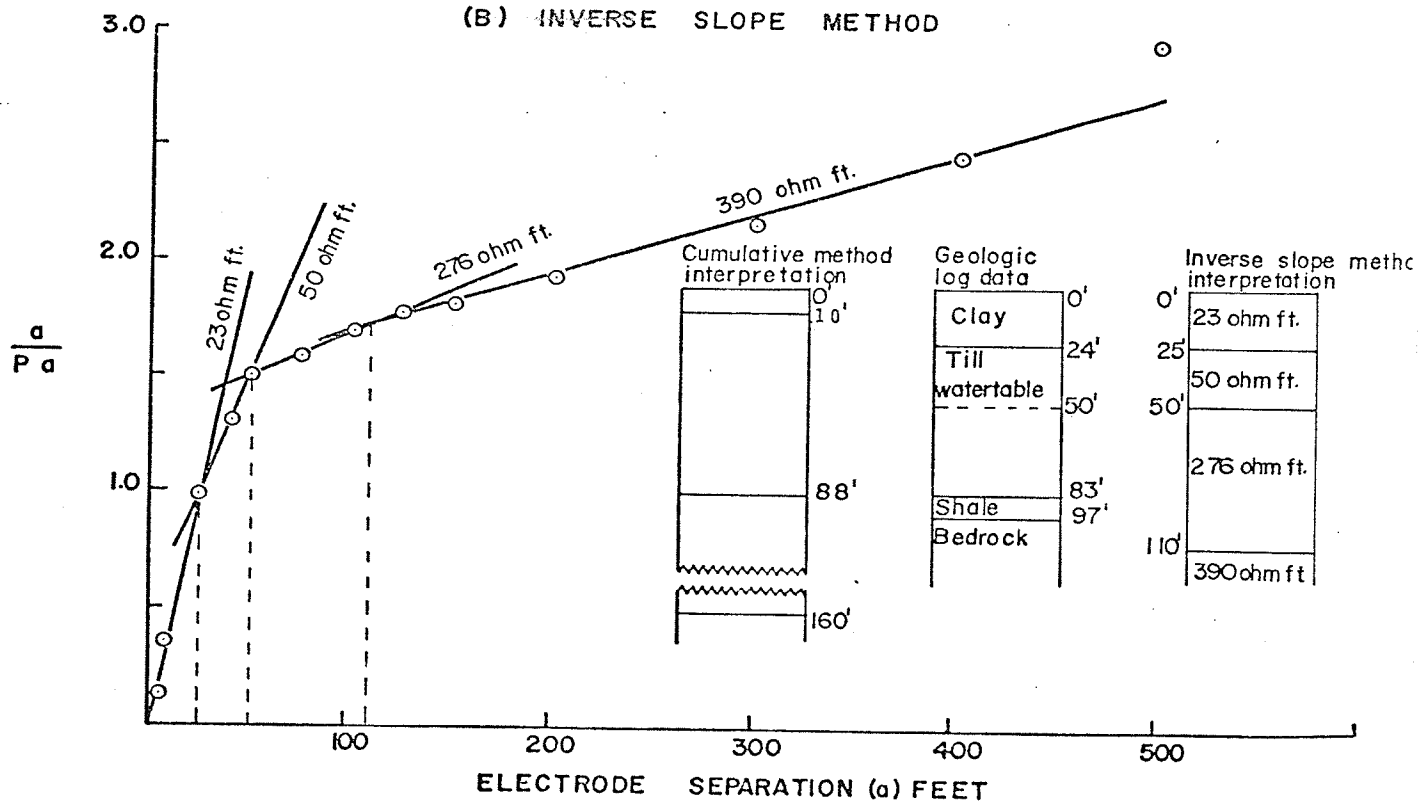


Fig. 35. Resistivity sounding #112, near MO 5, Metro Winnipeg area.

- (a) cumulative method
- (b) inverse slope method

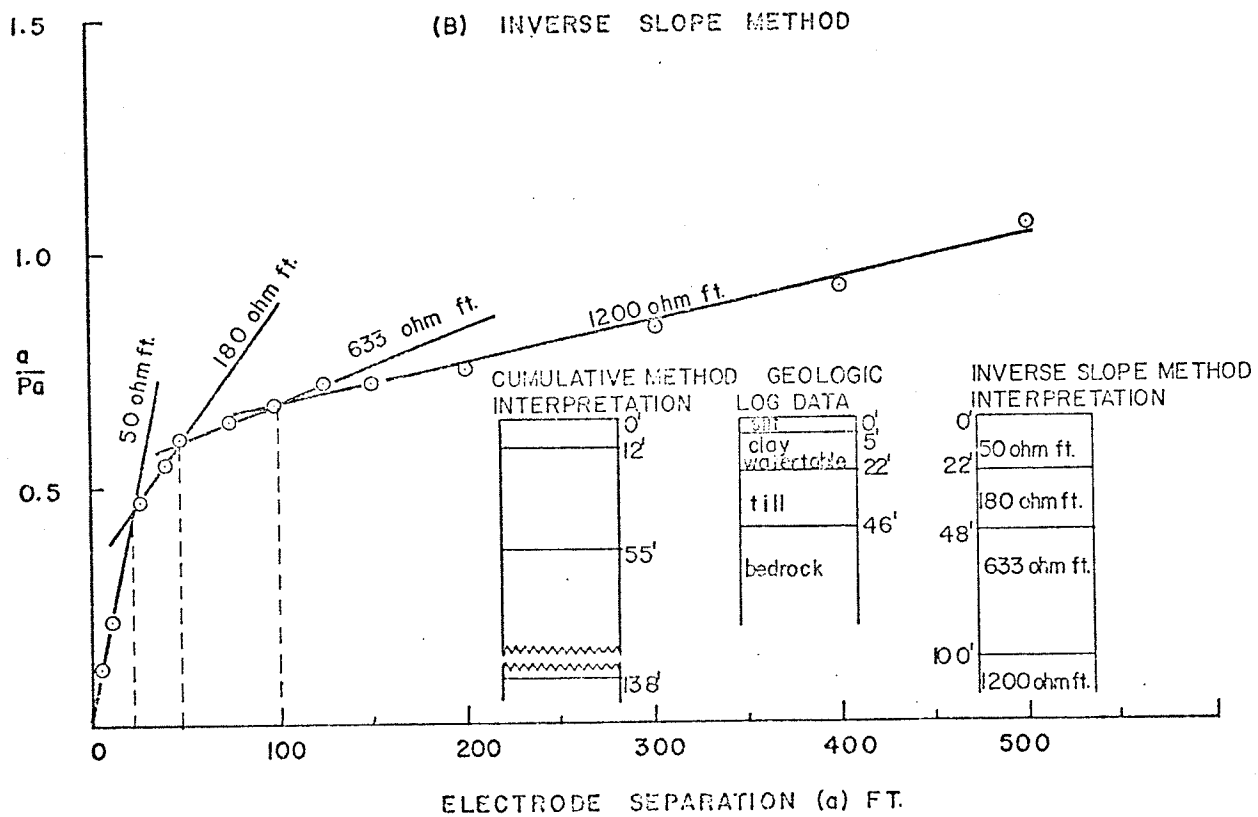
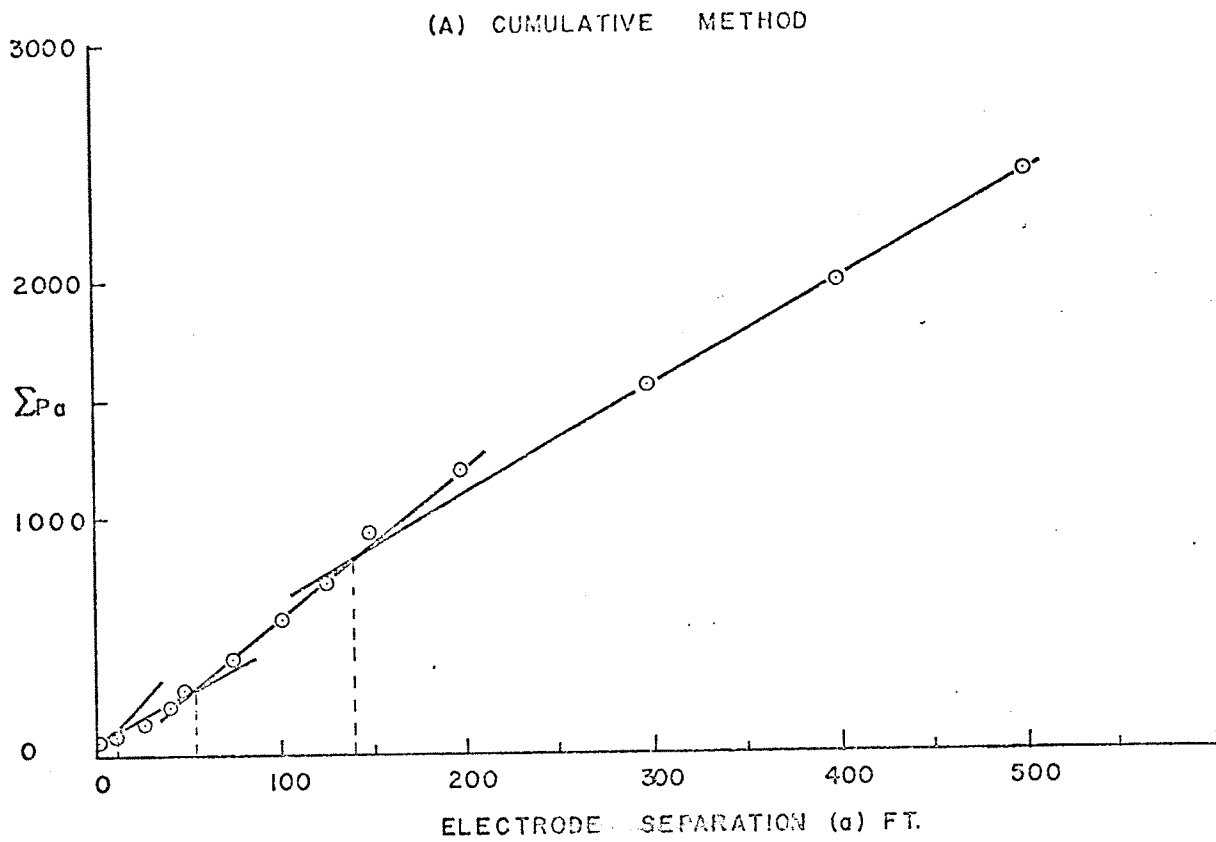


Fig. 36. Resistivity sounding #120, near well 047, Metro Winnipeg area.
 (a) cumulative method
 (b) inverse slope method

lithologic contact the water table has been defined by the data. The percentage error encountered in depth determination using the resistivity data in this area is considerably less than in the other areas studied. The reason for this lies in the fact that the thickness of the drift in this area is more than in the other areas studied. By the very character of the method, depth determinations may be more accurate if potential readings are taken at more frequent electrode separations.

The depths obtained from the cumulative method are given in Table XII. Interpreted depths from this method for soundings #112 and #120 are shown in Fig. 35 and Fig. 36. In general, the depths obtained from this interpretation are in reasonable agreement for 50 percent of the soundings. In half of the cases the agreement is very poor.

Seismic Results

The seismic profile locations are shown in Fig. 30. Nine reversed profiles were done in this area. All of the profiles were located near test well locations.

The depth determinations are carried out using the time-distance plots. The calculated depths along with the velocities are given in Table XIII. The normalized histogram of the velocities encountered is given in Fig. 37. Nearly 30 percent of the velocities range from 2,500 to 3,500 ft./sec. Nearly 55 percent of the velocities are scattered between 9,500 and 19,500 ft./sec. The variation

Table XIII

Velocity and Depth Data from Seismic Interpretations, Metro Winnipeg Area

<u>Seismic Profile Number</u>	<u>Location</u>	<u>Velocity (V₁ in ft/sec)</u>	<u>Velocity (V₂ in ft/sec)</u>	<u>Velocity (V₃ in ft/sec)</u>	<u>h₁ (ft)</u>	<u>h₂ (ft)</u>
400	Near Well 040	3100	7800	14900	37	115
401	1000' SE of Well 040	3200	7800	14000	37	85
402	Well 040	3500	8000	12500	39	123
403	Well 040	3500	8000	10500	39	103
404			9850	19300	90	260
405	Near Well 041	5200	12500			
406	Near Well 02	2800	10500	16400	44	114
407		3300	10500	15900	44	128
408		2600	11500	18400	40	143
409	1000' NE of Well 02	3000	12900	18200	54	161
410	Near Well 012	3000	10000	16400	40	121
411		2900	11500	14500	50	111
412	1000' West of Well 012	2800	15600		59	
413		3300	13600		50	
414	Near Well 014	3100	13500		49	
415		2900	13000		47	
416	1000' East of Well 014	2900	13800		35	
417		1700	14400		38	

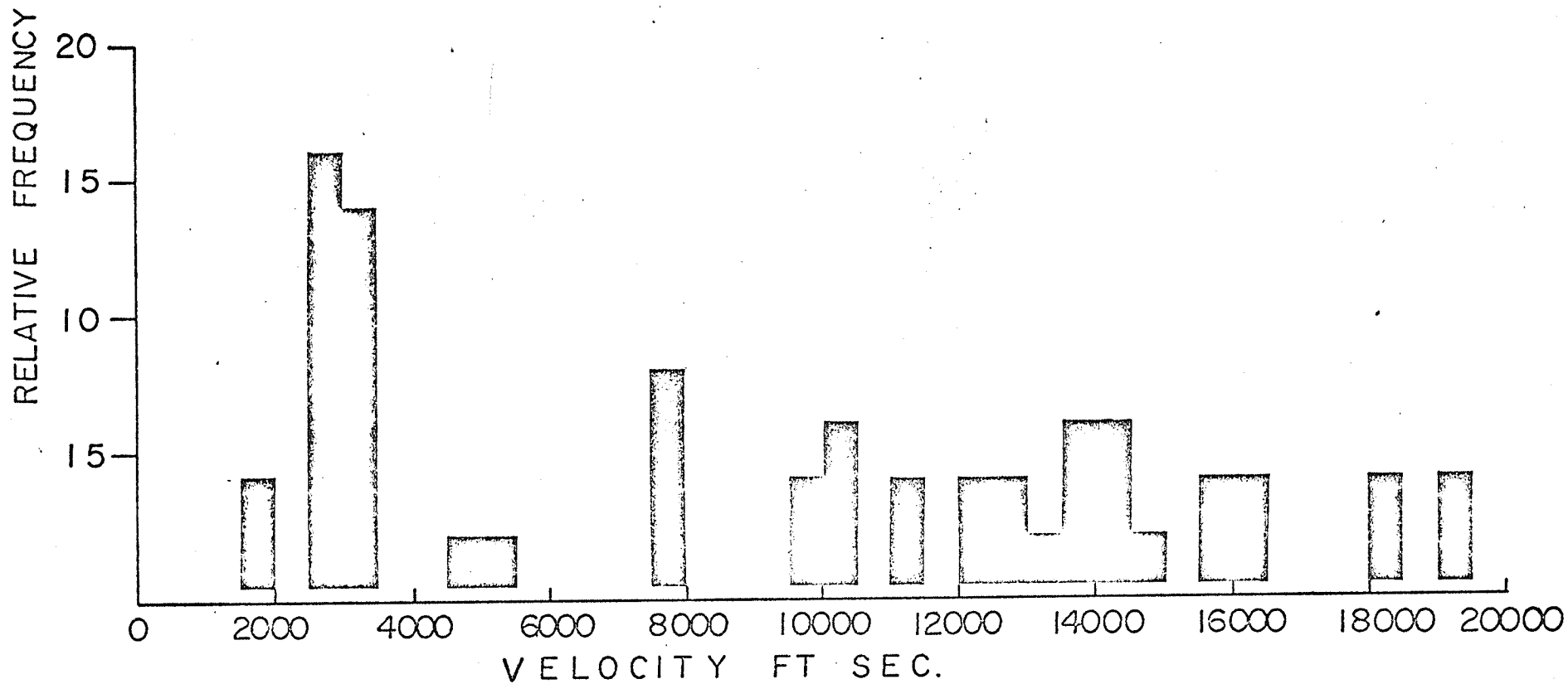


Fig. 37. Normalized histogram of seismic velocities, Metro Winnipeg Area.

in velocities obtained with the bedrock may be due to the fractured nature of the bedrock.

The seismic profiles were situated at five different locations in the area. From geologic log data at three of these locations (well 040, well 012, and well 014) the thickness of the till layer under the clay unit is only 12 ft. on the average. At the other two locations (well 041 and well 02) the thickness of the till below the clay unit is nearly 40 ft. As the geophones were spaced 110 ft. apart no segment has been recorded on the time-distance plot in many locations. Whenever the thickness is small no attempt has been made to introduce the velocity segment for the till layer on the time-distance plot. Where the unit is thick a velocity segment is introduced whenever it is not observed on the time-distance plot. This value is taken from the other profiles where a clear velocity segment has been observed. At well 012 and well 014 a layer nearly 10 ft. thick of sand and gravel is present below the till unit. As the thickness is small no distinct time delay has occurred on the time-distance plot. The depths calculated to the bedrock are in fair agreement with the known information. In some instances a change in velocity has occurred at depths greater than 100 ft., and some of these are in agreement with the resistivity results. A time-distance plot along with the known geologic information is shown in Fig. 38. The velocity range of 2,500 to

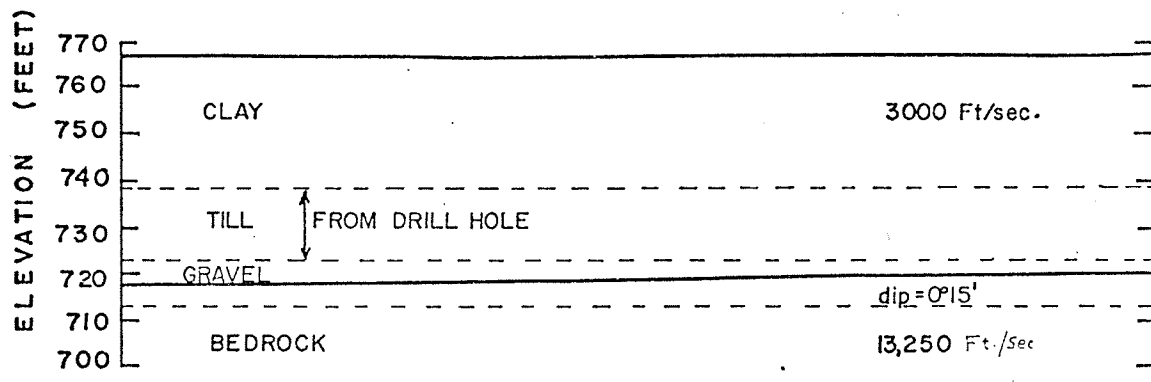
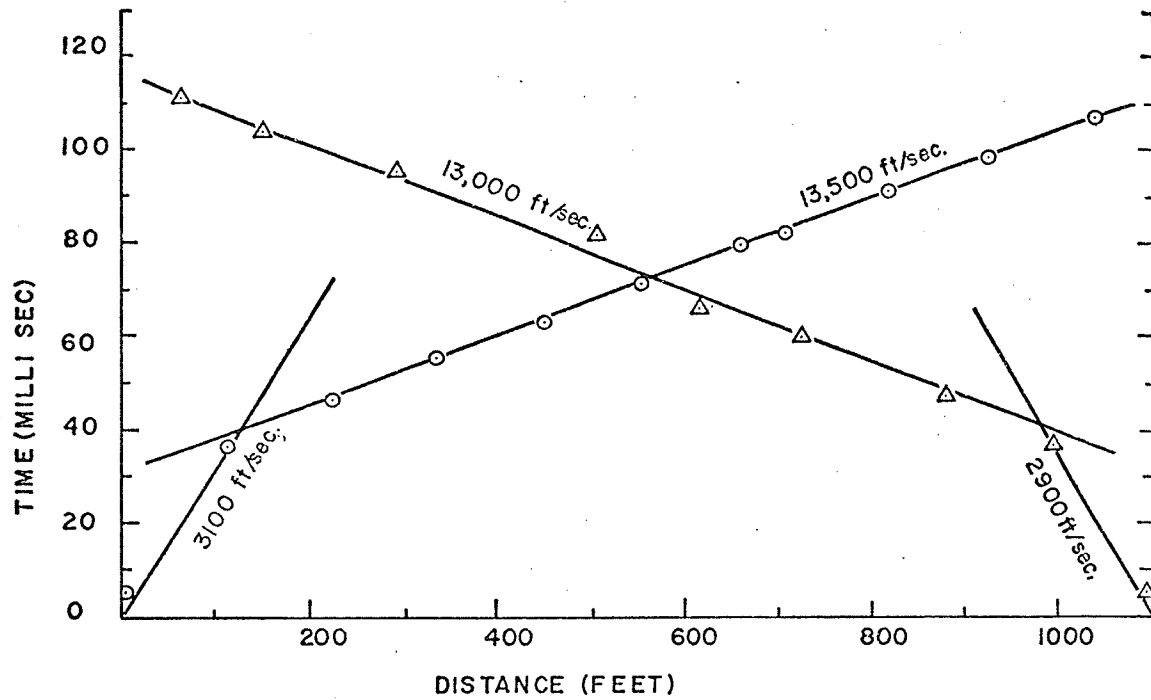


Fig. 38. Seismic profile 414-415, near well 014, Metro Winnipeg Area.
Seismic interpretation with drill hole data shown.

3,500 ft./sec. observed in the first layer in many instances is attributed to the clay unit. The evaluation of the drift materials would be clearer if closer geophone spacings had been used.

Conclusions

In general, it may be pointed out that the resistivity surveys in this area yields quite useful information. Since a distinct change in resistivity exists between the various drift materials, this may be used in evaluation of the various units and to map the bedrock topography in this area. More detailed information may be possible if closer electrode spacings were used.

The curve matching method and the inverse slope method are consistent with each other. Particularly the inverse slope method seems to be quite reliable in this area and giving more information here than in any of the other areas studied. A distinct change in resistivity has been observed at the water table at many locations. The information obtained from the cumulative method would be unreliable without the use of the curve matching and inverse slope methods.

The observed resistivities of the various units in this area are shown in Fig. 33. In general, the clay unit resistivity is 6.0 to 20.0 ohm.m., the till unit resistivity is 0.0 to 60.0 ohm.m. In general, the bedrock resistivities

are much higher and vary considerably. Resistivities as high as 1,500 ohm.m. are obtained for the bedrock.

The seismic refraction method in this area indicates that it may be used for mapping the bedrock topography. The interpretations may be ambiguous if a thick, sand and gravel layer is present below the till. Because of the inadequate data no definite conclusions can be drawn whether seismic refraction method is useful to differentiate the drift materials or not. It may be pointed out that if units are thick enough it would be possible to differentiate clay and till as there exists velocity contrast between these two. The seismic velocities obtained for the bedrock are indicative of the nature of the bedrock.

Wilson Creek Experimental Watershed, McCreary

Geology of the Area

The Wilson Creek experimental watershed is located on the slope of the Manitoba escarpment along the eastern boundary of Riding Mountain National Park, approximately six miles southwest of McCreary, Manitoba. The geology of the Wilson Creek Basin is reported by Carr (1965). A report on the hydrogeology of the area is given by Newbury *et al.* (1969). The study area is shown in Fig. 1. The rocks in the study area were reported to be mainly Upper Cretaceous in age and are comprised predominantly of grey shale, intercalated with limestone and bentonite. Only the Riding Mountain Formation was found to be exposed in the basin. The bedrock is predominantly a hard, light grey, siliceous shale of the Odanah Formation. Two lithologically distinct tills which occur in the ground moraine, overlie the Riding Mountain Formation. The lower till presumably lodgement till, is grey in color and is composed of numerous grey shale fragments and a few small igneous pebbles in a matrix of silt and clay. Overlying this is a light brown stony till presumably ablation till, containing igneous and metamorphic pebbles, cobbles and boulders. In the study area the creek banks are formed predominantly of slumped shale, alluvium and colluvium, with occasional outcrops of relatively undisturbed shale units. In the upper reaches of

the watershed thick deposit of glacial drift (more than 400 ft.) overlies the shale. The topography and the accessibility of the area is shown in Fig. 39.

Resistivity Results

Eight resistivity soundings were done in this area, five of which are within the boundaries of the watershed. The location of the resistivity soundings are shown on Fig. 40.

Mooney and Wetzel four-layer master curves give the best fits in all the cases. The fits are reasonable. The resistivity and depth information obtained from the curve matching method is given in Table XIV. A normalized histogram of resistivities is given in Fig. 41. All the resistivities obtained for the top layer are less than 100 ohm.m. Nearly 90 percent of the resistivities obtained for the second layer are between 0 and 200 ohm.m., the rest being in 400 to 450 ohm.m. range. In the third layer 90 percent of the resistivities are below 100 ohm.m. and the remaining in 300 to 350 ohm.m. range. All the resistivities obtained for the fourth layer are less than 50 ohm.m. Resistivity values of 3 to 13 ohm.m. are obtained for the bedrock (Riding Mountain Formation shale) at Broomhill Experimental Watershed, Melita. In general, the drift resistivities obtained in this area are in close agreement with the resistivities obtained for till at the Broomhill Experimental Watershed.

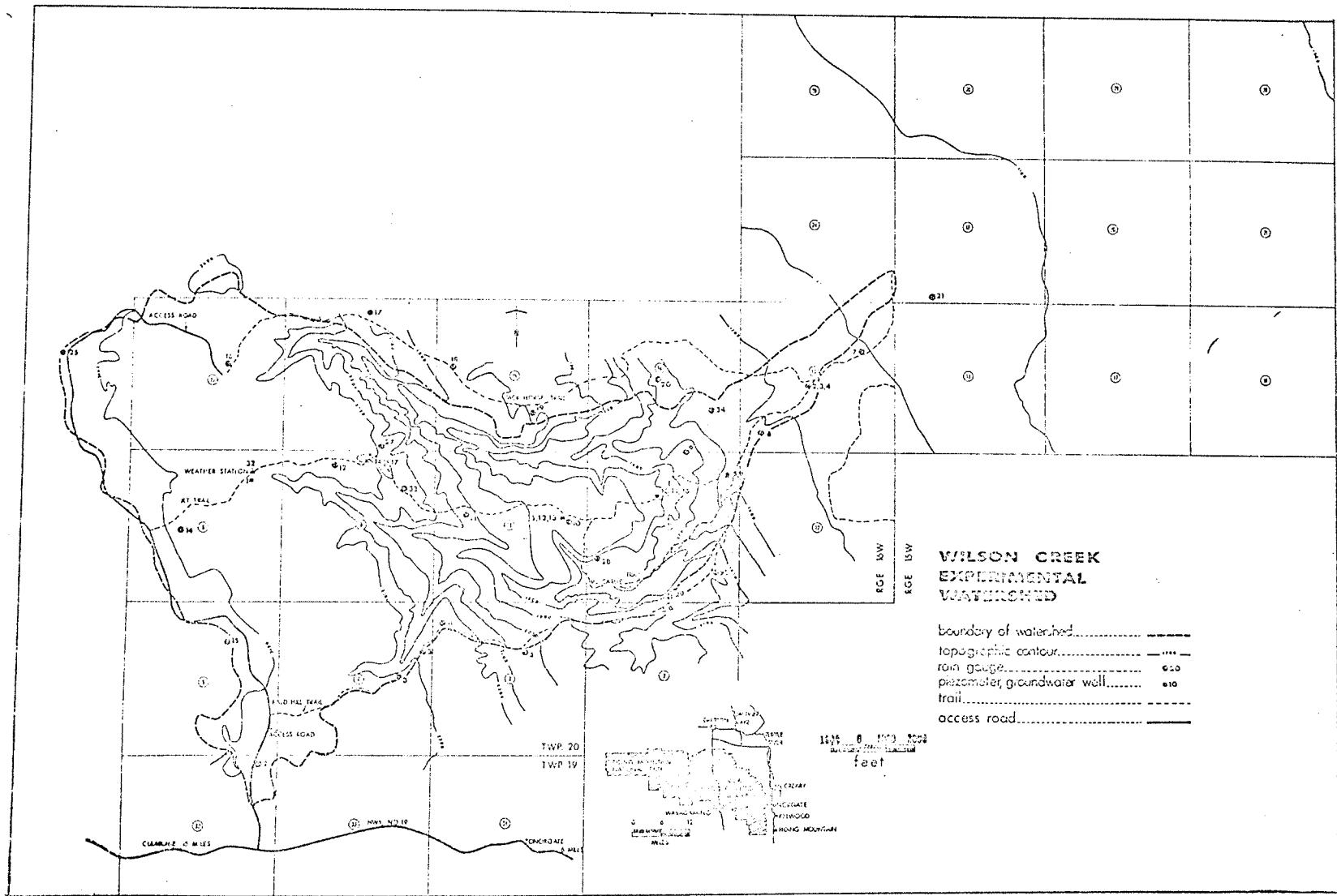


Fig. 39. Map showing topography and accessibility of the area.

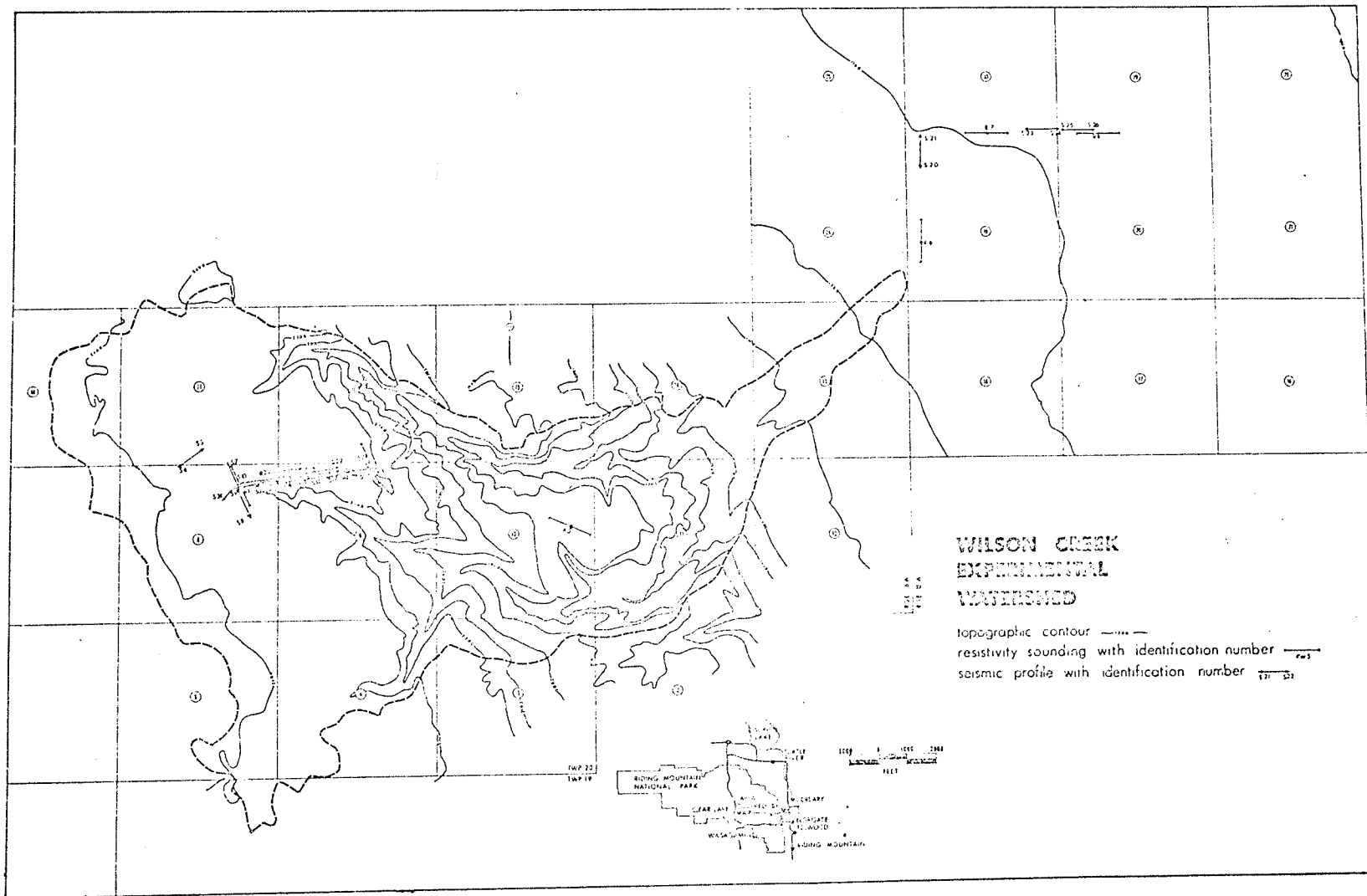


Fig. 40. Map showing resistivity sounding-seismic profile locations.

Table XIV

Resistivity and Depth Values from Curve Matching Method, Wilson Creek Experimental Watershed, McCreary

<u>Resistivity Sounding</u>	ρ_1 (ohm.m.)	ρ_2 (ohm.m.)	ρ_3 (ohm.m.)	ρ_4 (ohm.m.)	h_1 (ft)	h_2 (ft)	h_3 (ft)
1	42.6	462.4	14.3	42.6	8	12	24
2	39.6	118.8	39.6	13.1	47	93	280
3	51.8	155.3	51.8	17.4	45	75	90
4	32.0	96.0	319.8	3.2	34	50	100
5	57.9	19.2	5.8	19.2	17	67	100
6	48.7	16.1	48.7	4.9	107	133	160
7	56.3	18.9	56.3	5.8	18	46	55
8	35.0	105.1	35.0	11.6	5	10	31

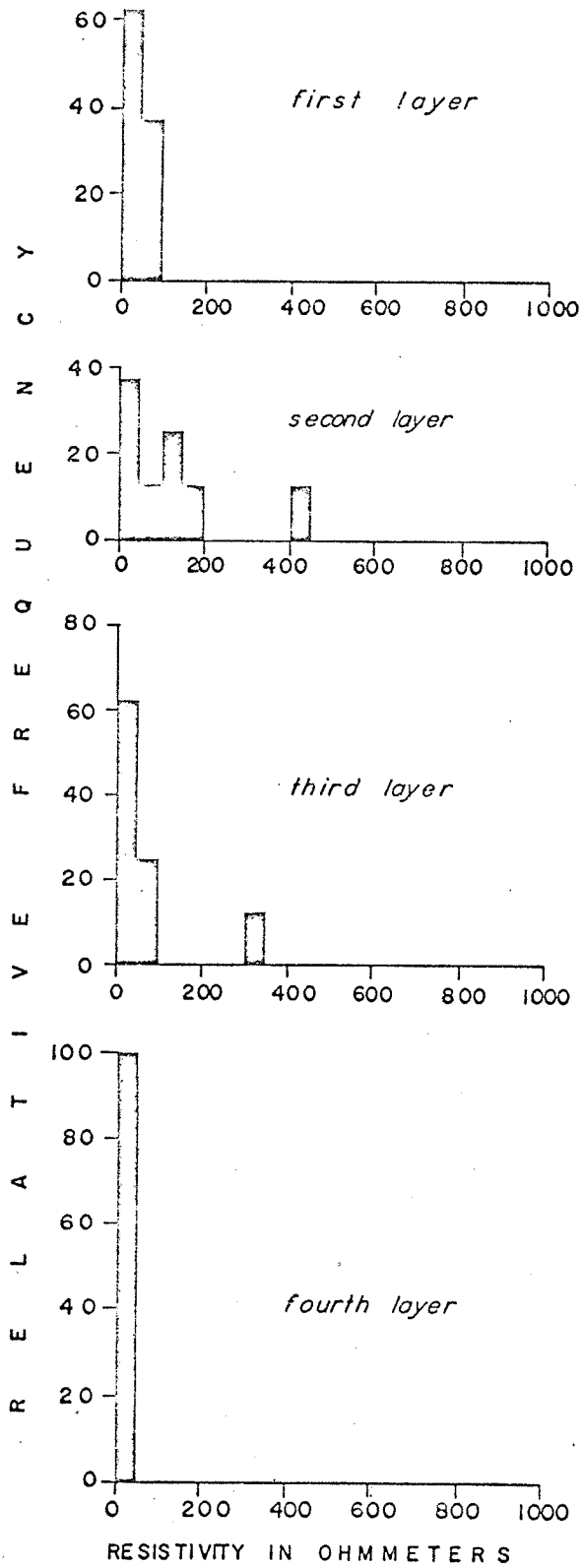


Fig. 41. Histogram of resistivities, Wilson Creek Experimental Watershed.

The increase in resistivity obtained in the second layer may be due to variations in the sandy silt content or to variations within the till itself. A typical resistivity sounding from the area with the interpretation from curve matching method is shown in Fig. 42.

The resistivity and depth values obtained from inverse slope method are given in Table XV. The results from this method are in fair agreement with the curve matching method. In some instances changes in resistivities at deeper depths are obtained in this method which are not observed in curve matching method. Interpretation from this method is shown in Fig. 43 for the example given in curve matching method.

All the soundings have also been interpreted using cumulative method. The depth information obtained from this is given in Table XVI. The interpretation from this method is shown in Fig. 44 for the same soundings given by the other methods.

Seismic Results

Fourteen reversed seismic profiles were conducted in this area and the locations are shown in Fig. 40.

Depth interpretations were carried out using the time-distance plots. The velocities and depths obtained are given in Table XVII. In nearly 80 percent of the cases only two segments are obtained on the time-distance plot and the remaining cases three segments are obtained. After the final

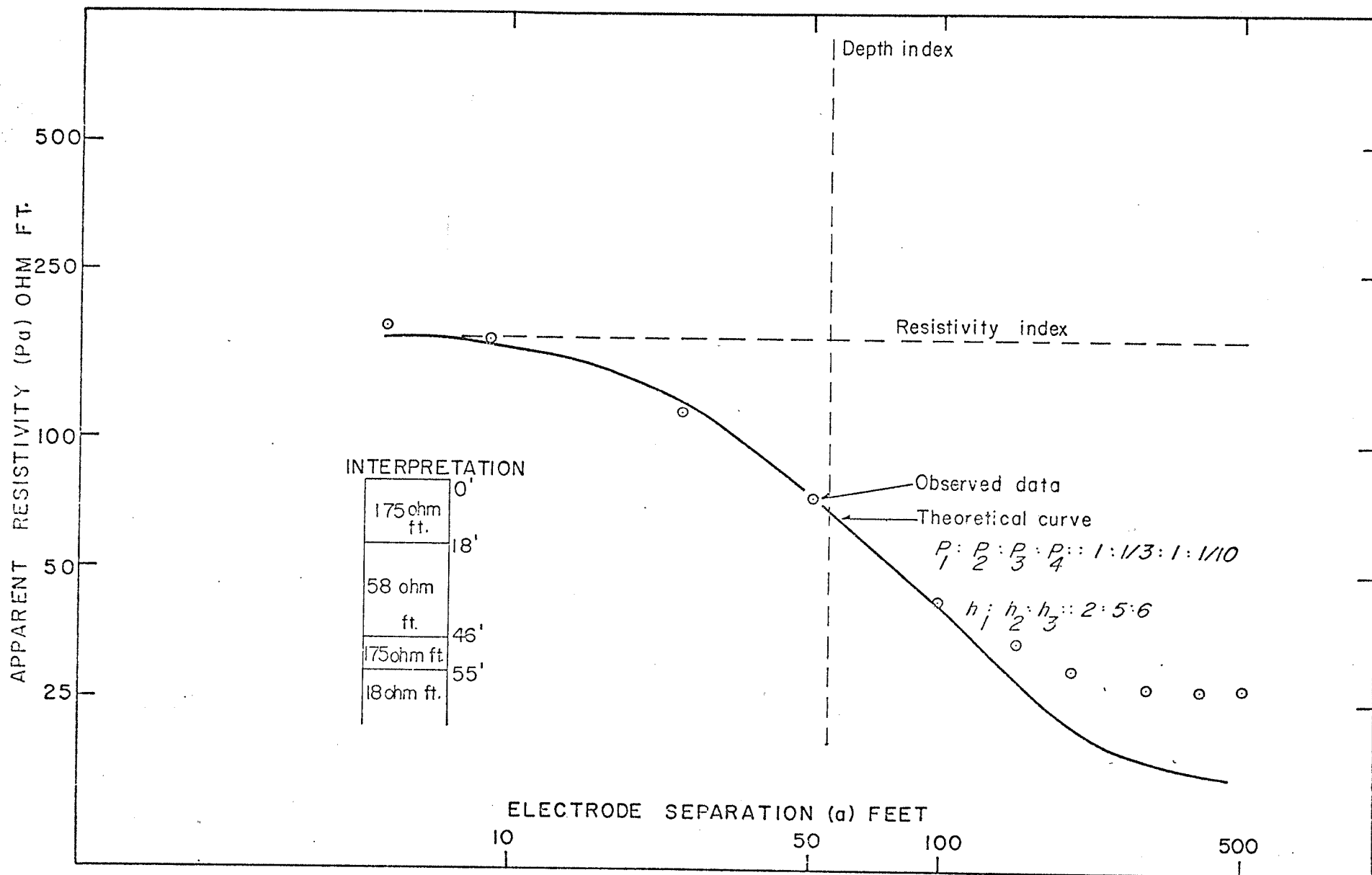


Fig. 42. Resistivity sounding #7, curve matching method, Wilson Creek Experimental Watershed. 66

Table XV

Resistivity and Depth Values from Inverse Slope Method, Wilson Creek Experimental Watershed, McCreary

<u>Resistivity Sounding</u>	ρ_1 (ohm.m.)	ρ_2 (ohm.m.)	ρ_3 (ohm.m.)	ρ_4 (ohm.m.)	h_1 (ft)	h_2 (ft)	h_3 (ft)
1	56.3	34.4	26.2		37	129	
2	35.0	60.3	17.4		15	275	
3	53.0	30.5	21.6		119	259	
4	37.8	147.1	50.0	23.8	33	109	196
5	53.9	11.3			23		
6	52.1	37.5	7.9		20	178	
7	57.3	17.4	7.3		18	72	
8	52.1	9.1	5.5	10.7	38	155	300

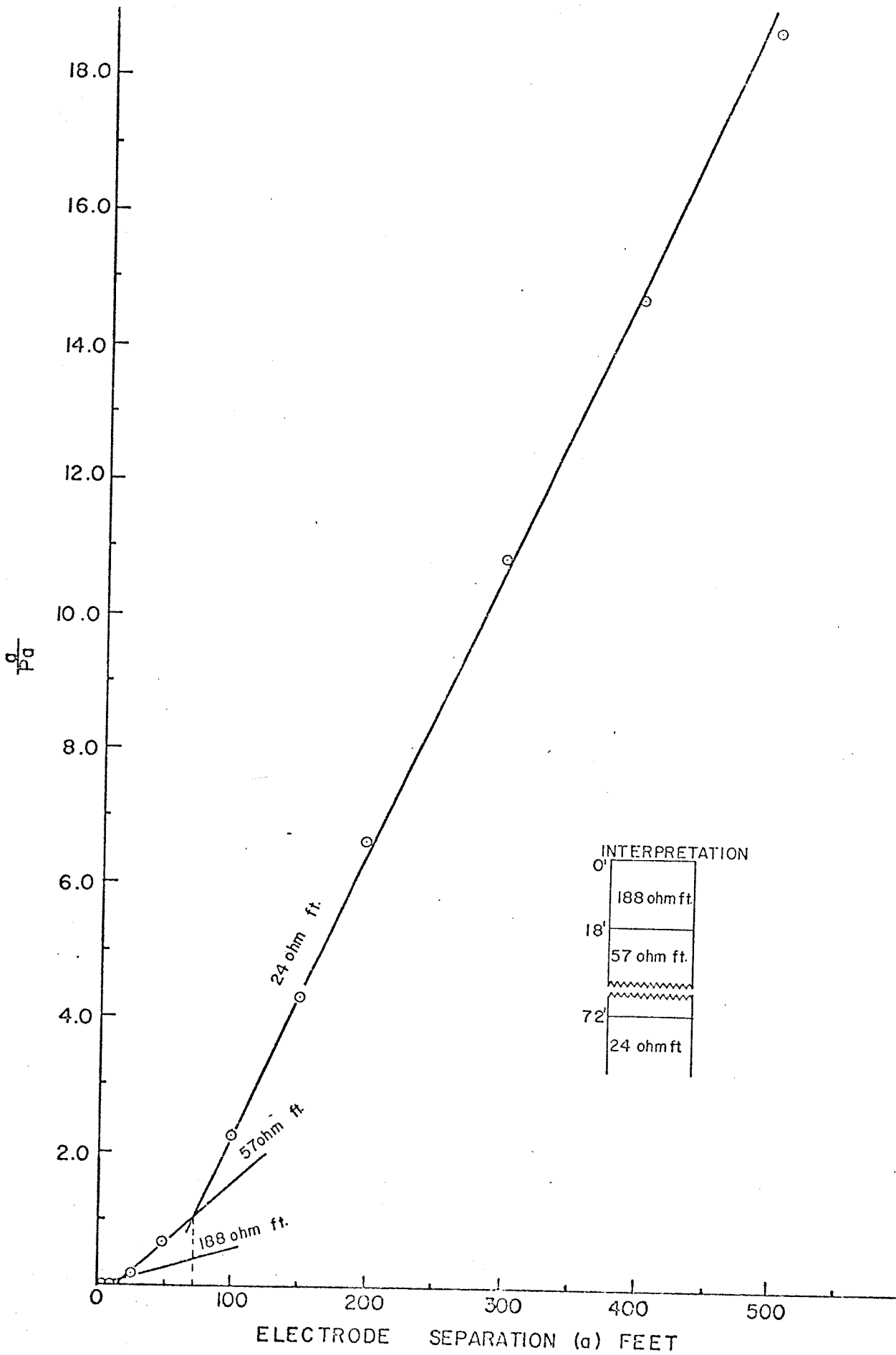


Fig. 43. Resistivity sounding #7, inverse slope method, Wilson Creek Experimental Watershed, McCreary.

Table XVI

Depth Data from Cumulative Method,
Wilson Creek Experimental Watershed, McCreary

<u>Resistivity Sounding</u>	<u>h₁ (ft)</u>	<u>h₂ (ft)</u>	<u>h₃ (ft)</u>
1	10	38	193
2	10	47	214
3	11	49	178
4	11	44	192
5	10	45	203
6	12	57	193
7	28	191	
8	28	157	

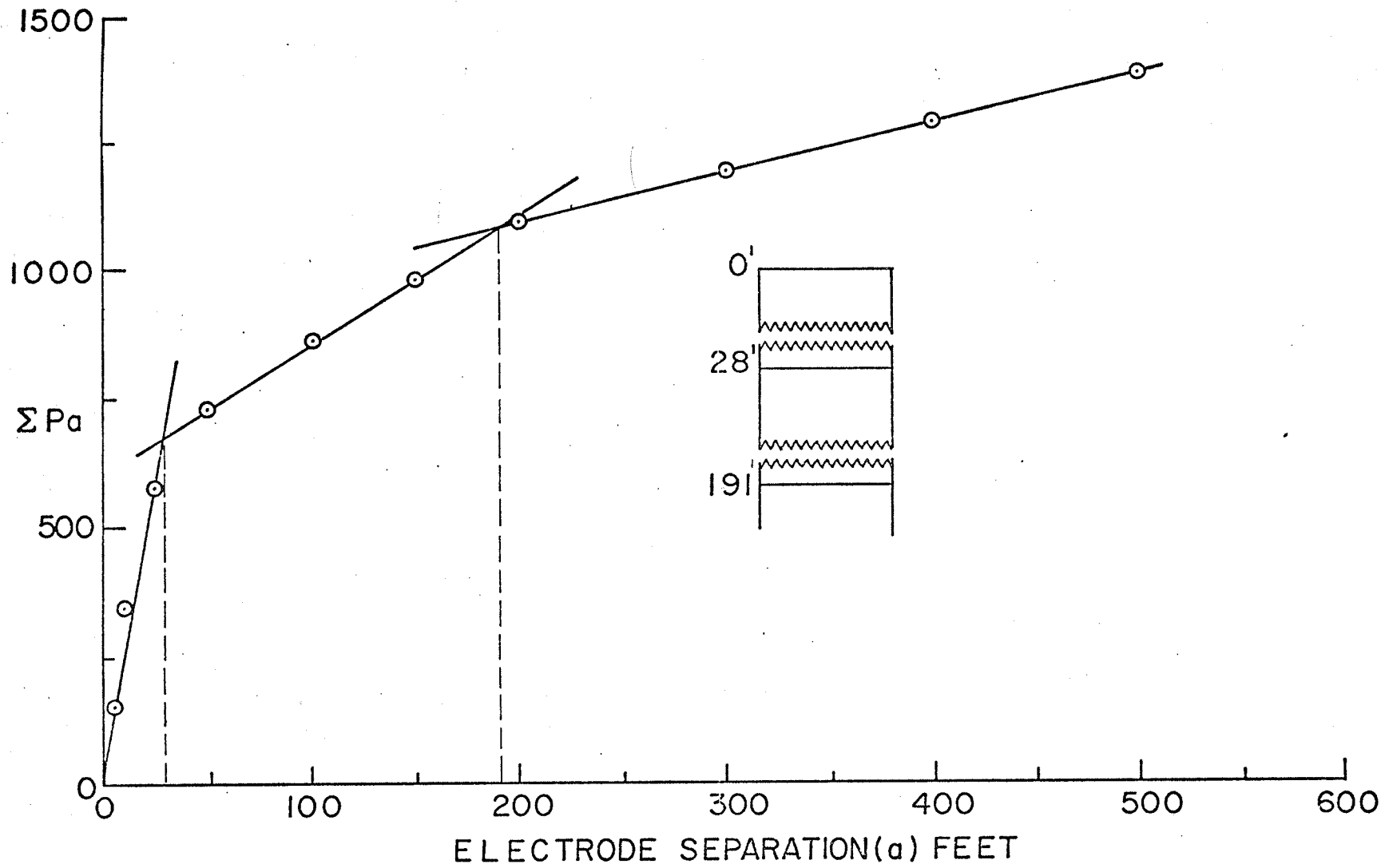


Fig. 44. Resistivity sounding #7, cumulative method, Wilson Creek Experimental Watershed.

Table XVII

Seismic Velocities and Calculated Depths, Wilson Creek Experimental Watershed - McCreary

<u>Seismic Profile Number</u>	<u>Velocity (V₁ in ft/sec)</u>	<u>Velocity (V₂ in ft/sec)</u>	<u>Velocity (V₃ in ft/sec)</u>	<u>h₁ (ft)</u>	<u>h₂ (ft)</u>
3	5550	8000		180	
4	5150	7850		160	
7	3250	5650		27	
8	950	5100	5900	10	66
9	700	4600	5550	3	55
10	3500	6100		36	
11	3300	5600		33	
14	5100	8500		214	
15	5200	7250		168	
16	4600	6500		130	
17	4450	7100		164	
18	2200	4750	6100	30	127
19	2300	5150	6400	41	151
20	3500	6200		45	
21	3350	6600		63	
23	2800	7000		69	
24	2400	6300		44	

<u>Seismic Profile Number</u>	<u>Velocity (V₁ in ft/sec)</u>	<u>Velocity (V₂ in ft/sec)</u>	<u>Velocity (V₃ in ft/sec)</u>	<u>h₁ (ft)</u>	<u>h₂ (ft)</u>
25	2800	7250		55	
26	2750	8000		61	
27	2400	5300	6950	33	185
28	3000	5300	6150	33	148
29	4600	5200		135	
30	4600	5900		202	
31	4800	6250		184	
32	4700	6000		143	
33	4300	5200		69	
34	4300	5850		83	

segment in many instances the velocities started to decrease approaching the velocity of the first layer. This character may be due to structures in the bedrock (Heiland, p. 518).

A normalized histogram of the velocities obtained in this area is given in Fig. 45. All the velocities are less than 8,000 ft./sec. the major peak being at 5,000 to 5,500 ft./sec. The velocities obtained for the drift is always less than 5,500 ft./sec. An example of a time-distance plot from this area is given in Fig. 46 with interpretation.

Conclusions

The results obtained in this area were not compared with any drill hole information as no specific information is available. In general, the three resistivity interpretations are fairly consistent with each other. In general, and particularly within the watershed, the depths obtained from seismic refraction method and resistivity soundings are not in good agreement. The locations of the resistivity soundings were selected at minimum topographic variations, the depths obtained from resistivity soundings may be approximate, as the interpretation theory demands horizontal layers. The resistivities obtained for shale are in the same range as those obtained at Broomhill Experimental Watershed. In some instances in this area the shale resistivities are as high as 20 ohm.m. The till resistivities are higher in this area with values of 30 to 50 ohm.m.

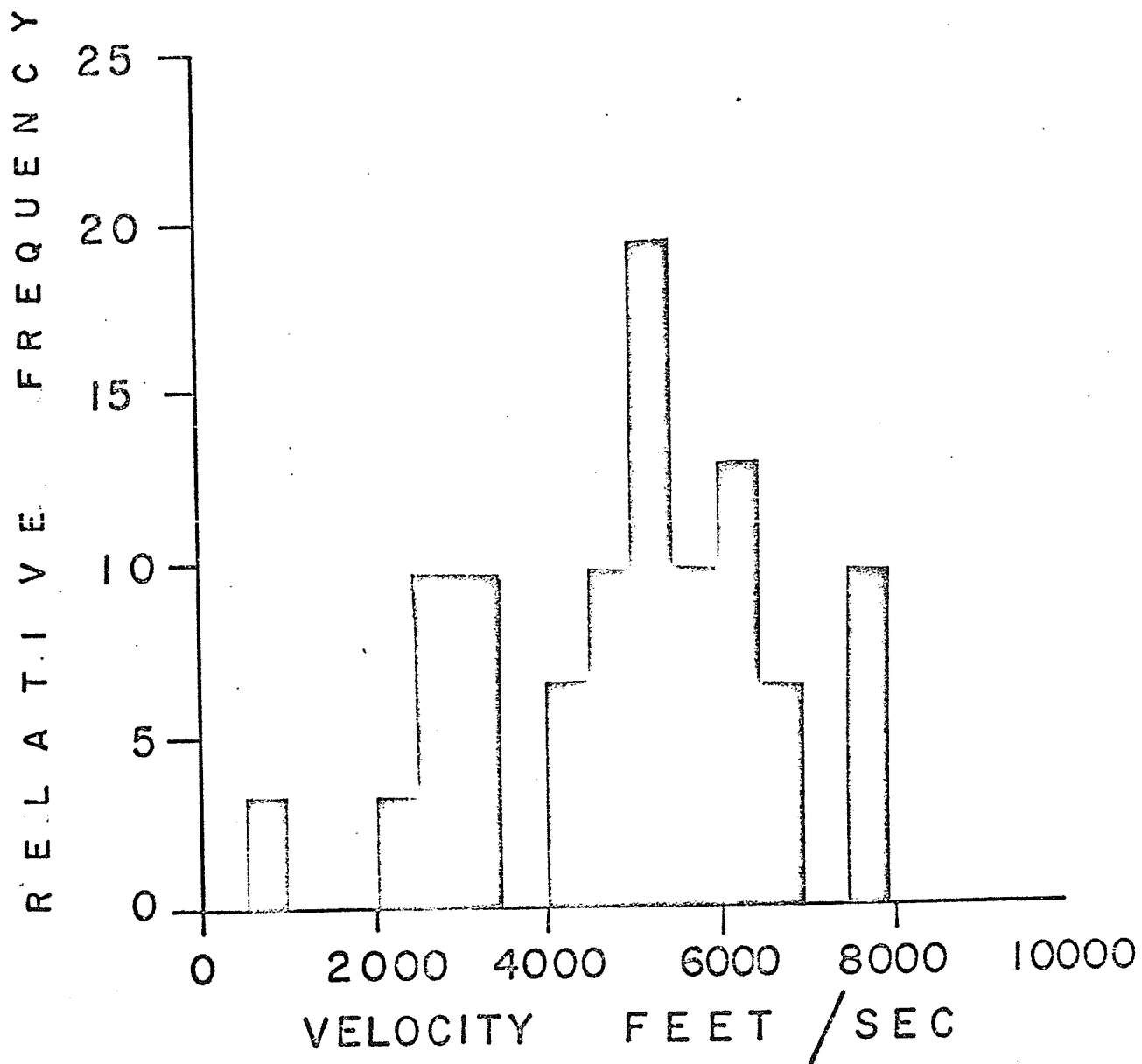


Fig. 45. Histogram of velocities, Wilson Creek Experimental Watershed.

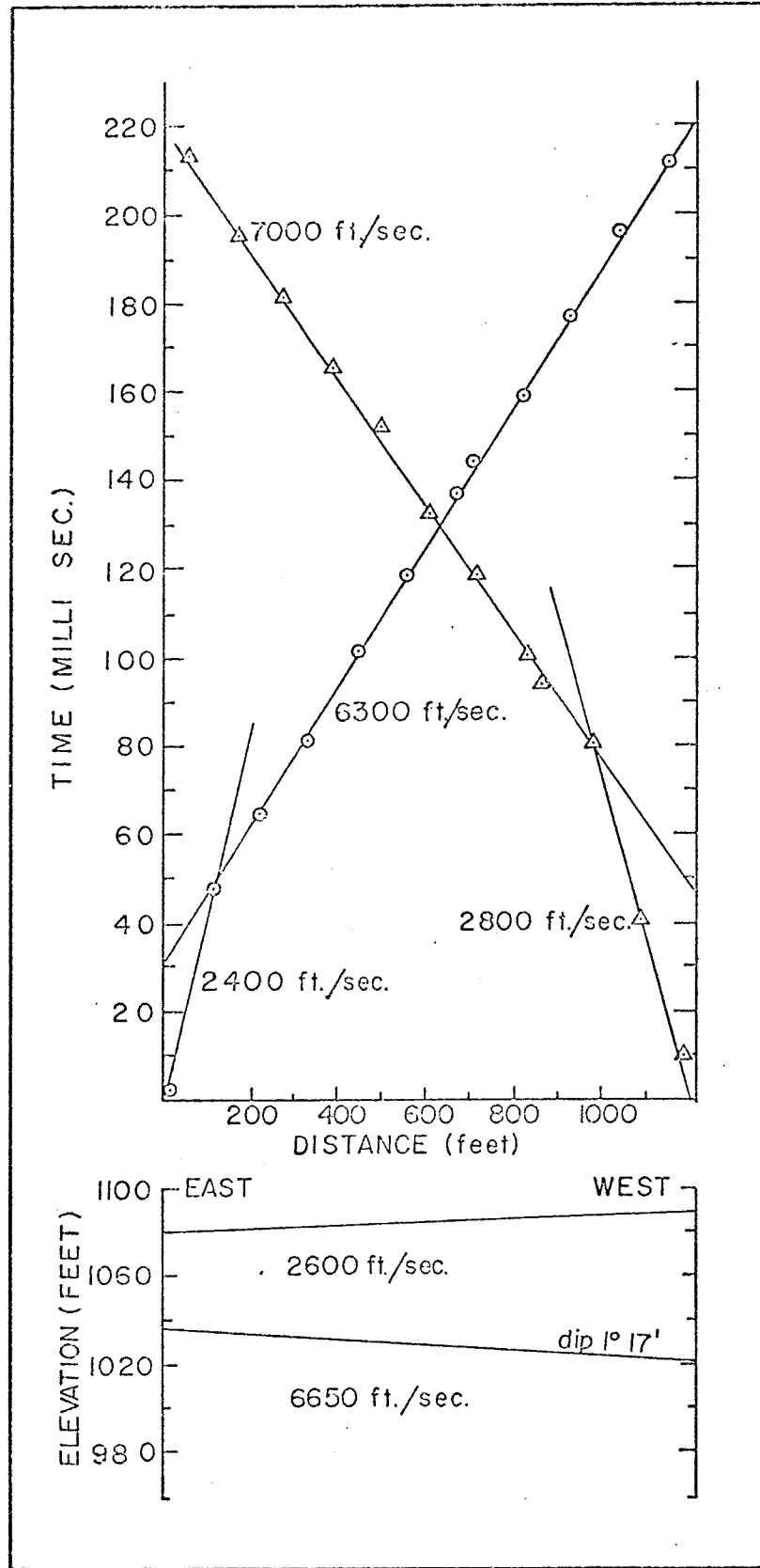


Fig. 46. Seismic profile 24-23. Time-distance plot with interpretation Wilson Creek Experimental Watershed.

Seismic surveys in this area suggest irregular bedrock topography or in some instances structures within the bedrock. The velocity obtained for drift in this area is less than 5,500 ft./sec. This indicates that the till in this area is unconsolidated and contains more silty or clayey fraction. The bedrock velocities in this area vary from 5,500 to 8,000 ft./sec.

No comment can be made on the validity of the depth information obtained from seismic and resistivity in this area since there is no known drill hole information, but it is clear that there exists a resistivity change within the till unit and between till and the bedrock shale.

CHAPTER IV

GENERAL CONCLUSIONS

The resistivity method was successful both in evaluating the individual superficial deposits and mapping the overburden-bedrock interface. The seismic refraction method was found less sensitive to the character of the individual deposits but reliable in mapping the overburden-bedrock interface.

The resistivity data was interpreted using the curve matching method. Inverse slope and cumulative methods were also applied but the success was limited. Curve matching is the best and most reliable of the methods used.

In the Broomhill area the geologic sequence from top to bottom is sand and gravel, and till over a bedrock of shale. The results from the resistivity surveys were in good agreement with drill hole information. The seismic refraction survey indicated that the outwash deposit is saturated at several locations. At these locations it is not possible to determine the thickness of the outwash deposit using seismic refraction methods.

At the Pinawa site the general sequence of layers is lacustrine clay and silty clay, lacustrine sand and gravel, sandy till over a bedrock of granite. The resistivity method

in this area was successful in differentiating the superficial deposits and in mapping the overburden-bedrock interface. The seismic refraction method was useful in mapping the overburden-bedrock interface but not in differentiating the individual deposits.

In the Winnipeg area the general sequence of formations is clay and till over a bedrock of limestone and dolomite. The resistivity method was reliable in differentiating the drift materials and in mapping the drift-bedrock interface. The seismic method was reliable only in mapping the drift-bedrock interface. More information is necessary to determine the usefulness of the seismic method in differentiating the drift materials.

In the Wilson Creek area the geological sequence is glacial drift comprised of sand, gravel and till over a bedrock of shale. Drill hole information was not available to compare with the results from the geophysical surveys. In general, the results from the resistivity interpretation method were consistent with each other. The seismic refraction surveys indicate possible structures in the bedrock. The results from the resistivity surveys and the seismic refraction surveys are in poor agreement. More data is necessary to arrive at any firm conclusions about a subsurface in this area.

In general geophysics does not replace drilling. But certainly this can be used as a tool especially in

groundwater projects. No one can deny the fact that the information obtained from dilling is quite localized and is expensive. In favorable situations certainly resistivity and seismic methods do reduce the amount of drilling which means saving of considerable amount of time and money. For example, on an average day a three man crew could do six resistivity soundings with 500 feet maximum electrode separation. On an average day a three man crew could complete easily 6 or 7 reversed seismic profiles with 1200 ft. span. The initial investment for both the seismic refraction unit and resistivity equipment is less than \$10,000. Drilling operations costs \$100 per day, in which only 100 ft. can be drilled with a two man crew and comparing these costs with those for geophysical operations one agrees that geophysical operations are a considerably cheaper way of obtaining information about the subsurface.

This study indicates that geophysics can be used to extend the known information to unknown areas economically if selected drilling is also done. Without the use of known geology or drill hole information geophysical interpretations may be ambiguous and complicated in shallow investigations. It is certainly economical, at least in favourable locations, to use geophysics as a tool in groundwater problems.

In summary it is recommended that future studies of the Pleistocene deposits in Manitoba be made using selected

geophysical methods as well as drilling. It would also be advisable to use closer spacings of measurement than was used in this work. However, the individual methods to be applied and the spacings to be used depends on the specific problem under consideration and the features of the deposits to be studied.

LIST OF REFERENCES

- Bhaktiari, H., 1971. Hydrogeology of the Broomhill Experimental Aquifer. Unpubl. M.Sc. thesis, University of Manitoba.
- Carr, P.A., 1965. Geological and hydrogeological reconnaissance of the Wilson Creek Basin, Manitoba, Geological Survey of Canada, Topical Report No. 106.
- Cherry, J.A., Beswick, B.T. and Clister, W.E., 1970. Hydrogeologic factors in subsurface radioactive waste management at the Whiteshell Nuclear Research Establishment Plant Site, Pinawa, Manitoba. Dept. of Earth Sciences, University of Manitoba, Winnipeg.
- Dobrin, M.B. 1960. Introduction to geophysical prospecting. New York, McGraw Hill Book Company.
- Davies, J.F., Bannatyne, B.B., Barry, G.S. and McCabe, H.R., 1962. Geology and mineral resources of Manitoba. Manitoba Mines Branch Publication, 350 p.
- Groundwater Availability in the Melita area, Groundwater availability studies Report No. 1, Department of Mines and Natural Resources, Province of Manitoba, July, 1968, pp. 4-14.
- Heiland, C.A., 1963. Geophysical Exploration, New York, Hafner Publishing Company.
- Hobson, G.D., 1964. Geotechnical Investigations of Red River Floodway, Winnipeg, Manitoba. Geological Survey of Canada Paper 64-18.
- Lancaster-Jones, E., 1930. The earth resistivity method of electrical prospecting. Mining Magazine, vol. 43, No. 2, pp. 19-29.
- Lennox, D.H. and Carlson, V., 1967. Integration of geophysical methods for groundwater exploration in prairie provinces, Canada. Mining and Groundwater Geophysics (ed.) pp. 517-533.

- McGinnis, L.D., 1961. Integrated seismic, resistivity and geologic studies of glacial deposits. Ill. Geol. Survey circ. 323.
- McPherson, R.A., 1968. Pleistocene stratigraphy of the Winnipeg River in the Pine Falls - Seven Sisters Falls area, Manitoba. Unpubl. M.Sc. thesis, Dept. of Geology, University of Manitoba.
- Meidav, T., 1960. An electrical resistivity survey for Groundwater. Geophysics, vol. 25, pp. 1077-1093.
- Mooney, H.M. and Wetzel, W.W. 1956. The potentials about a point electrode and apparent resistivity curves for a two, three and four layer earth. Minneapolis, The University of Minnesota Press.
- Moore, R.W., 1945. An empirical method of interpretation of earth resistivity measurements. A.I.M.E. Geophysics, vol. 164, pp. 197-223.
- Nettleton, L.L., 1940. Geophysical prospecting for oil. New York, McGraw Hill Book Company.
- Newbury, R.W., Cherry, J.A., Cox, R.A., 1969. Groundwater stream flow systems in Wilson Creek Experimental Watershed. Can. Jour. of Earth Sciences, vol. 6, 613 p.
- Pirson, S.J., 1934. Interpretation of three layer resistivity curves. A.I.M.E. Trans., vol. 110, pp. 148-158.
- Render, F.W., 1970. Geohydrology of the Metropolitan Winnipeg area as related to groundwater supply and construction. Can. Geotechnical Jour., vol. 7, No. 3, pp. 250-258.
- Sankernarain, P.V. and Ramanujachary, 1967. An inverse slope method of determining absolute resistivity. Geophysics, vol. 32, pp. 1036-1040.
- Tagg, G.F. 1934. Interpretations of resistivity measurements. A.I.M.E. Trans., vol. 110, pp. 135-145.
- Van Nostrand, R.G. and Cook, K.L., 1966. Interpretation of resistivity data. U.S.G.S. Prof. Paper 499.
- Wenner, F., 1915. A method of measuring earth resistivity. U.S. Bureau Standards Bull., vol. 12, pp. 469-478.